IntechOpen

Autonomous Vehicle

Edited by Andrzej Zak

AUTONOMOUS VEHICLE

Edited by **Andrzej Zak**

Autonomous Vehicle
http://dx.doi.org/10.5772/61898
Edited by Andrzej Zak

Contributors

Changle Xiang, Yue Ma, Bin Xu, Yang Wang, Khuram Shahzad, Weria Khaksar, Feng Gao, Shengbo Eben Li, Ibrahim Kutay Yilmazcoban, Antonio Virga, Kwang Sub Song

Notice

First published in Croatia, 2016 by INTECH d.o.o.
eBook (PDF) Published by IN TECH d.o.o.
Place and year of publication of eBook (PDF): Rijeka, 2019.
IntechOpen is the global imprint of IN TECH d.o.o.
Printed in Croatia

Legal deposit, Croatia: National and University Library in Zagreb

Additional hard and PDF copies can be obtained from orders@intechopen.com

Autonomous Vehicle
Edited by Andrzej Zak

p. cm.

Print ISBN 978-953-51-2584-6

Online ISBN 978-953-51-2585-3

eBook (PDF) ISBN 978-953-51-5789-2

Meet the editor

Dr. Andrzej Zak comes from Poland. He graduated from Military University of Technology with master's degree in Science and Engineer Degree in Computer Science. In Polish Naval Academy, Dr. Zak earned his degree of a Doctor of Technical Sciences. His doctoral thesis covered dynamics identification and modeling of underwater vehicles using artificial neural networks. The AGH University of Science and Technology awarded him with a degree of doctor habilitated in technical science in the field of automation and robotics in specialization autonomous underwater vehicles. His habilitation monography is concerned with the control team of cooperated autonomous underwater vehicles using game theory and multi-agent systems. Dr. Zak has published monographs and many articles and conference papers covering topics related directly or indirectly to autonomous vehicles.

Contents

Preface

From earliest times, mankind has been searching for ways of convenient and fast travel and transport of goods. In ancient times people built various types of vehicles used to move through the lands, as well as boats and ships to move along the surface of the water and the oceans. It was not until the late nineteenth century that planes became means of transport. Currently, land, air, water surface, or underwater transport no longer represent a problem, but still new solutions are sought in these areas.

In the early period of the development of means of transport, manned vehicles were used, controlled by a well-trained man or group of people located on the vehicle. Since the 1950s we saw the development of remotely operated unmanned vehicles. Nowadays they are offering all the characteristic features of a robot: mobility and manipulation, the ability of the technical observation of the environment, and sometimes self-decision making especially in typical and repetitive situations. Unmanned vehicles have become the basic equipment of many companies, private and public institutions particularly active in military, police, and rescue, and are also at the disposal of research and development centers. Unmanned vehicles are used in various fields of human activity both on land and sea or air. In recent years, one of the main tasks carried out by unmanned vehicles are recognition and survey tasks, which became important in the security dimension, especially in terms of terrorist threats.

The development of autonomous vehicle began in the early 1960s. During this period, the main problem was the computer technology, which in the 1970s and 1980s was relatively undeveloped. The situation was similar to the mobile energy sources required for autonomous operation of the vehicle. In the past almost 50 years, substantial progress was made in both areas. Currently, most developed and developing countries are working on few of their own autonomous vehicles, and some countries are developing technology borrowed from other countries. In most cases, these systems are built on behalf of the army and perform typical military missions, although gradual autonomous vehicle technology also comes from the civilian market. For example, offshore industry started to use autonomous underwater vehicles (AUV) to support the work of drilling, which reduces labor costs in many areas of oil production.

Currently, the aim is to ensure that vehicles can realize a number of common tasks without human intervention, e.g., moving to a specified point in conditions of disruptions and restrictions of trajectory, positioning at a given point, avoiding obstacles, retrieving data about the state of the environment etc. These efforts are manifested by permanent growth in usage of autonomous vehicles in the implementation of various tasks. In such scenarios, the operator enters only superior orders, as the coordinates of the area of operation, the options of the work, orders to stop operations, etc., and the vehicle autonomously performs the task. Un-

fortunately, giving vehicles or generally any technical device, features of autonomy raises some issues. They are primarily associated with the need to "teach" machine to think logically, of course, in a limited range of the nature of the mission, as well as to make the right decisions in both typical and atypical situations. Currently, despite the attempts to give the machines features of artificial intelligence that should enable autonomous operations to a limited extent, this area is still being continuously developed, there are no concrete solutions that can be applied in real life, and there is still a lot to be done.

Autonomous vehicle technology is still being developed, which can be seen even with reports of attempts to construct biomechanical vehicles which are imitating the actions of animals or even humans. Recently a new trend has appeared: concept of many autonomous vehicles collectively working together to pursue a specific tasks and achieve a common goal. This is considered the latest trend in the development of robotics.

In this book, scientists from research institutions and universities of various countries of the world present their achievements in the field of autonomous vehicles. According to the presented messages, the impact of these vehicles on the improvement of human life is invaluable especially because of the wide field of its application. I hope that this book will provide closer insight on some of the problems related to the autonomy of various vehicles and will inspire further research in the field of robotics, in general.

Andrzej Zak
Polish Naval Academy
Poland

Chapter 1

Cloud Robotics and Autonomous Vehicles

Khuram Shahzad

Additional information is available at the end of the chapter

http://dx.doi.org/10.5772/64064

Abstract

Recently, a good amount of research has been focused on the development of the autonomous vehicles. Autonomous vehicles possess great potential in numerous challenging applications, for example, autonomous armoured fighting vehicles, automated highway systems, etc. To enable the usage of autonomous vehicles in such challenging applications, it is important to ensure the safety, efficiency, reliability and robustness of the system. Most of the existing implementations of the autonomous vehicles operate as standalone systems limited to onboard capabilities (computations, memory, data, etc.), which limit their potential and performance in real-world applications. The advent of the Internet and emerging advances in the cloud infrastructure suggests new methodologies where vehicles are not limited to onboard capabilities. Processing is also performed remotely on cloud to support different operations and to increase the proficiency of decision-making. This chapter surveys the research to date in the evolution of autonomous vehicles, cloud and cloud-enabled autonomous vehicles, with the limitations of existing systems, research challenges and possible future directions. The chapter can help new researchers in the field to understand and evaluate different approaches for the design of the autonomous vehicular systems.

Keywords: cloud robotics, cloud computing, big data, crowdsourcing, open-source, open-access, vehicular cloud

1. Introduction

The advancements in the vehicular industry have immensely benefited different related industries and served the humanity by increasing the efficiency of our routine activities. Take the example of agriculture industry, one can cultivate a piece of land so quickly (using tractors and other equipment) than compared to 100 years ago. The same applies to the transportation industry—nowadays, one can travel from one point to another so quickly compared to

travelling few decades ago. However, vehicular industry still requires further advancements to decrease/eliminate the human error/involvement. If we take the example of transportation industry, only in the USA, motor-vehicles-traffic-related injuries result in around 34,000 deaths every year, and it is the leading cause of death every year for people aged between 4 and 34 [1]. If we look worldwide, over 1.20 million people die every year as a result of road traffic accidents and between 20 and 50 million more people suffer from non-fatal injuries including physical disabilities, etc. [2]. 90 plus percent of these accidents are caused by human error [2]. Hence, a need arises for the technology that always pays attention to it, never gets distracted and has no/minimal human involvement. Such goals can be achieved through autonomous vehicles.

(a) On-Road vehicles

(b) Off-Road vehicle: Jeep

(c) Water vehicles: Submarine and battleships

(d) Aerial vehicle: Fighter Jet Lockheed Martian F-35 Lightening II

(e) Space vehicle: NASA Spaceship

(f) Amphibious vehicle: AeroMobil 3.0 © AeroMobil

Figure 1. Different types of vehicles used in real life applications for travelling in different mediums such as land, water, air and space.

http://dx.doi.org/10.5772/64064

Vehicles can be generally categorized into on road, off road, water, aerial, space and amphibious vehicles. **Figure 1(a)–(f)** shows examples of different types of vehicles from real life. On-road vehicles require paved or gravel surface for their driving. These vehicles involve sports cars, passenger cars, pickup trucks, school/passenger buses, etc. Off-road vehicles are vehicles which are capable of driving both on as well off the paved surface. These vehicles are generally characterized with deep large tires or caterpillar tracks, flexible suspension and open treads. Tractors, bulldozers, tanks, 4WD army trucks are examples of such type of vehicles. Both on-road and off-road vehicles require land as a medium of travelling. Water vehicles are vehicles which are capable of driving/travelling on water, under water or both on as well under water. Ships, boats and submarines are examples of such vehicles. Aerial vehicles are vehicles which are capable of flying in the air by gaining air support. Aeroplanes, helicopters, drone planes are examples of aerial vehicles. Space vehicles are vehicles which are capable of travelling/flying in the outer space. They are used to carry payload such as humans or satellites between the earth and the outer space. These vehicles are rocket-powered vehicles, which also require an oxidizer to operate in vacuum space. Spacecrafts and rockets are examples of space vehicles. Amphibious vehicles are vehicles, which inherit characteristics of multiple mediums of travelling and can travel in those mediums efficiently. These mediums can be land, water, air and space. AeroMobil 3.0 and LARC-V (Lighter, Amphibious Resupply, Cargo, 5 ton) are examples of amphibious vehicles.

Automation of these different types of vehicles can increase the safety, reliability, robustness and efficiency of the systems through standardization of procedural operations with minimal human intervention. With the advancements in technology, autonomous vehicles have become forefront public interest and active discussion topic recently. Based on a recent survey conducted in the USA, UK and Australia, 56.8% peoples had positive opinion, 29.4% had neutral opinion and only 13.8% had negative opinion about the autonomous or self-driving vehicles [3]. These stats give us a good picture of the general public's interest in the autonomous vehicles; however, they do have high levels of concerns regarding safety, privacy and performance issues. There are generally five levels of autonomous or self-driving vehicles ranging from Level 0 to Level 4 [4]. The brief description of these levels is as follows (taken from [4]):

- Level 0 means no automation.
- Level 1 achieves critical function-specific automation.
- Level 2 achieves combined functions automation by coordinating two or more Level 1 functions.
- Level 3 provides limited self-driven automation.
- Level 4 provides completely self-driven unmanned vehicle. The vehicle controls all its operations by itself.

These levels of automations are drafted for the on-road vehicles; however, they can be extended for the other types of vehicles. Based on a recent survey conducted in the USA, UK and Australia, 29.9% people were very concerned, 30.5% were moderately concerned, 27.5% were slightly concerned and only 12.1% people were not at all concerned about riding in a Level-4

autonomous vehicle [3]. These statistics show that major efforts are required for the usage and acceptability of the autonomous vehicles in real-world practical applications.

Autonomous vehicle is an active area of research and possesses numerous challenging applications. The earlier implementations of the autonomous vehicles and other autonomous systems were standalone implementations; rather, most of the existing implementations are still operating independently [5]. In such standalone implementations, the system is limited to the onboard capabilities such as memory, computations, data and programs, and also the vehicles cannot interact with each other or have access to each other's information or information about their surroundings [5]. To achieve Level-4 autonomous vehicles and self-driven automation in other robotic systems, it is important to overcome these limitations and go beyond the onboard capabilities of such systems. With the advent of Internet and emerging advances in the cloud robotics paradigm, new approaches have been enabled where systems are not limited to the onboard capabilities and the processing is also performed remotely on the cloud to support different operations. The cloud-based implementation of different types of vehicles has been illustrated in **Figure 2**. The cloud-based infrastructure has potential to enable a wide range of applications and new paradigms in robotics and automation systems. Autonomous vehicle is one example of such systems, which can highly benefit from cloud infrastructure and can overcome the limitations posed by standalone implementations. Cloud infrastructure enables ubiquitous, convenient and on-demand network access to a shared pool of configurable computing resources [6]. These computing resources can include services, storage, servers, networks and applications [6]. These resources can be rapidly provisioned and released with minimal service provider interaction or management effort [6]. The cloud model is characterized with five important characteristics (on-demand self-services, broad

Figure 2. Example of vehicular cloud where vehicles act as nodes to access shared pool of computing resources, including services, storage, servers, networks and applications.

http://dx.doi.org/10.5772/64064

network access, resource pooling, rapid elasticity and measured service), three service models (Software as a Service, Platform as a Service and Infrastructure as a Service, abbreviated as SaaS, PaaS and IaaS, respectively) and four deployment models (private, community, public and hybrid clouds), and see Ref. [6] for more detail.

An example of cloud-based implementation is the online document-processing facility offered by Microsoft through Office 365 and OneDrive. One can perform different operations online, such as one can create, edit and share MS Office documents (Word, Excel, PowerPoint, etc.) online without the need of installing the MS Office locally. The documents' data and software installations reside on the cloud remote servers, which can be accessed through the Internet. These servers share their computing capabilities such as processors, storage and memory. Cloud-based implementations provide economics of scale and take care of the software and hardware updates. The infrastructure also facilities backup of data as well sharing of resources across different applications and users.

Cloud-enabled robots and autonomous systems are not limited to onboard capabilities and rely on data from a cloud network to support their different operations. In 2010, James Kuffner explained the potential benefit of cloud-enabled robots and coined the term "Cloud Robotics" [7]. The vehicular industry is rapidly evolving; nowadays, vehicles are equipped with different ranges of sensors and cloud collaborations, which facilitate drivers with the desired information, for example, weather forecasts, GPS location, traffic situation on the road, road condition, directions and time to reach the destination with different alternative paths and speeds, etc. Through cloud robotics, we can develop a network of autonomous vehicles (such as vehicular cloud or Internet of vehicles), by which autonomous vehicles can collaborate with each other or can perform different computing activities that they cannot perform locally, to achieve their well-defined utility functions (e.g. timely delivery of the passengers or payload, safety, environment friendly, etc.). Google's self-driving car demonstrates the cloud-robotics-based implementation of the autonomous vehicles. It uses cloud services for the accurate localization and manoeuvring. Google tested the autonomous vehicle deployment on different types of cars including Audi TT, Lexus RX450h, Toyota Prius and their own custom vehicle [8, 9]. As of March 2016, Google had tested their autonomous self-driven vehicles a total of 1,498,214 miles (2,411,142 km) [10]. The project is limited to the on-road implementation of the autonomous vehicle; also it has many limitations that need to be addressed before it can be released to the commercial public. These limitations involve driving in heavy rain or snowy weather, driving on unmapped intersections or routes, veer unnecessarily due to difficulty in objects identification and other limitations cause of LIDAR technology to spot different signals (e.g. police officer signalling the car to stop), etc. [11, 12].

The rest of the chapter is organized as follows: In Section 2, we have presented the historical backgrounds of the evolution of autonomous vehicles, cloud computing and cloud-enabled autonomous vehicles. In this section, we have also presented different high level architectures of autonomous vehicle and cloud-enabled autonomous vehicles proposed in literature. In Section 3, we have discussed five potential benefits of cloud-enabled autonomous vehicles, namely cloud computing, big data, open-source/open-access, system learning and crowd-

sourcing. Section 4 describes active research challenges and possible future directions in the field, and conclusion appears in Section 5.

2. Historical backgrounds

Autonomous vehicle is an active area of research with rich history. The research performed in the early 1980s and 1990s on autonomous driving demonstrated the possibilities of developing vehicles that can control their movements in the complex environments [13, 14]. Initial prototypes of autonomous vehicles were limited to indoor use [15–17]. First study on visual road vehicle was performed in Mechanical Engineering Laboratory, Tsukuba, Japan, using vertical stereo cameras [18]. In the early 1980s, completely onboard autonomous vision system for vehicles was developed and deployed with digital microprocessors [13, 19]. First milestone towards the development of road vehicles with machine vision was accomplished in the late 1980s, with the fully autonomous longitudinal and lateral demonstrations of UBM's (Universität der Bundeswehr München) test vehicle and computer vision VaMoRs on a free stretch of Autobahn over 20 km at 96 km/h [13]. These encouraging results led the inclusion of computer vision for vehicles in the European EUREKA-project "Prometheus" (1987–1994) and also sparked European car industrialists and universities for research in the field [13]. The major focus of these developments was to demonstrate which functions of the autonomous vehicles could be automated through computer vision [13, 14]. The promising results of such demonstrations kicked-off many initiatives [13, 20].

The Intermodal Surface Transportation Efficiency Act (ISTEA) passed the transportation authorization bill in 1991 and instructed United States Department of Transportation (USDOT) for demonstrating an autonomous vehicle and highway system by 1997 [20, 21]. The USDOT built partnerships with academia, state, local and private sectors in conducting the program, and made extraordinary progress with revolutionizing developments in vehicle safety and information systems [21]. The USDOT program also motivated US Federal Highway Administration (FHWA) to start National Automated Highway System Consortium (NAHSC) program with different partners including California PATH, General Motors, Carnegie Mellon University, Hughes, Caltrans, Lockheed Martian, Bechtel, Parsons Brinkerhoff and Delco Electronics [20]. The Intelligent Vehicle Initiative (IVI) program was announced in 1997 and was legalized in 1998 Transportation Equity Act for the 21st Century (TEA-21), with the purpose to speed-up the development of driver-assistive systems by focusing on crash prevention rather than mitigation and vehicle-based rather than highway-based applications [22]. The IVI program resulted in a number of successful developments and deployments in the field operational tests which include different commercial applications such as lane change assist, lane departure/merge warning, adaptive cruise control, adaptive forward crash warning and vehicle stability system [22]. Commercial versions of these systems were manufactured shortly, and ever since their evolution and industrial penetration have been increasing [22].

The increasing advancements in the computational and sensing technologies have further impelled interest in the field of autonomous vehicles and developing cost-effective systems [5].

http://dx.doi.org/10.5772/64064

The present state of the art autonomous vehicles can sense their local environment, identify different objects, have knowledge about the evolution of their environment and can plan complex motion by obeying different rules. Many advancements have been made in the recent 1.5 decade, evidenced through different successful demonstrations and competitions. The most prominent historical series of such competitions/challenges were organized by US Department of Defence under Defence Advanced Research Projects Agency (DARPA). The competition was initially launched as DARPA Grand Challenge (DGC), and there are five such competitions held so far—first in March 2004, second in October 2005, third in November 2007, fourth from October 2012–June 2015 and fifth one from January–April 2013 [5, 23–25]. The fourth challenge, named as DARPA Robotics Challenge (DRC), was aimed at the development of semi-autonomous emergency maintenance ground robots [23, 25], and the fifth challenge, named as Fast Adaptable Next-Generation Ground Vehicle (FANG GV), was aimed at adaptive designs of the vehicles [24]. Both FANG and DRC were not aiming for self-driven/autonomous/robotic vehicles; hence, we have not discussed them in this chapter. In the first three challenges, hundreds of autonomous vehicles from the USA and around the world participated in the competition and exhibited their different levels of versatilities. The first and second challenges were aimed to examine vehicles' ability in off-road environment. Autonomous vehicles had to navigate in a desert up to 240 km at speed up to 80 km/h [5]. Only five vehicles were able to travel more than a mile, in the first competition. Out of those five vehicles the furthest travelling vehicle covered only 7.32 miles (11.78 km) [5]. None of the vehicles completed the route; hence, there was no winner, and the second challenge was scheduled for October 2005. By the second challenge, five vehicles were able to successfully complete the route, and Stanley from Stanford University, Palo Alto, California, secured the first place in the competition. The third challenge, named as DARPA Urban Challenge (DUC), was shifted to the urban area. The route involved 60 miles of travelling to be completed within 6 h, and vehicles had to obey all traffic regulations during their autonomous driving. Out of the 11 final teams, only 6 were able to successfully complete the route, and Boss from Carnegie Mellon University, Pittsburgh, Pennsylvania, secured the first place in the competition [5].

The participating teams in the DGC competitions adopted different types of system architectures, with standalone implementations. However, on a higher level, they decomposed the system architecture in four basic subsystems, namely, sensing, perception, planning and control (see **Figure 3** for the pictorial representation) [5]. The sensing unit takes raw measurements from different on-/off-board sensors (e.g. GPS, radar, LIDAR, odometer, vision, inertial measurement unit, etc.) for perceiving the static and dynamic environment. Sensor unit passes the raw data to the perception unit, which then generates the usable information about the vehicle (e.g. pose, map relative estimations, etc.) and its environment (e.g. lanes of other vehicles, obstacles, etc.), based on provided data. The planner unit takes the usable information/estimations from the perception unit, reasons about the provided information and plans about the vehicle's actuations in the environment, such as path, behavioural, escalation and map planning, etc. to maximize their well-defined utility functions. Finally, the planner unit passes the ultimate information/commands to the control unit, which is responsible for actuating the vehicle.

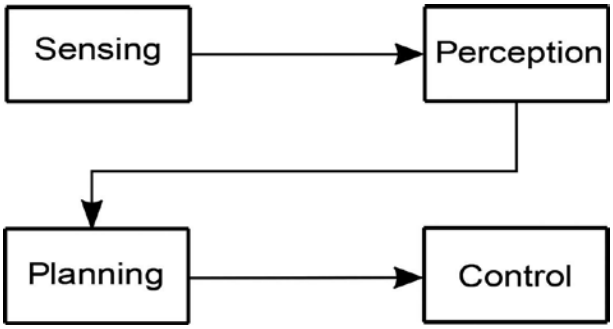

Figure 3. High-level system architecture of the autonomous vehicles.

One of the main lessons learned from the DARPA challenges was the need for the autonomous vehicles to be connected, that is, the ability to interact with each other and to have access to each other's information or information about their surroundings [5]. This also provides us some idea about the importance of cloud infrastructure in accomplishing dreams of autonomous vehicles. In the 2000s, cloud computing was evolving and came into existence. Amazon introduced its Elastic Compute Cloud (EC2) as a web service in 2006 [26]. Amazon EC2 was aimed to provide resizable computing capabilities in the cloud servers [26]. In 2008, NASA's OpenNebula become the first open-source software to provide private and hybrid clouds [27]. In the same year, Azure was announced by Microsoft, aiming to provide cloud computing services and was released in early 2010 [28]. In the mid-2010, OpenStack project was jointly launched by NASA and Rackspace Hosting, with the intentions to help organizations to set up cloud computing services (mostly IaaS) on their standard hardware [29]. Oracle Cloud was announced by Oracle in year 2012, with the aim to provide access to integrated set of IT solutions, including SaaS, PaaS and IaaS [30].

The importance of connecting machines in manufacturing automation systems through networking was realized 3.5 decades ago when General Motors developed Manufacturing Automation Protocol in 1980s [31]. Before the discovery of World Wide Web (WWW), different types of incompatible protocols were adopted by different vendors. In the early 1990s, the discovery of WWW promoted the Hypertext Transfer Protocol (HTTP) over Internet Protocol (IP) [32]. In 1994, the first industrial robot was integrated with WWW so that it can be teleoperated by different users through graphical user interface [33]. In the mid- and late-1990s different types of robots were integrated with the web to explore robustness and interface issues that initiated study in a new field named as "Network Robotics" [34, 35]. In 1997, Inaba et al. investigated the benefits of remote computing to accomplish control of remote-brained robots [36]. The technical committee on networked robotics established the IEEE robotics and automation society in 2001 [37]. The initial focus of the society was on Internet-based teleported robots which was later on extended to different range of applications [37]. In 2006, MobEyes system was proposed, which exploits vehicular sensors networks to record surrounding environment and events for the purpose of urban monitoring. RoboEarth project was announced in 2009, with the purpose to use WWW for robots, such that they can share their data and learn from each other [38]. In 2010, James Kuffner explained the concept of 'Remote

http://dx.doi.org/10.5772/64064

Brained' robots (i.e. physical separation of the robotics hardware and the software) and introduced the term "Cloud Robotics" with potential applications and benefits of cloud-enabled robots [7]. In the same year, the term "Internet of Things (IoT)" was introduced to exploit the network of physical things (e.g. vehicles, household appliances, buildings, etc.) that consists of sensors, software and ability for network connectivity for exchanging information with other objects [39]. Different vehicular ad-hoc networks (VANETs) were proposed in 2011, with the purpose to provide several cloud services for the next generation automotive systems [40, 41]. The term "Industry 4.0" was introduced in the same year for the fourth industrial revolution, with the purpose to use networking to follow the first three revolutions [42].

In 2012, M. Gerla discussed different design principles, issues and potential applications of the Vehicular Cloud Computing (VCC) [43]. In the same year, S. Kumar et al. proposed the Octree-based cloud-assisted design for autonomous driving of vehicles to assist them in planning their trajectories [44]. The high level system architecture can be visualized as presented in **Figure 4**. The purpose of sensing, planner and controller unit is same as explained for **Figure 3**, with the modification that the perception unit has been merged into the planner unit, and planner unit has been divided into two sub-units namely onboard planner and planner over cloud. Both planner units can communicate with each other to exchange desired information and for vehicle to vehicle (V2V) communication. Cloud planner can generate requests to various autonomous vehicles for providing sensors' data, which is then aggregated to generate the information about the obstacles, path planning, localization and emergency control, etc. Onboard planner unit communicates with the cloud planner for planning the optimal trajectory and passes the ultimate information to the controller unit, which then actuates the vehicle as required.

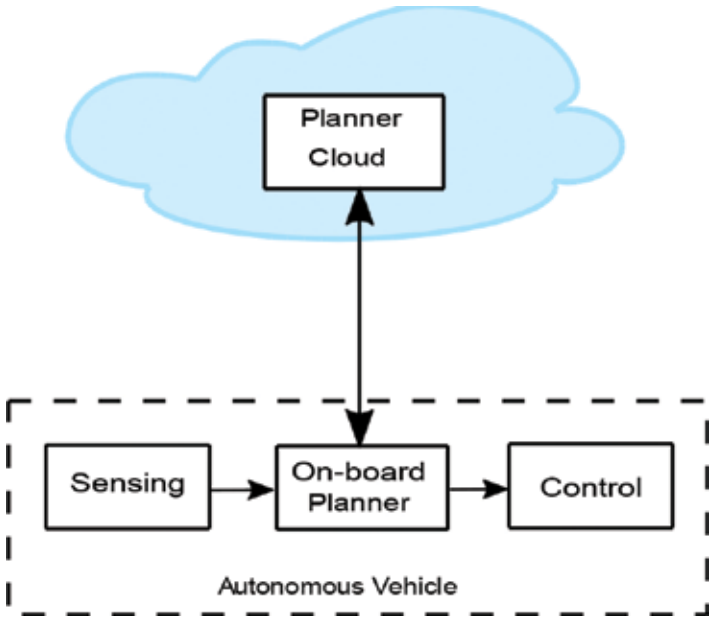

Figure 4. High-level system architecture of the cloud-assisted design of the autonomous vehicles.

In the same year 2012, the term "Industrial Internet" was introduced by General Electric, with the purpose to connect industrial equipment over network for exchanging their data [45]. In 2014, Gerla et al. investigated the vehicular cloud and deduced that it will be a core system for autonomous vehicles that will make the advancements possible [46]. In the same year, Ashutosh Saxena announced the "RoboBrain" project, with the aim to build a massive online brain for all the robots of the world from publically available internet data [47, 48]. In early 2016, HERE announced the launch of their cloud-based mapping service for autonomous vehicles, aiming to enhance automated driving features of the vehicles [49]. In February 2016, Maglaras et al. investigated the concept of Social Internet of Vehicles (SIoV), discussed its different design principles, potential applications and research issues [50].

3. Potential benefits

As discussed in the previous section, cloud-based automation has gained massive interest of researches around the world and sparked many initiatives such as RoboEarth, Remote Brained Robots, IoT, Industry 4.0, VCC Industrial Internet, RoboBrain and SIoV. In this section, we have discussed potential of cloud to enhance automation of vehicle (also applicable to all robotics automation systems in general) by improving performance though five potential benefits, as follows:

3.1. Cloud computing

Autonomous vehicles require intensive parallel computation cycles to process sensors' data and efficient path planning in the real-world environment [5]. It is certainly not practical to deploy massive onboard computing power with each agent of autonomous vehicle. Such deployments will be cost-intensive and may have certain limitations in parallel processing. Cloud provides massively parallel on demand computation, up to the computing power of super computers [51], which was previously not possible in standalone onboard implementations. Nowadays, a wide range of commercial sources (including Amazon's EC2 [26], Microsoft's Azure [28] and Google's Compute Engine [52]) are available for cloud computing services, with the aim to provide access to tens of thousands of processors for on-demand computing tasks [53]. Initially, web/mobile apps developers used such services; however, they have increasingly been used in technical high-performance applications. Cloud computing can be used for computationally extensive tasks, such as to find out uncertainties in models, sensing and controls, analysis of videos and images, generate rapidly growing graphs (e.g. RRT*) and mapping, etc. [53]. Many applications require real-time processing of computational tasks, in such applications cloud can be prone to varying network latency and quality of service (QoS), and this has been an active research area nowadays [51, 53].

3.2. Big data

Big data refers to extremely large collection of datasets that cannot be handled with conventional database systems and require analysis to find out different patterns, associations, trends,

etc. [54]. Autonomous vehicles require access to vast amount of data, for example, sensors' network data, maps, images, videos, weather forecasts, programs, algorithms, etc., which cannot be maintained on board and surpass the processing capabilities of conventional database systems. Cloud infrastructure offer access to unlimited on-demand elastic storage capacities over cloud servers that can store large collections of big data as well facilitate in their intensive computations [54–56]. Shared access of big datasets can also facilitate more accurate machine learning of autonomous vehicles, which can help the planners in optimal decision-making. It is essential to recognize that big datasets may require high-performance IaaS tools for performing intensive computations on the gigantic amount of data. These may include Amazon's EC2 [26], Microsoft's Azure [28] and Google's Compute Engine [52], as described in previous section. Active research challenges in cloud-based big data storage include defining cross platform formats, working with sparse representation for efficient processing and developing new approaches that can be more robust to dirty data [55, 56].

3.3. Open-source/open-access

Open-source refers to free access to original source code of software and models in case of hardware, which can be modified and redistributed without any discrimination [56]. Open-access refers to free access of the algorithms, publications, libraries, designs, models, maps, datasets, standards and competitions, etc. [57]. In open set-up, different organizations and researchers contribute and share such resources to facilitate their development, adoption and distribution. For standalone autonomous vehicles, it is not possible to maintain such open-source software and resources and take maximum advantages of the facilities. Cloud infrastructure facilitates by providing well-organized access to such pools of resources [6]. A prominent example of the success of the open resources in the scientific community is the Robot Operating System (ROS), which provides access to the robotics tools and libraries to facilitate the development of the robotics applications [58]. Furthermore, many simulation tools and libraries (e.g. GraspIt, Bullet, Gazebo, OpenRAVE, etc.) are available open-source and can be customized as per the application's requirement, which can certainly speed up the research and development activities.

3.4. System learning

System learning refers to collective learning of all the agents (e.g. autonomous vehicles) in the system. Autonomous vehicles need to learn from each other's experiences, for example, if a vehicle identifies a new situation that was not part of the initial system, then the learning outcome of that instance needs to be reflected in all the vehicles in the systems. Accomplishing such goals is not possible with standalone implementation of the autonomous vehicles [5]. Cloud infrastructure enables shared access on the data [6]. Instances of physical trials and new experiences are also stored in that shared pool for collective leaning of all the vehicles. Instances can hold initial and anticipated conditions, boundary conditions and outcome of the execution. A good example of collective learning is the "Lightning" framework, which indexes paths of different robots in the system over several tasks and then use cloud computing for path planning and variations in different new situations [59].

3.5. Crowdsourcing

Crowdsourcing can be defined as a process to obtain desired information, service, input or ideas on a specific task (which surpass computer capabilities) from human(s), typically over the Internet [60, 61]. In case of autonomous vehicles, crowdsourcing can be performed to solve a number of problems, for example, during operation vehicles identify new obstacles/routes which were not labelled previously and require human(s) input. Standalone implementations limit vehicles' ability for accomplishing such objectives [5]. Cloud-enabled systems facilitate in conducting crowdsourcing activities with specific or cloud crowd [61]. Cloud-based crowdsourcing has captured much attention of the researchers and industrialists/enterprises to achieve automation in their different processes [61]. A prominent example of cloud-based crowdsourcing is Amazon's Mechanical Turk (MTurk), which provides marketplace to perform tasks that surpass computer capabilities and require human intelligence [62].

4. Research challenges and future directions

In this section, we have summarized different potential research challenges and future directions for cloud-enabled autonomous vehicles.

- **Effective load balancing:** New algorithms and policies are required for balancing computations between vehicle's onboard and cloud computers.
- **Scalable parallelization:** Advancements in the cloud infrastructure are required for cloud computing parallelization scheme to scale based upon the size of autonomous vehicular system.
- **Effective sampling and scaling of data:** New algorithms and approaches are required, which scale to the size of big data and are more robust to dirty data [56].
- **Ensure privacy and security:** The data collected through different autonomous vehicles (using sensors, cams, route maps, etc.) can include potential secretes (e.g. private home data, corporate business planes, etc.), and over cloud it can be prone to theft or criminal use. Hence, privacy and security of the data over cloud needs to be ensured.
- **Ensure control and safety:** The control of autonomous vehicles over cloud can be exposed to potential hacking threats. A hacker could remotely control the vehicle and use it for unethical purpose or to cause certain damage. Hence, the control and safety of the vehicle needs to be ensured.
- **Cope with varying network latency and QoS:** For real-time applications, new algorithms and approaches are needed to handle varying network latency and QoS.
- **Fault tolerant control:** For autonomous vehicular system failures can lead to undesirable hazardous situations, hence are not acceptable. New approaches are required for onboard and cloud-based fault tolerant control.
- **Verification and validation of the system:** A primary problem for the autonomous vehicular system is the ability to substantiate that the system can operate safely, effectively

and robustly, with safety being the major concern [5]. New methods are required for verifying and validating the desired functioning of the autonomous vehicular system [5].

- **Standards and protocols:** Research in new standards and protocols is required such as to define cross platform formats of data and to work with sparse representation for efficient processing etc.
- **Crowdsourcing quality control:** Crowdsourcing has normally been prone to generating nosier/erroneous data [59]. Hence, new mechanisms are required for improving and ensuring the quality of data collected through crowdsourcing.

5. Conclusion

In this chapter, we have provided an overview of the evolution of the cloud robotics and autonomous vehicles through different phases of the history. We discussed that automation of different types of vehicles (e.g. on-road, off-road, water, aerial, space and amphibious vehicle) can increase the safety, reliability, robustness and efficiency of the system. We examined that autonomous vehicle is an active area of research with rich history, and it possesses great potential in numerous challenging applications. We analysed that the cloud robotics paradigm enabled new approaches, where autonomous vehicles are not limited to onboard capabilities and relies on data from a cloud network to support their different operations. Cloud provides economics of scale and facilitates backup and sharing of data across different agents. We also discussed potential of cloud to enhance automation of vehicles by improving performance though different potential benefits including cloud computing, big data, open-source/open-access, system learning and crowdsourcing. In the end we analysed different active research challenges and possible future directions in the field.

The chapter can help new researchers in the field to get an overview of the current state-of-the-art systems and start research activities in possible future directions. We believe that a comprehensive design of autonomous vehicular systems based on cloud infrastructure can significantly increase the reliability, robustness and safety of autonomous vehicles that can be exploited for different potential applications.

Author details

Khuram Shahzad*

Address all correspondence to: 12mscskshahzad@seecs.edu.pk

National University of Sciences and Technology (NUST), Islamabad, Pakistan

References

[1] M.D. Jiaquan Xu, B.S. Sherry, L. Murphy, M.A. Kenneth, D. Kochanek, B.S. Brigham, A. Bastian. Deaths: Final Data for 2013. NVSR. 2016;64(2). Available from: http://www.cdc.gov/nchs/data/nvsr/nvsr64/nvsr64_02.pdf [Accessed: 2016-02-21].

[2] M. Peden, R. Scurfield, D. Sleet, D. Mohan, A.A. Hyder, E. Jarawan, C. Mathers, editors. World Report on Road Traffic Injury Prevention. Geneva: World Health Organization; 2004. Available from: http://whqlibdoc.who.int/publications/2004/9241562609.pdf?ua=1 [Accessed: 2016-02-21].

[3] B. Schoettle, M. Sivak. A Survey of Public Opinion about Autonomous and Self-driving Vehicles in the US, the UK, and Australia. University of Michigan, Ann Arbor, Transportation Research Institute; 2014. Report No. UMTRI-2014-21. Available from: https://deepblue.lib.umich.edu/bitstream/handle/2027.42/108384/103024.pdf [Accessed: 2016-03-21].

[4] U.S. National Highway Traffic Safety Administration. Preliminary Statement of Policy Concerning Automated Vehicles [Internet]. 2013. Available from: http://www.nhtsa.gov/staticfiles/rulemaking/pdf/Automated_Vehicles_Policy.pdf [Accessed: 2016-03-21].

[5] M. Campbell, M. Egerstedt, J.P. How, R.M. Murray. Autonomous driving in urban environments: approaches, lessons and challenges. Philosophical Transactions of the Royal Society of London A: Mathematical, Physical and Engineering Sciences. 2010;368:4649–4672. DOI: 10.1098/rsta.2010.0110

[6] P. Mell, T. Grance. The NIST Definition of Cloud Computing. Computer Security Division, Information Technology Laboratory, National Institute of Standards and Technology Gaithersburg; 2011. Available from: http://nvlpubs.nist.gov/nistpubs/Legacy/SP/nistspecialpublication800-145.pdf [Accessed: 2016-03-21].

[7] J.J. Kuffner. Cloud-enabled Robots. IEEE-RAS International Conference on Humanoid Robotics, Nashville, TN; 2010. Available from: http://www.scribd.com/doc/47486324/Cloud-Enabled-Robots [Accessed: 2016-03-21].

[8] D. Lavrinc. Exclusive: Google Expands Its Autonomous Fleet with Hybrid Lexus RX450h [Internet]. 2012-04-16. Available from: http://www.wired.com/2012/04/google-autonomous-lexus-rx450h/ [Accessed: 2016-03-21].

[9] G. Nelson. Automotive News. Google in Talks with OEMs, Suppliers to Build Self-driving Cars [Internet]. 2015-01-14. Available from: http://www.autonews.com/article/20150114/OEM09/150119815/google-in-talks-with-oems-suppliers-to-build-self-driving-cars [Accessed: 2016-03-21].

[10] Google. Google Self-Driving Car Project Monthly Report March 2016 [Internet]. 2016-03-31. Available from: https://static.googleusercontent.com/selfdrivingcar/files/reports/report-0316.pdf [Accessed: 2016-04-01].

[11] J. Muller. No Hands, No Feet: My Unnerving Ride in Google's Driverless Car [Internet]. 2013-03-21. Available from: http://www.forbes.com/sites/joannmuller/2013/03/21/no-hands-no-feet-my-unnerving-ride-in-googles-driverless-car/#5528586261b6 [Accessed: 2016-03-21].

[12] L. Gomes. Hidden Obstacles for Google's Self-Driving Cars [Internet]. 2014-08-28. Available from: https://www.technologyreview.com/s/530276/hidden-obstacles-for-googles-self-driving-cars/ [Accessed: 2016-03-21].

[13] E.D. Dickmanns. The Development of Machine Vision for Road Vehicles in the Last Decade. Intelligent Vehicle Symposium. IEEE. 2002;1:268–281. DOI: 10.1109/IVS.2002.1187962

[14] C. Thorpe, M.H. Hebert, T. Kanade, S.A. Shafer. Vision and Navigation for the Carnegie–Mellon Navlab. IEEE Transactions on Pattern Analysis and Machine Intelligence. 1988;10(3):362–373. DOI: 10.1109/34.3900

[15] N.J. Nilsson. A Mobile Automaton: An Application of Artificial Intelligence Techniques. Proceedings of the 1st International Joint Conference on Artificial Intelligence; 1969. pp. 509–521. Available from: http://dl.acm.org/citation.cfm?id=1624562.1624607 [Accessed: 2016-03-21].

[16] D.B. Gennery. A Stereo Vision System for an Autonomous Vehicle. Proceedings of the 5th International Joint Conference on Artificial Intelligence, Cambridge, USA. 1977;2:576–582. Available from: http://dl.acm.org/citation.cfm?id=1622943.1622945 [Accessed: 2016-03-21].

[17] H.P. Moravec. The Stanford Cart and the CMU Rover. Proceedings of the IEEE. 1983;71(7):872–884. DOI: 10.1109/PROC.1983.12684

[18] S. Tsugawa, T. Yatabe, T. Hirose, S. Matsumoto. An Automobile with Artificial Intelligence. Proceedings of the 6th International Joint Conference on Artificial Intelligence, Tokyo, Japan. 1979;2:893–895. ISBN: 0-934613-47-8. Available from: http://dl.acm.org/citation.cfm?id=1623050.1623117 [Accessed: 2016-03-21].

[19] H.G. Meissner. Steuerung dynamischer Systeme aufgrund bildhafter Informationen [thesis]. Doctoral Dissertation (in German), Aerospace Department, German Armed Forces University Munich, Germany, LRT; 1982. 175 p.

[20] Transportation Research Board. National Automated Highway System Research Program: A Review. Transportation Research Board. Special Report 253; 1998. 87 p. ISBN: 030906452X.

[21] C.M. Johnson. The National ITS Program: Where We've Been and Where We're Going [Internet]. Sept/Oct 1997. Available from: https://www.fhwa.dot.gov/publications/publicroads/97septoct/p97sept6.cfm [Accessed: 2016-03-21].

[22] K. Hartman, J. Strasser. Saving Lives through Advanced Vehicle Safety Technology: Intelligent Vehicle Initiative Final Report. Federal Highway Administration, FHWA-JPO-05-057; Sep 2005. Available from: http://ntl.bts.gov/lib/jpodocs/repts_pr/14153_files/ivi.pdf [Accessed: 2016-03-21].

[23] DARPA. DARPA Robotics Challenge (Broad Agency Announcement). DARPA-BAA-12-39. 2012-04-10. Available from: http://www.androidworld.com/DARPA_Robotics_Challenge.pdf [Accessed: 2016-03-23].

[24] DARPA. DARPA Announces Winner of the First FANG Challenge [Internet]. 2013-04-22. Available from: http://www.darpa.mil/news-events/2013-04-22 [Accessed: 2016-03-23].

[25] E. Ackerman, E. Guizzo. DARPA Robotics Challenge: Amazing Moments, Lessons Learned, and What's Next [Internet]. 2015-06-11. Available from: http://spectrum.ieee.org/automaton/robotics/humanoids/darpa-robotics-challenge-amazing-moments-lessons-learned-whats-next [Accessed: 2016-03-23].

[26] Amazon. Announcing Amazon Elastic Compute Cloud (Amazon EC2) - Beta [Internet]. 2006-08-24. Available from: https://aws.amazon.com/about-aws/whats-new/2006/08/24/announcing-amazon-elastic-compute-cloud-amazon-ec2---beta/ [Accessed: 2016-04-02].

[27] B. Rochwerger, D. Breitgand, E. Levy, A. Galis, K. Nagin, I.M. Llorente, R. Montero, Y. Wolfsthal, E. Elmroth, J. Caceres, et al. The Reservoir Model and Architecture for Open Federated Cloud Computing. IBM Journal of Research and Development. 2009;53(4): 535–545. DOI: 10.1147/JRD.2009.5429058

[28] Microsoft. Windows Azure General Availability [Internet]. 2010-02-01. Available from: http://blogs.microsoft.com/blog/2010/02/01/windows-azure-general-availability/#sm.000zygf6310ttetpyqo2hls18kvmn [Accessed: 2016-04-02].

[29] Business Wire. OpenStack Launches as Independent Foundation, Begins Work Protecting, Empowering and Promoting OpenStack [Internet]. 2012-09-19. Available from: http://www.businesswire.com/news/home/20120919005997/en/OpenStack-Launches-Independent-Foundation-Begins-Work-Protecting [Accessed: 2016-04-02].

[30] T.P. Morgan. Oracle's Big Cloud Announcement, Again [Internet]. 2012-06-07. Available from: http://www.theregister.co.uk/2012/06/07/oracle_cloud_rehash_platinum_services/ [Accessed: 2016-04-02].

[31] J.D. Irwin. The Industrial Electronics Handbook. 2nd ed. CRC Press LLC, 2000 Corporate Blvd NW, Boca Raton, Florida 33431, USA; 1997. 1728 p. ISBN: 9780849383434

[32] M. Narita, S. Okabe, Y. Kato, Y. Murakwa, K. Okabayashi, S. Kanda. Reliable Cloud-based Robot Services. In: Conference of the IEEE Industrial Electronics Society. IEEE; 2013. pp. 8317–8322. DOI: 10.1109/IECON.2013.6700526

[33] K. Goldberg. Beyond the Web: Excavating the Real World via Mosaic. In: Second International WWW Conference; 1994. DOI: 10.1.1.299.6262. Available from: http://www.ieor.berkeley.edu/~goldberg/pubs/Beyond-the-Web-Excavating-Oct-1994.pdf [Accessed: 2016-04-01].

[34] K. Goldberg, B. Chen. Collaborative Control of Robot Motion: Robustness to Error. In: IEEE/RSJ International Conference; 2001. pp. 655–660. DOI: 10.1109/IROS.2001.976244

[35] G. McKee. What Is Networked Robotics? Springer, Berlin, Heidelberg; 2008. pp. 35–45. DOI: 10.1007/978-3-540-79142-3_4. Available from: http://dx.doi.org/10.1007/978-3-540-79142-3_4 [Accessed: 2016-04-01].

[36] M. Inaba. Remote-brained Robots. International Joint Conference on Artificial Intelligence; 1997. pp. 1593–1606. Available from: http://www.ijcai.org/Proceedings/97-2/Papers/118.pdf [Accessed: 2016-04-01].

[37] IEEE. IEEE Society of Robotics and Automation's Technical Committee on Networked Robots [Internet]. 2001. Available from: http://www-users.cs.umn.edu/~isler/tc/ [Accessed: 2016-04-02].

[38] M. Waibel. RoboEarth: A World Wide Web for Robots [Internet]. 2011-02-05. Available from: http://spectrum.ieee.org/automaton/robotics/artificial-intelligence/roboearth-a-world-wide-web-for-robots [Accessed: 2016-04-02].

[39] L. Atzori, A. Iera, G. Morabito. The Internet of Things: A Survey. Computer Networks. 2010;54(15):2787–2805. DOI: 10.1016/j.comnet.2010.05.010

[40] A. Iwai, M. Aoyama. Automotive Cloud Service Systems Based on Service-Oriented Architecture and Its Evaluation. In: IEEE International Conference on Cloud Computing (CLOUD); 4–9 July 2011; Washington, DC. pp. 638–645. DOI: 10.1109/CLOUD.2011.119

[41] J. Wang, J. Cho, S. Lee, T. Ma. Real Time Services for Future Cloud Computing Enabled Vehicle Networks. In: IEEE International Conference on Wireless Communications and Signal Processing (WCSP); 9–11 Nov. 2011; Nanjing. pp. 1–5. DOI: 10.1109/WCSP.2011.6096957

[42] R. Drath, A. Horch. Industrie 4.0: Hit or Hype? [Industry Forum]. IEEE Industrial Electronics Magazine. 2014;8(2):56–58. DOI: 10.1109/MIE.2014.2312079

[43] M. Gerla. Vehicular Cloud Computing. In: The 11th Annual Mediterranean on Ad Hoc Networking Workshop (Med-Hoc-Net); 19–22 June 2012; Ayia Napa. pp. 152–155. DOI: 10.1109/MedHocNet.2012.6257116

[44] S. Kumar, S. Gollakota, D. Katabi. A Cloud-assisted Design for Autonomous Driving. In: Proceedings of the First Edition of the MCC Workshop on Mobile Cloud Computing; Helsinki, Finland; ACM; 2012. pp. 41–46. DOI: 10.1145/2342509.2342519

[45] P.C. Evans, M. Annunziata. Industrial Internet: Pushing the Boundaries of Minds and Machines. General Electric. 2012. Available from: http://www.ge.com/docs/chapters/Industrial_Internet.pdf [Accessed: 2016-04-03].

[46] M. Gerla, E.K. Lee, G. Pau, U. Lee. Internet of Vehicles: From Intelligent Grid to Autonomous Cars and Vehicular Clouds. In: IEEE World Forum on Internet of Things (WF-IoT); 6–8 March 2014; Seoul. pp. 241–246. DOI: 10.1109/WF-IoT.2014.6803166

[47] A. Saxena, A. Jain, O. Sener, A. Jami, D.K. Misra, H.S. Koppula. Robobrain: Large-scale Knowledge Engine for Robots. arXiv:1412.0691. 2014; Available from: http://arxiv.org/pdf/1412.0691.pdf [Accessed: 2016-04-04].

[48] D. Hernandez. The Plan to Build a Massive Online Brain for All the World's Robots [Internet]. 2014-08-25. Available from: http://www.wired.com/2014/08/robobrain/ [Accessed: 2016-04-04].

[49] P. Pajarillo. HERE Launches Cloud-Based Mapping Service For Autonomous Vehicles [Internet]. 2016-01-05. Available from: http://www.itechpost.com/articles/17137/20160105/here-launches-cloud-based-mapping-service-for-autonomous-vehicles.htm [Accessed: 2016-04-04].

[50] L.A. Maglaras, A.H. Al-Bayatti, Y. He, I. Wagner, H. Janicke. Social Internet of Vehicles for Smart Cities. Journal of Sensor and Actuator Networks. 2016; 5(1):1–22. DOI: 10.3390/jsan5010003

[51] M. Armbrust, A. Fox, R. Griffith, A.D. Joseph, R. Katz, A. Konwinski, G. Lee, D. Patterson, A. Rabkin, I. Stoica, M. Zaharia. A View of Cloud Computing. Communication of the ACM. 2010;53(4):50–58. DOI: 10.1145/1721654.1721672

[52] O. Malik. Google Launches Amazon Rival, Compute Engine [Internet]. 2012-06-28. Available from: https://gigaom.com/2012/06/28/taking-on-amazon-google-launches-compute-on-demand-rival-to-ec2/ [Accessed: 2016-04-05].

[53] Z. Li, H. Zhang, L. O'Brien, R. Cai, S. Flint. On Evaluating Commercial Cloud Services: A Systematic Review. Journal of Systems and Software. 2013;86(9):2371–2393. DOI: 10.1016/j.jss.2013.04.021

[54] N. Marz, J. Warren. Big Data: Principles and Best Practices of Scalable Realtime Data Systems. 1st ed. Greenwich, CT, USA: Manning Publications Co.; 2015. 425 p. ISBN: 978-1617290343

[55] H. Elazhary. Cloud Computing for Big Data. MAGNT Research Report. 2014;2(4):135–144. Available from: https://www.researchgate.net/profile/Hanan_Elazhary/publication/285692839_Cloud_Computing_for_Big_Data/links/56629d4e08ae192bbf8e241f.pdf [Accessed: 2016-04-06].

[56] Robotics Virtual Organization. A Roadmap for U.S. Robotics: From Internet to Robotics 2013 Edition. Presented to Congressional Robotics Caucus; 2013. Available from: https://robotics-vo.us/sites/default/files/2013%20Robotics%20Roadmap-rs.pdf [Accessed: 2016-04-10].

[57] E.M. Corrado. The Importance of Open Access, Open Source, and Open Standards for Libraries. Issues in Science and Technology Librarianship. 2005;42:1092–1206. DOI: 10.5062/F42F7KD8

[58] M. Quigley, K. Conley, B. Gerkey, J. Faust, T. Foote, J. Leibs, R. Wheeler, A.Y. Ng. ROS: An Open-source Robot Operating System. In: ICRA Workshop on Open Source Software; 2009. Available from: http://pub1.willowgarage.com/~konolige/cs225B/docs/quigley-icra2009-ros.pdf [Accessed: 2016-04-06].

[59] D. Berenson, P. Abbeel, K. Goldberg. A Robot Path Planning Framework That Learns from Experience. In: IEEE International Conference on Robotics and Automation (ICRA); 14–18 May 2012; Saint Paul, MN. 2012. pp. 3671–3678. DOI: 10.1109/ICRA.2012.6224742

[60] M. Lease. On Quality Control and Machine Learning in Crowdsourcing. In: Workshops at the Twenty-Fifth AAAI Conference on Artificial Intelligence; 2011. Available from: http://www.aaai.org/ocs/index.php/WS/AAAIW11/paper/viewFile/3906/4255 [Accessed: 2016-04-07].

[61] M. Vukovic. Crowdsourcing for Enterprises. In: Congress on Services – I; 2009. DOI: 10.1109/SERVICES-I.2009.56

[62] Amazon. Introduction to Amazon Mechanical Turk [Internet]. 2014-08-15. Available from: http://docs.aws.amazon.com/AWSMechTurk/latest/AWSMechanicalTurkGettingStartedGuide/SvcIntro.html [Accessed: 2016-04-10].

Chapter 2

Application of Sampling-Based Motion Planning Algorithms in Autonomous Vehicle Navigation

Weria Khaksar, Khairul Salleh Mohamed Sahari and Tang Sai Hong

Additional information is available at the end of the chapter

http://dx.doi.org/10.5772/64730

Abstract

With the development of the autonomous driving technology, the autonomous vehicle has become one of the key issues for supporting our daily life and economical activities. One of the challenging research areas in autonomous vehicle is the development of an intelligent motion planner, which is able to guide the vehicle in dynamic changing environments. In this chapter, a novel sampling-based navigation architecture is introduced, which employs the optimal properties of RRT* planner and the low running time property of low-dispersion sampling-based algorithms. Furthermore, a novel segmentation method is proposed, which divides the sampling domain into valid and tabu segments. The resulted navigation architecture is able to guide the autonomous vehicle in complex situations such as takeover or crowded environments. The performance of the proposed method is tested through simulation in different scenarios and also by comparing the performances of RRT and RRT* algorithms. The proposed method provides near-optimal solutions with smaller trees and in lower running time.

Keywords: autonomous vehicle, motion planning, sampling-based planning, optimality, low runtime

1. Introduction

As information technology and artificial intelligence develop rapidly, it is becoming possible to use computers to assist daily driving, even to make the driving process entirely autonomous. Due to the recent research advances in robotics and intelligent transportation systems, autonomous vehicles have attracted dramatic attentions in the past decades [1].

An important milestone has been reached in the field of autonomous driving on the urban road, which can be seen in DARPA Urban Challenge (DUC) [2]. As an important achievement in the progress of autonomous vehicle, the suggested vehicle navigation systems in DUC have been well accepted as the instruction for the design process of autonomous vehicle systems [3, 4]. The majority of the available architectures for autonomous vehicle focused on autonomous driving in structured roads and unstructured parking environments, and thus the performance of these proposals for more complicated driving scenarios is not clear, and despite interesting solutions for this problem in the literature, it is still a basic challenge to design an efficient motion planner for navigation in dynamic and cluttered environments where high number of obstacles, extensive effects of failure and safety considerations make it even more challenging [1].

One of the challenging research areas in autonomous vehicle is the development of an intelligent motion planner that is able to guide the vehicle in dynamic changing environments. Motion planning is an essential and fundamental part of autonomous vehicle [5], which can find solutions for the problem of finding a set of control values or feasible motion states for the vehicle to manoeuvre among obstacles from a given initial configuration towards a final one, taking into account the vehicle's kinematic and dynamic systems [6]. Furthermore, the traffic regulations and the available information on the geometric structures of roads are also included in the motion planning for autonomous driving.

Motion planning can be considered as one of the basic challenges within robotics sciences which have been studied by many researchers over the past few decades resulting in different algorithms with various specifications. Motion planning for an autonomous vehicle is a procedure to find a path from an initial position to a final state, while avoiding any collision with obstacles. In the simplest form of motion planning problem, which is called the piano mover's problem, the running time of each algorithm is exponentially the degrees of freedom, which indicates that the path-planning problem is NP-Complete. It is also shown that the motion planner needs memory exponential in the degrees of freedom, which proves that the problem is PSPACE-Complete [7].

When the environment is not known for the robot, the path planning is called online, local or sensor-based. During the past few decades, online path planning has been a challenging but attractive field for many robotic researchers. In unknown environments, there are two main aspects. First, the motion decisions are based on local information, and second, sensing is contemporaneous to the decision-making process. In this class of path planning, the robot acquires the information via its sensors that could be touch or vision sensors [8].

The field of sensor-based path planning has been studied by many researchers resulting in various algorithms with different characteristics. One of the earliest and simplest online path-planning algorithms is the Bug algorithm [9] that acquires information from touch sensors and guides the robot to the goal through the boundaries of obstacles. An extension of the classic Bug algorithm is Tangent Bug [10], which incorporates vision sensor information with the algorithm. A performance comparison between different Bug-like algorithms can be found in [11]. Despite interesting performances of the conventional motion planning methods in

http://dx.doi.org/10.5772/64730

robotics, their efficiency in navigation of autonomous vehicle is considerably low due to the complex and unstable dynamics of such systems.

Another well-known class of path-planning algorithms is sampling-based path planning. In this class of algorithms, the only source of information is a collision detector, and hence, there is no need to characterize all possible collision situations. Sampling-based methods operate several strategies for creating samples in free space and for connecting them with collision-free paths in order to provide a solution for path-planning problem. Three of the more popular sampling-based approaches include probabilistic roadmap (PRM) [12], randomized potential fields (RPFs) [13] and rapidly exploring random trees (RRTs) [14]. PRM approach finds collision-free samples in the environment and adds them to a roadmap graph. Afterwards, by using a cost function, best samples are chosen in the graph and a simple local path planner is used to connect them together. RPFs approach builds a graph by connecting the local minimums of the potential function defined in the environment. Then, the planner searches this graph for paths. RRTs are specially proposed to deal with non-holonomic constraints and high degrees of freedom. This approach builds a tree by randomly choosing a node in the free space and finding the nearest node in the tree. Next, the planner expands this nearest node in the direction of the random node. Several extension of RRT for solving sensor-based path-planning problems has been proposed. In [15], a new data structure called sensor-based random tree (SRT) is proposed, which represents a roadmap of the visited area. Similar to the RRT, the SRT is a tree of already visited nodes with a local safe region. The tree is increasingly expanded towards a random direction. An improvement of RRT is proposed in [16]. This method directs the robot in an RRT-derived direction while avoiding collision. In [17], two heuristics are added to the RRT to handling unknown environments. The first heuristic checks if the goal is reachable from the current position of the robot. The second heuristic tries to avoid the robot from getting close to the obstacles. Despite interesting solutions for this problem in the literature, it is still a basic challenge to design an efficient motion planner for navigation in dynamic and cluttered environments where high number of obstacles, extensive effects of failure and safety considerations make it even more challenging. Due to the interesting advantages and properties of sampling-based motion planning algorithms, they seem to be efficient and powerful tools for autonomous vehicle navigation. In this chapter, a novel motion planning architecture is proposed for autonomous vehicle navigation, which employs recent advances in sampling-based motion planning. The resulted approach is capable of planning safe and efficient motions in different situations such as following the course of the road, overtaking the front vehicle and following the front vehicles while overtaking is not possible. The proposed architecture employs the optimal strategy proposed in RRT* planner [18] to avoid meandering paths. The proposed planner also utilizes a unique low-dispersion strategy [19] to reduce the running time of the planner which is essential in autonomous vehicle navigation. The rest of the chapter is organized as follows. In Section 2, the category of sampling-based motion planning algorithms is summarized. The existing applications of sampling-based planners in autonomous vehicle navigation are reviewed in Section 3. Then, the proposed architecture is introduced in Section 3, supported by the simulation studies in Section 4. Finally, discussion and conclusion is provided in Section 5.

2. Sampling-based motion planning

Naturally, offline path-planning algorithms need a complete map of the configuration space which usually increases the cost and runtime of the search in most problems. Sampling-based motion planning was proposed to solve navigation queries without trying to construct the map of the entire configuration space. Instead, they only depend on a procedure that decides on whether a given configuration of the robot is in collision with obstacles or not. The available sampling-based path-planning algorithms can be categorized into two main classes, namely, roadmap-based or multi-query algorithms and tree-based or single-query algorithms [19]. Roadmap-based algorithms are normally applicable in multi-query scenarios as they form a graph that later will be used to solve different navigation problems. The graph is the main structure used for saving the environmental information, where the nodes represent different configurations in the robot's configuration space. An edge exist between any two configurations if the corresponding geometrical properties satisfy a set of conditions such as vicinity, and the autonomous agent can navigate from one point to another without any collision. A typical algorithm consists of two main stages: learning or observation stage and search stage. In the first stage, the graph structure is constructed. Collision-free positions or samples are chosen randomly and considered as the vertices of the graph. In the search stage, each vertex is tested to be connected to the closest neighbour configurations, and the resulted successful connection will be an edge in the roadmap. To answer a given planning task, the initial and final configurations are added to the existing graph and a normal search technique is considered for finding the shortest path. The most important factor in the efficiency of the algorithm is how effectively the roadmap can learn the free-space connectivity of the configuration space. In addition, the main problem in the performance of such algorithm is the construction of the graph because the search algorithms usually perform satisfactory in terms of speed and runtime. The original form of PRM planner consists of the following steps. First, a random configuration is selected from the configuration space and is tested if it lies in the free configuration space. If the sample passes this, it will be included in the roadmap structure as a vertex or a node. Second, a search technique takes place to find the closest neighbours in the graph to the new node. Finally, a local planner attempts to connect the closest neighbour and the new configurations based on criteria posed by the planning query. This connection will be added to the graph as a new edge if it is collision free. In several situations, quickly finding a solution for a particular problem is the main objective. In these situations, single-query algorithms can be implemented. In these algorithms, the base of the data structure is normally a tree. The basic idea is to find an initial configuration (the starting configuration) that is the root of the tree and all incrementally generated configurations will be connected to other configurations already included in the tree. The initial tree-based algorithm is the rapidly exploring random tree (RRT) planner [20]. Started to grow from the start configuration, a tree continuously grows in the free configuration space until it gets close enough to the final configuration. An essential feature of this planner is that configurations with larger Voronoi regions (i.e. the part of the free configuration space that is closer to that node than to other members of the tree) have higher chances to be selected in the process of tree expansion. Therefore, the tree normally grows towards yet unknown parts of the environment, circumfusing rapidly in the free

http://dx.doi.org/10.5772/64730

configuration space. The initial version of the RRT consists of the following steps. First, a random sample is generated in the free search environment. Then, the planner searches the tree for a particular configuration, which is the nearest node to this newly generated sample. Next, a new node is created by moving a predefined distance from in the direction of the selected node using a local planner or an interpolation technique that relies on the robotic system. And, finally, if the new node is a valid point that falls in free configuration space, and if the local path between it and the nearest node is collision free, then, the new node is added to the tree as a new node and an edge is created between the tree and the new node. This process is repeated until the goal configuration can be connected to the tree or a maximum number of iterations are reached.

One of the key issues in sampling-based planners is that they usually result in undesirable lengthy resulted paths that stray within the free configuration space. Recently, the RRT planner has been proven not to be able to find the optimum answer [18]. Thus, the optimal improved forms of original sampling-based algorithms, i.e. PRM* and RRT*, have been proposed and proven to possess the asymptotical optimality in which the chance of generating the optimum path approaches unity as the cardinality of the generated structure approaches infinity. The RRT* planner contains a unique ability which is the sufficiency to find the optimal path from the start position to any configuration within the free space [18]. **Figure 1** shows the performance of PRM* and RRT* algorithms in a 2D indoor environment.

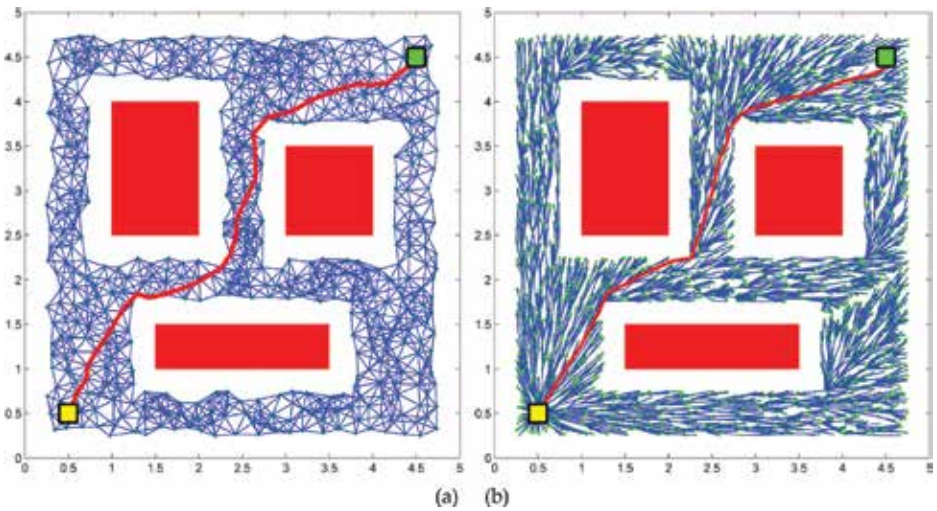

Figure 1. Performances of (a) PRM* and (b) RRT* algorithms in a simple 2D environment. Start and goal configurations are shown by yellow and green squares, respectively.

3. Related work

Over the past two decades, sampling-based motion planning algorithms have attracted the attention of researchers in the field of autonomous vehicle resulting in various approaches

with different advantages and drawbacks. In this section, some of the well-known past applications of sampling-based methods in autonomous vehicle navigation is summarized.

In one of the first reports of such applications, a probabilistic planning process has been proposed to deal with dynamic systems in dealing with static and dynamic obstacles [21]. This planner evaluates the dynamic limitations of the vehicle's movement and provides a steady and solid decoupling between low-level control and motion planning at the same time. This planning method maintains the convergence characteristics of its kinematic peers. The safety of the system is also considered in the form of finite running times by checking the behaviour of the planner when the existed embedded computational resources are moderate, and the motion generation process must take place in real time. This method is capable of dealing with vehicles if their dynamics are defined by ordinary differential equations or even by other hybrid complex representations [22].

A detailed analysis of the motion planning subsystem for the MIT DARPA Urban Challenge [2] vehicle based on the rapidly exploring random tree (RRT) algorithm has been provided [22]. The purpose was to present the numerous extensions made to the standard RRT algorithm that enables the online use of RRT on robotic vehicles with complex, unstable dynamics and significant drift, while preserving safety in the face of uncertainty and limited sensing.

A real-time motion planning algorithm has been introduced based on the rapidly exploring random tree (RRT) approach for autonomous vehicle operating in an urban environment [23]. For several motivations, such as the need to generate dynamically feasible plans in real time, safety requirements and the constraints dictated by the uncertain operating (urban) environment, several extensions to the standard RRT planner have been considered.

A rapidly exploring random tree (RRT) based on path planner has been implemented for autonomous vehicle parking problem, which treats all the situations in a unified manner [24]. As the RRT method sometimes generates some complicated paths, a smoothing sub-process has also been implemented for smoothing generated paths.

The use of rapidly exploring random trees (RRT) for the planning of multiple vehicles in traffic scenarios has been proposed [25]. According to this method, the controller for each car uses RRT to produce a navigation plan. Spline curves are used for smoothing the route resulted from the RRT, which includes non-holonomic constraints. Priority is taken into consideration as a coordination method where a vehicle with higher priority attempts to avoid all lower priority vehicles. This algorithm attempts to find the maximum possible velocity at which the vehicle can travel and the corresponding path.

Time-efficient manoeuvres for an off-road vehicle taking tight turns with high speed on a loose surface have been studied using the RRT* planner [26]. The experimental results have shown that the aggressive skidding manoeuvre, normally known as the trail-braking manoeuvre, naturally rises from the RRT* planner as the minimum-time path. Along the way, the RRT* planner has been extended to deal with complicated dynamical systems, such as systems that are explained by nonlinear differential equations and include high-dimensional state spaces, which may be of independent interest. The RRT* has also been exploited as an anytime computation framework for nonlinear optimization problems.

http://dx.doi.org/10.5772/64730

An efficient motion planning method for on-road driving of the autonomous vehicle has been reported based on the rapidly exploring random tree (RRT) algorithm [27]. To address the issue and taking into account the realistic context of on-road autonomous driving, they have proposed a fast RRT planner that utilizes a rule-template set according to the traffic scenes and an aggressive extension strategy for searching the tree. Both justification result in a faster and more accurate RRT planner towards the final state compared with the original RRT algorithm. Meanwhile, a model-based post-process estimation approach has been taken into account, where the resulted paths can be more smoothed and a feasible control sequence for the vehicle would be prepared. Furthermore, in the cases with moving obstacles, a combined method of the time-efficient RRT algorithm and the configuration-time space has been used to improve the quality of the resulted path and the re-planning.

A human-RRT (rapidly exploring random tree) collaborative algorithm has been presented for path planning in urban environments [28]. The well-known RRT algorithm has been modified for efficient planning in cluttered yet structured urban environments. To engage the expert human knowledge in dynamic re-planning of autonomous vehicle, a graphical user interface has been developed that enables interaction with the automated RRT planner in real time. The interface can be used to invoke standard planning attributes such as way areas, space constrains and waypoints. In addition, the human can draw desired trajectories using the touch interface for the RRT planner to follow. Based on new information and evidence collected by human, state-dependent risk or penalty to grow paths based on an objective function can also be specified using the interface.

An online motion planner has been proposed based on the drivers' visual behaviour-guided rapidly exploring random tree (RRT) approach that is valid for on-road driving of autonomous vehicle [29]. The main contribution of this work is the implementation of a guidance system for drivers' visual search behaviour in the form of the RRT navigation algorithm. RRT usually performs poorly in various planning situations such as on-road driving of autonomous vehicles because of the uncanny trajectory, wasteful sampling and low-speed exploration strategy. In order to overcome these drawbacks, they have proposed an extension of the RRT planner that utilizes a powerful supervised sampling strategy according to the drivers' on-road behaviour in visual search and a continuous-curvature smoothing technique based on B-spline.

A sampling-based planning technique for planning manoeuvring paths for semi-autonomous vehicle has been reported where the autonomous driving system may be taking over the driver operation [30]. They have used rapidly exploring random tree star (RRT*) and have proposed a two-stage sampling strategy and a particular cost function to adjust RRT* to semi-autonomous driving, where, besides the standard goals for autonomous driving such as collision avoidance and lane maintenance, the deviations from the estimated path planned by the driver are accounted for. They have also proposed an algorithm to remove the redundant waypoints of the path returned by RRT*, and, by applying a smoothing technique, our algorithm returns a G-squared continuous path that is suitable for semi-autonomous vehicles.

Despite the great effort that has been put to employ sampling-based methods for autonomous vehicle navigation, there are still some problems with the performance of the current methods.

For instance, there is no proper method for takeover which is one of the most common behaviours in driving. Takeover is a complicated and critical task that sometimes is not avoidable and the motion planner should be able to plan takeovers while considering the safety issues. Furthermore, the running time of the planner is usually too high which makes the method less practical. Finally, the quality of the generated solutions, i.e. paths, is a critical issue. The quality of the resulted paths from sampling-based methods is normally low and finding the optimal path is usually a challenging task in randomized algorithms.

4. Proposed approach

In this work, a new sampling-based motion planner is introduced for autonomous vehicle navigation. The proposed method is based on the optimality concept of the RRT* algorithm [18] and the low-dispersion concept of the LD-RRT algorithm [19]. Furthermore, this planner utilizes a novel procedure that divides the sampling domain based on the updates received from the vehicle's sensory system.

$V \leftarrow \{q_{start}\}$
$E \leftarrow \emptyset$
For $i = 1, \dots, n$ **Do**
  $q_{rand} \leftarrow Collision\_Free\ Sample$
  $q_{nearest} \leftarrow Nearest\ \{(V, E), q_{rand}\}$
  $q_{new} \leftarrow Steer(q_{nearest}, q_{rand})$
  If$(q_{nearest}, q_{new}) is\ Collision\_Free$ **Then**
  $Q_{neighbor} \leftarrow Neighbor\{(V, E), q_{new}, \min(r^*(n), step)\}$
  $V \leftarrow V \cup q_{new}$
  $q_{min} \leftarrow q_{nearest}$
  $Cost_{min} \leftarrow Cost(q_{nearest}) + Cost(q_{nearest}, q_{new})$
  For All$q_{neighbor} \in Q_{neighbor}$ **Do**
  If $(q_{neighbor}, q_{new}) is\ Collision\_Free$ **AND**
  $Cost(q_{neighbor}) + Cost(q_{neighbor}, q_{new}) < Cost_{min}$ **Then**
  $q_{min} \leftarrow q_{neighbor}$
  $Cost_{min} \leftarrow Cost(q_{neighbor}) + Cost(q_{neighbor}, q_{new})$
  $E \leftarrow E \cup \{(q_{min}, q_{new})\}$
  For All$q_{neighbor} \in Q_{neighbor}$ **Do**
  If$(Q_{neighbor}, q_{new}) is\ Collision\_Free$ **AND**
  $Cost(q_{new}) + Cost(q_{new}, q_{neighbor}) < Cost(q_{neighbor})$ **Then**
  $q_{parent} \leftarrow Parent(q_{neighbor})$
  $E \leftarrow (E \backslash \{(q_{parent}, q_{neighbor})\}) \cup \{(q_{new}, q_{neighbor})\}$
Return(V, E)

Algorithm 1. RRT* Planner

The first component of the proposed planner is the RRT* algorithm that can be described in **Algorithm 1**.

http://dx.doi.org/10.5772/64730

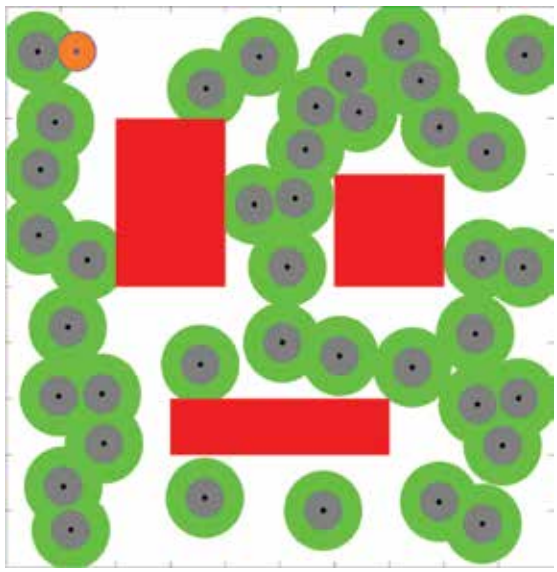

Figure 2. The implementation of the boundary sampling in a simple 2D environment with three obstacles. The new sample (orange circle) will be generates on the boundary of the union of forbidden region after the occurrence of the first rejection.

In the RRT* algorithm, the important recoveries can be seen in Algorithm 1, where an edge is added to the tree only if it can be connected to the latest generated point through a set of path segments with minimal cost. Then, if other nodes exist in the vicinity of the current node with better costs, these nodes will take the position of the parent for the current node. These improvements facilitate the RRT* algorithm with the unique capability of finding the optimal solution. **Figure 2** shows the optimality behaviour of the RRT* algorithm in an empty environment.

The second component of the proposed method is the low-dispersion properties of the LD-RRT planner. This component utilizes the poison disk sampling strategy to reduce the number of samples required to capture the connectivity of the sampling domain. The proposed method performance is similar to the PRM*/RRT* algorithms with a basic different in the sampling technique. Unlike the original planners that would let any collision-free samples to be included in the tree, the proposed method contains an extra checking procedure that makes sure that the samples possess the Poisson-disk distribution property.

There are various efficient techniques for creating fast Poisson-disk structures. In this research, the boundary sampling technique [31] is selected for generating the Poisson-disk samples for its simplicity and implementation facility. In this method, the existing neighbourhood of all samples reduces to a set of spheres located at the sample's position with the radius of r^s. The first result of such arrangement is that the existing neighbourhood can be represented by a set of spherical ranges at which a point can be placed on the boundary. **Figure 3** shows the sampling phase as proposed in [31] where the Poisson disks and the forbidden sampling areas are illustrated by grey and green circles, respectively. After the first rejection, the boundary of

the union of the forbidden areas will be selected and a random sample is generated accordingly as shown by the orange circle. The sampling radius is defined as follows:

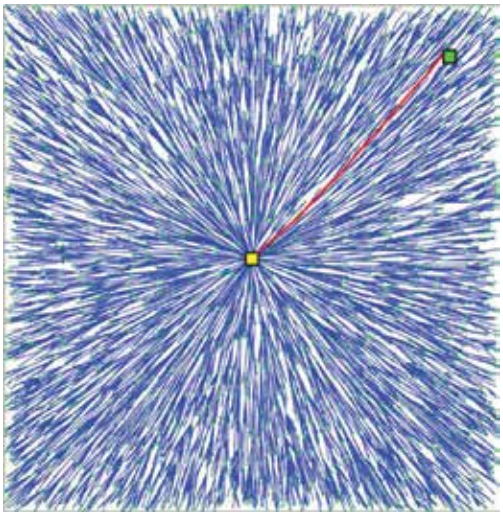

Figure 3. The optimal behaviour of RRT* algorithm in a planar empty environment.

1	$V \leftarrow \{q_{start}\}$
2	$E \leftarrow \emptyset$
3	**For** $i = 1, \ldots, n$ **Do**
4	$q_{rand} \leftarrow Collision_{Free} Sample,\ r^s(n)$
5	$q_{nearest} \leftarrow Nearest\ \{(V, E), q_{rand}\}$
6	$q_{new} \leftarrow Steer(q_{nearest}, q_{rand})$
7	**If**$(q_{nearest}, q_{new}) is\ Collision\_Free$ **Then**
8	$Q_{neighbor} \leftarrow Neighbor\{(V, E), q_{new}, \min(r^*(n), step)\}$
9	$V \leftarrow V \cup q_{new}$
10	$q_{min} \leftarrow q_{nearest}$
11	$Cost_{min} \leftarrow Cost(q_{nearest}) + Cost(q_{nearest}, q_{new})$
12	**For All**$q_{neighbor} \in Q_{neighbor}$ **Do**
13	**If** $(q_{neighbor}, q_{new}) is\ Collision\_Free$ **AND** $Cost(q_{neighbor}) + Cost(q_{neighbor}, q_{new}) < Cost_{min}$ **Then**
14	$q_{min} \leftarrow q_{neighbor}$
15	$Cost_{min} \leftarrow Cost(q_{neighbor}) + Cost(q_{neighbor}, q_{new})$
16	$E \leftarrow E \cup \{(q_{min}, q_{new})\}$
17	**For All**$q_{neighbor} \in Q_{neighbor}$ **Do**
18	**If**$(Q_{neighbor}, q_{new}) is\ Collision\_Free$ **AND** $Cost(q_{new}) + Cost(q_{new}, q_{neighbor}) < Cost(q_{neighbor})$ **Then**
19	$q_{parent} \leftarrow Parent(q_{neighbor})$
20	$E \leftarrow (E \backslash \{(q_{parent}, q_{neighbor})\}) \cup \{(q_{new}, q_{neighbor})\}$
21	**Return**(V, E)

Algorithm 2. The proposed asingle–uery algorithm

http://dx.doi.org/10.5772/64730

$$r^s(n) \le \tau\sqrt{Q_{\text{free}}/n} \tag{1}$$

where τ is a scaling coefficient ranging within (0, 1]. The main idea behind this radius is that the volume of the space should be approximately equal to $n(r^s)^2$ in order to fill an obstacle-free square space with n disks with radius r^s. Compelling the samples to follow the Poisson-disk distribution usually decreases the cardinality of the resulted graph. In other words, it is almost impossible to find n samples with $\tau\sqrt{Q_{\text{free}}/n}$ distance from one another with a randomized sample generator. Upon the generation of the Poisson-disk samples, the algorithm will follow normal steps in the original PRM*/RRT*. The pseudo code of the proposed algorithms can be seen in **Algorithm 2**.

As can be seen in Algorithm 2, the Poisson-disk sampling takes place at line 4 by forcing the generated samples to satisfy the sampling radius rule. The rest of both algorithms are same as the originals. The relevance between the neighbourhood and sampling radii is an important index about the performance of the proposed algorithm. It is essential for the sampling radius to be smaller than the connection radius. Otherwise, it will not be possible to connect any two samples and the resulted structure will be a set of separate configurations. **Figure 4** shows the relation between these two radii along with the ratio of $r^s(n)$ over $r^*(n)$.

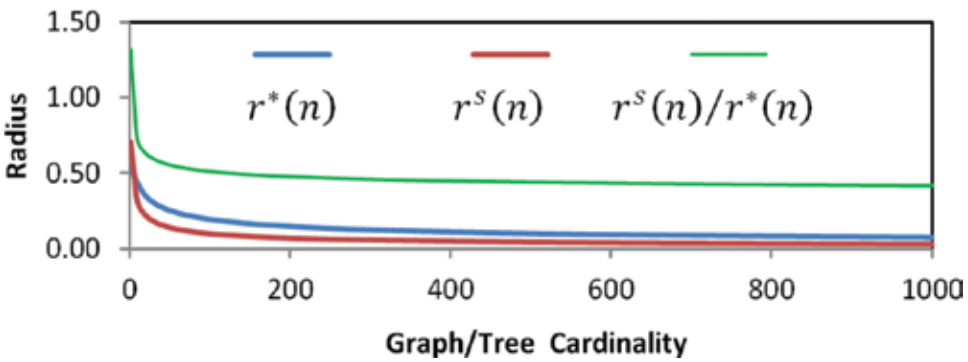

Figure 4. Different values for neighbourhood and sampling radii and the corresponding ratio for $\mu(Q_{\text{free}}) = 1$ and $\tau = 1$. For $n \ge 4$, the neighbourhood radius is always greater than the sampling radius.

According to the definitions of neighbourhood and sampling radii, the cardinality of the graph/tree should follow the following rule:

$$n \ge 10^{\pi\tau^2/6} \tag{2}$$

This requirement ensures that there will be at least one eligible sample within the neighbourhood region of the current sample. Considering the acceptable range of τ, i.e. (0, 1], the sampling radius in a 2D configuration space is smaller than the neighbourhood radius if and only if the number of samples exceeds four.

Another important property of the proposed planner takes place in the RRT* algorithm where the steering factor in the original RRT*, which is 'step', will be automatically replaced by the sampling radius. As stated before, the samples will be created randomly from the perimeter of the current Poisson disks. As a result, the highest distance between any two samples exactly equals the sampling radius $r^s(n)$. As stated before, the cost of the final optimum solution can be calculated as the total Euclidean distance between all members (nodes) of the optimum path which can be calculated as follows:

$$c\left(\omega^*\right) = \sum_{i=1}^{n^*} \| \, \omega_{i+1}^* - \omega_i^* \, \| \tag{3}$$

where n^* is the number of nodes in the optimal path resulted from the algorithm. Considering the fact that $\left\|\omega_{i+1}^* - \omega_i^*\right\| < r^s(n)$, now it is possible to find an upper bound for the path of the optimal solution:

$$c\left(\omega^*\right) = \sum_{i=1}^{n^*} \| \, \omega_{i+1}^* - \omega_i^* \, \| \tag{4}$$

This upper bound merely depends on the size of the final graph/tree structure. On the other hand, reducing the total number of samples (n), will reduce the number of samples in any solution. Therefore, it can be concluded that using a Poisson-disk distribution as the sampling domain will improve the cost of the final solution and maintains the asymptotic optimality property of the proposed algorithm. **Figure 5** illustrates the graph construction phase for the PRM* planner.

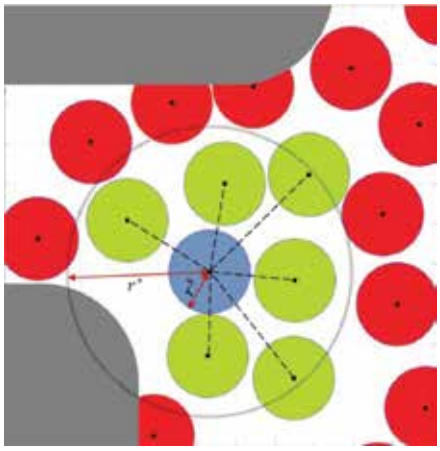

Figure 5. The connection strategy in the proposed algorithm.

http://dx.doi.org/10.5772/64730

The next component of the proposed method is a novel procedure that divides the sampling domain into different sampling segments based on the information received online from the sensory system of the vehicle. The proposed approach divides the sampling domain into two regions namely tabu region and valid region. The sampling procedure takes place only in the valid region and the tabu region is forbidden to be included in the sampling. **Figure 6** shows different possibilities of tabu and valid segments in a sampling domain.

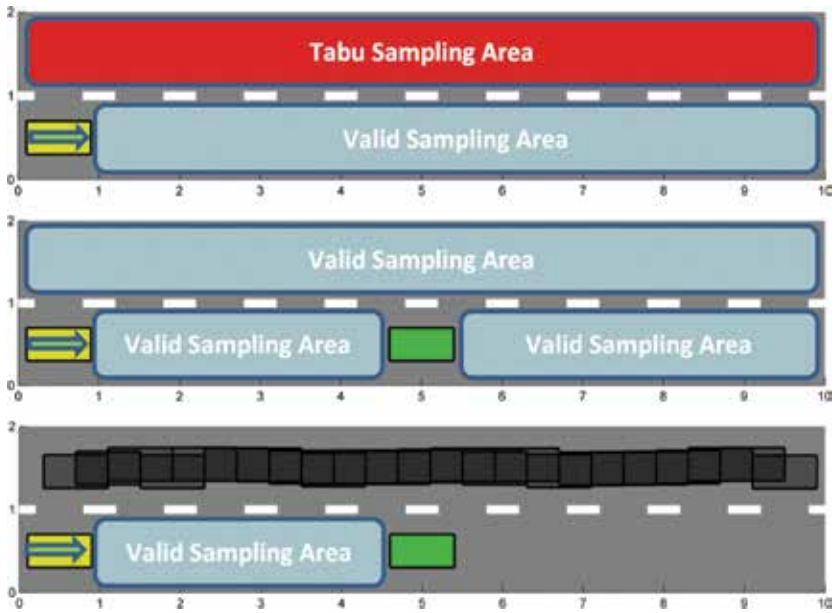

Figure 6. The performance of the segmentation procedure. The sampling domain is divided into different valid or tabu segments.

Three different scenarios have been considered in the simulation studies. In the first one, there is no vehicle in front of the autonomous car and the sampling domain is only the current lane. In the second situation, there is a vehicle in front but takeover is possible and the valid sampling region is expanded to include proper space for the takeover. Finally, when takeover is not possible, the valid sampling domain is restricted to the available space between the two vehicles.

5. Simulation studies

According to the properties of the proposed algorithm, three different situations have been designed for simulation studies. **Figure 7** depicts an instance of the solutions in these scenarios. The proposed method is able to plan difficult motions for the vehicle such as following or takeover. As can be seen in **Figure 7**, when there are no other vehicles, the planner restricts the sampling domain to the current lane and other parts of the road are not included in the sampling procedure. When there is another car in front but takeover is not an option, the

generated rapidly exploring random tree just follows the front vehicle with a proper distance. Finally, when takeover is possible, the sampling domain will be expanded to include suitable space.

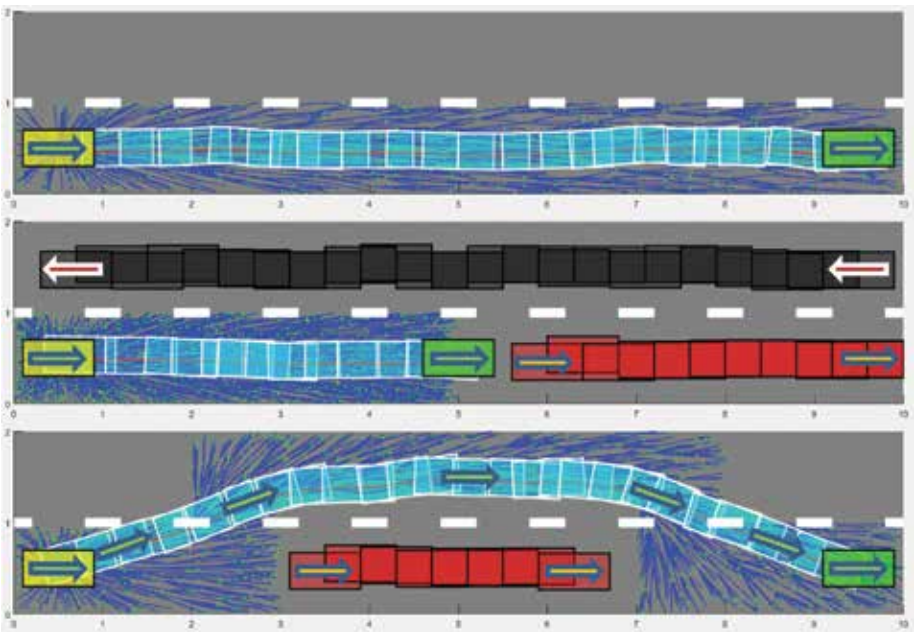

Figure 7. Simulation results in different scenarios. The initial and final positions of the vehicle are shown by yellow and green, respectively.

The average results of the performance of the proposed planner as well as the performances of RRT and RRT* planners are shown in **Table 1**.

Scenario	Variable	RRT	RRT*	Proposed algorithm
Free drive	Average number of samples	314.2	203.7	138.8
	Average optimality (%)	63.4	93.8	93.9
	Average runtime (s)	87.6	114.0	48.3
Takeover	Average number of samples	627.2	808.5	316.4
	Average optimality (%)	50.7	91.4	91.4
	Average runtime (s)	134.2	168.9	93.5
Follow	Average number of samples	223.1	418.5	108.8
	Average optimality (%)	68.6	93.5	93.4
	Average runtime (s)	73.5	108.6	46.4

Table 1. Simulation average results for the proposed algorithm, RRT and RRT* planners.

http://dx.doi.org/10.5772/64730

As can be seen, the proposed planner provides optimal solutions with surprisingly smaller set of samples. The runtime of the planner is also less than other planners. **Figure 8** shows the variations of performance variables for 1000 iterations of each planner.

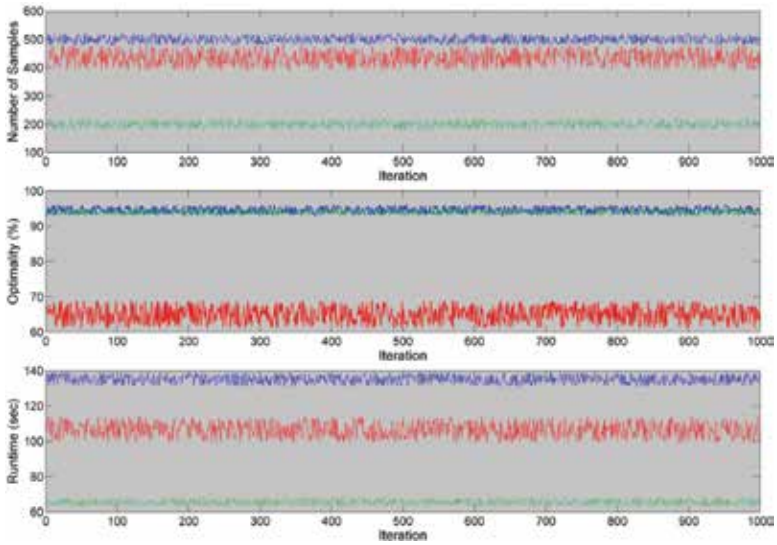

Figure 8. Variation of the results over 1000 iterations for the proposed algorithm (green), RRT (red) and RRT* (blue) in terms of the number of nodes, optimality (%) and runtime (s).

6. Conclusion

In this chapter, a novel sampling-based navigation architecture has been introduced that is capable of driving autonomous vehicles in crowded environments. The proposed planner utilizes the optimal behaviour of the RRT* algorithm combined with the low runtime requirements of low-dispersion sampling-based motion planning. Furthermore, a novel segmentation procedure is introduced which differentiates between valid and tabu segments of the sampling domain in different situations.

Simulation results show the robust performance of this planner in different scenarios such as following the front car and takeover. This method also outperforms the classical RRT and RRT* planners in terms of runtime and the size of the generated tree while maintaining the same optimality rate as RRT*.

Acknowledgements

This research was supported by the Malaysia Fundamental Graduate Research Scheme (FRGS) under grant no. FRGS/2/2014/TK06/UNITEN/02/7.

Author details

Weria Khaksar[1*], Khairul Salleh Mohamed Sahari[1] and Tang Sai Hong[2]

*Address all correspondence to: weria@uniten.edu.my

1 Centre of Advanced Mechatronics and Robotics (CAMARO), College of Engineering, National Energy University (UNITEN), Kajang, Selangor, Malaysia

2 Department of Mechanical and Manufacturing Engineering, Faculty of Engineering, University Putra Malaysia (UPM), Serdang, Malaysia

References

[1] W. Liu, Z. Weng, Z. Chong, X. Shen, S. Pendleton, and B. Qin, et al., "Autonomous vehicle planning system design under perception limitation in pedestrian environment," in *2015 IEEE 7th International Conference on Cybernetics and Intelligent Systems (CIS) and IEEE Conference on Robotics, Automation and Mechatronics (RAM)*, 2015, pp. 159–166.

[2] C. Urmson, J. Anhalt, D. Bagnell, C. Baker, R. Bittner, and M. Clark, et al., "Autonomous driving in urban environments: boss and the urban challenge," *Journal of Field Robotics*, 25, 425–466, 2008.

[3] J. Markoff, "Google cars drive themselves, in traffic," *The New York Times*, 10, 9, 2010.

[4] A. Broggi, P. Medici, E. Cardarelli, P. Cerri, A. Giacomazzo, and N. Finardi, "Development of the control system for the vislab intercontinental autonomous challenge," in *2010 13th International IEEE Conference on Intelligent Transportation Systems (ITSC)*, 2010, pp. 635–640.

[5] H. Cheng, Autonomous Intelligent Vehicles: Theory, Algorithms, and Implementation. Springer-Verlag London, 2011.

[6] T. M. Howard, M. Pivtoraiko, R. A. Knepper, and A. Kelly, "Model-predictive motion planning: Several key developments for autonomous mobile robots," *IEEE Robotics & Automation Magazine*, 21, 64–73, 2014.

[7] J. Canny, The Complexity of Robot Motion Planning. MIT Press, Cambridge, Massachusetts, 1988.

[8] N. S. Rao, S. Kareti, W. Shi, and S. S. Iyengar, Robot Navigation in Unknown Terrains: Introductory Survey of Non-heuristic Algorithms. Technical Report ORNL/TM-12410, Oak Ridge National Laboratory, 1993.

[9] A. V. J. Lumelsky and A. A. Stepanov, "Path-planning strategies for a point mobile automaton moving amidst unknown obstacles of arbitrary shape," *Algorithmica*, 2, 403–430, 1987.

[10] A. Kamon, E. Rimon, and E. Rivlin, "Tangentbug: a range-sensor-based navigation algorithm," *The International Journal of Robotics Research*, 17, 934–953, 1998.

[11] J. Ng and T. Bräunl, "Performance comparison of bug navigation algorithms," *Journal of Intelligent and Robotic Systems*, 50, 73–84, 2007.

[12] L. E. Kavraki, P. Švestka, J.-C. Latombe, and M. H. Overmars, "Probabilistic roadmaps for path planning in high-dimensional configuration spaces," *IEEE Transactions on Robotics and Automation*, 12, 566–580, 1996.

[13] J. Barraquand and J.-C. Latombe, "Robot motion planning: a distributed representation approach," *The International Journal of Robotics Research*, 10, 628–649, 1991.

[14] S. M. LaValle, "Rapidly-exploring random trees: a new tool for path planning, 1998.. Technical Report TR 98-11, Department of Computer Science; Iowa State University, 1993.

[15] G. Oriolo, M. Vendittelli, L. Freda, and G. Troso, "The SRT method: randomized strategies for exploration," in *2004 IEEE International Conference on Robotics and Automation, 2004. Proceedings. ICRA'04*, 2004, pp. 4688–4694.

[16] L. Chang-an, C. Jin-Gang, L. Guo-Dong, and L. Chun-Yang, "Mobile robot path planning based on an improved rapidly-exploring random tree in unknown environment," in *IEEE International Conference on Automation and Logistics, 2008. ICAL 2008*, 2008, pp. 2375–2379.

[17] J. Nieto, E. Slawinski, V. Mut, and B. Wagner, "Online path planning based on rapidly-exploring random trees," in *2010 IEEE International Conference on Industrial Technology (ICIT)*, 2010, pp. 1451–1456.

[18] S. Karaman and E. Frazzoli, "Sampling-based algorithms for optimal motion planning," *The International Journal of Robotics Research*, 30, 846–894, 2011.

[19] W. Khaksar, T. S. Hong, M. Khaksar, and O. Motlagh, "A low dispersion probabilistic roadmaps (LD-PRM) algorithm for fast and efficient sampling-based motion planning," International Journal of Advanced Robotic Systems, 10, 397, pp. 1-10, 2013.

[20] J. J. Kuffner and S. M. LaValle, "RRT-connect: an efficient approach to single-query path planning," in *IEEE International Conference on Robotics and Automation, 2000 Proceedings, ICRA'00*, 2000, pp. 995–1001.

[21] E. Frazzoli, M. A. Dahleh, and E. Feron, "Real-time motion planning for agile autonomous vehicles," *Journal of Guidance, Control, and Dynamics*, 25, 116–129, 2002.

[22] Y. Kuwata, G. A. Fiore, J. Teo, E. Frazzoli, and J. P. How, "Motion planning for urban driving using RRT," in *IEEE/RSJ International Conference on Intelligent Robots and Systems, 2008. IROS 2008*, 2008, pp. 1681–1686.

[23] Y. Kuwata, S. Karaman, J. Teo, E. Frazzoli, J. P. How, and G. Fiore, "Real-time motion planning with applications to autonomous urban driving," *IEEE Transactions on Control Systems Technology*, 17, 1105–1118, 2009.

[24] L. Han, Q. H. Do, and S. Mita, "Unified path planner for parking an autonomous vehicle based on RRT," in *2011 IEEE International Conference on Robotics and Automation (ICRA)*, 2011, pp. 5622–5627.

[25] R. Kala, and K. Warwick, "Planning of multiple autonomous vehicles using RRT," in *2011 IEEE 10th International Conference on Cybernetic Intelligent Systems (CIS)*, 2011, pp. 20–25.

[26] J. H. Jeon, S. Karaman, and E. Frazzoli, "Anytime computation of time-optimal off-road vehicle maneuvers using the RRT*," in *2011 50th IEEE Conference on Decision and Control and European Control Conference (CDC-ECC)*, 2011, pp. 3276–3282.

[27] L. Ma, J. Xue, K. Kawabata, J. Zhu, C. Ma, and N. Zheng, "Efficient sampling-based motion planning for on-road autonomous driving," *IEEE Transactions on Intelligent Transportation Systems*, 16, 2015, 1961–1976.

[28] S. S. Mehta, C. Ton, M. J. McCourt, Z. Kan, E. Doucette, and W. Curtis, "Human-assisted RRT for path planning in urban environments," in *2015 IEEE International Conference on Systems, Man, and Cybernetics (SMC)*, 2015, pp. 941–946.

[29] M. Du, T. Mei, H. Liang, J. Chen, R. Huang, and P. Zhao, "Drivers' visual behavior-guided RRT motion planner for autonomous on-road driving," *Sensors*, 16, 102, 2016.

[30] X. Lan and S. Di Cairano, "Continuous curvature path planning for semi-autonomous vehicle maneuvers using RRT," in *2015 European Control Conference (ECC)*, 2015, pp. 2360–2365.

[31] D. Dunbar, and G. Humphreys, "A spatial data structure for fast Poisson-disk sample generation," *ACM Transaction Graphic*, 25(3), 503–508, 2006.

Chapter 3

Robust Accelerating Control for Consistent Node Dynamics in a Platoon of CAVs

Feng Gao, Shengbo Eben Li and Keqiang Li

Additional information is available at the end of the chapter

http://dx.doi.org/10.5772/63352

Abstract

Driving as a platoon has potential to significantly benefit traffic capacity and safety. To generate more identical dynamics of nodes for a platoon of automated connected vehicles (CAVs), this chapter presents a robust acceleration controller using a multiple model control structure. The large uncertainties of node dynamics are divided into small ones using multiple uncertain models, and accordingly multiple robust controllers are designed. According to the errors between current node and multiple models, a scheduling logic is proposed, which automatically selects the most appropriate candidate controller into loop. Even under relatively large plant uncertainties, this method can offer consistent and approximately linear dynamics, which simplifies the synthesis of upper level platoon controller. This method is validated by comparative simulations with a sliding model controller and a fixed $\mathbf{H}_\infty$ controller.

Keywords: automated connected vehicles (CAVs), platoon control, acceleration control, robustness, multi-model

1. Introduction

The platoon driving of automated connected vehicles (CAVs) has considerable potential to benefit road traffic, including increasing highway capacity, less fuel/energy consumption and fewer accidents [1]. The R&D of CAVs has been accelerated with increasing usage of wireless communication in road transportation, such as dedicated short range communications (DSRC). Pioneering studies on how to control a platoon of CAVs can date back to 1990s, and as pointed out by Hedrick et al. , the control topics of a platoon can be divided into two tasks [2, 3]: (1) to implement control of platoon formation, stabilization and dissolution; and (2) to carry out

controls for throttle/brake actuators of each vehicle [4]. These naturally lead to a hierarchical control structure, including an upper level controller and a lower level controller [5, 6]. The upper one is to retain safe and string stable operation, whereas the lower one is to track the desired acceleration by determining throttle/brake commands.

The upper level control of a platoon of CAVs has been investigated extensively. An earlier work done by Shladover [2] introduced many known control topics, among which the most famous is the concept of string stability. The string stability ensures that range errors decrease as propagating along downstream [7]. Stankovic et al. [8] proposed a decentralized overlapping control law by using the inclusion principle, which decomposes the original system into multiple ones by an appropriate input/state expansion. Up to now, many other upper level control topics have already been explored, including the influence of spacing policies, information flow topologies, time delay and data loss of wireless communications, etc.

The lower level controller determines the commands for throttle and/or brake actuators. The lower level controller, together with vehicle itself, actually plays the role of node dynamics for upper level control. Many research efforts have been attempted on acceleration control in the past decades, but still few gives emphasis on the request of platoon level automation. Most platoon control relies on one critical assumption that the node dynamics are homogeneous and approximately linear. Then, the node dynamics can be described by simple models, e.g. double-integrator [9, 10] and three-order model [3, 7, 8, 11]. This requires that the behaviour of acceleration control is rather accurate and consistent, which is difficult to be achieved. One is because the salient non-linearities in powertrain dynamics, both traditional [12, 13] and hybridized [14], and any linearization, will lead to errors; the other is that such uncertainties as parametric variations and external disturbances significantly affect the consistence of control behaviour.

One of the major issues of acceleration control is how to deal with non-linearities and uncertainties. The majority to handle non-linearities are to linearize powertrain dynamics, including exact linearization [15, 16], Taylor linearization [17] and inverse model compensation [12, 18]. Fritz and Schiehlen [15, 16] use the exact linearization technique to normalize node dynamics for synthesis of cruising control. After linearization, a pole placement controller was employed to control the exactly linearized states. The Taylor expansion approach has been used by Hunt et al. [17] to approximate the powertrain dynamics at equilibrium points. The gain-scheduling technique was then used to conquer the discrepancy caused by linearization. The inverse model compensation is widely used in engineering practice, for example [12] and [19]. This method is implemented by neglecting the powertrain dynamics. For the uncertainties, the majority rely on robust control techniques, including sliding model control (SMC) [19], $\mathbf{H}_\infty$ control [20, 21], adaptive control [22–24], fuzzy control [25, 26], etc. Considering parametric variations, an adaptive SMC was designed by Swaroop et al. [19] by adding an on-line estimator for vehicle parameters, such as mass, aerodynamic drag coefficient and rolling resistance. Higashimata and Adachi [20] and Yamamura and Seto [21] designed a Model Matching Controller (MMC) based controller for headway control. This design used an $\mathbf{H}_\infty$ controller as feedback and a forward compensator for a faster response. Xu and Ioannou [23] approximated vehicle dynamics to be a first-order transfer function at equilibrium points, and

http://dx.doi.org/10.5772/63352

then the Lyapunov approach was used to design an adaptive thriller controller for tracking control of vehicle speed. Keneth et al (2008) designed an adaptive proportional-integral (PI) controller for robust tracking control in resistance to parametric variations. The adaptive law is designed by using the gradient algorithm [24]. The aforementioned robust controllers are useful to resist small errors and disturbances in vehicle longitudinal dynamics, but might not be always effective for large uncertainties. Moreover, the use of adaptive mechanism is only able to resist slowly varying uncertainties, but difficult to respond fast varying disturbances, e.g. instantaneous wind.

2. Node dynamic model for control

This chapter proposes a robust acceleration control method for consistent node dynamics in a platoon of CAVs. This design is able to offer more consistent and approximately linear node dynamics for upper level control of platoons even under large uncertainties, including vehicle parametric variation, varying road slop and strong environmental wind. The controlled node in the platoon is a passenger car with a 1.6 L gasoline engine, a 4-speed automatic transmission, two driving and two driven wheels, as well as a hydraulic braking system. **Figure 1** presents the powertrain dynamics. Its inputs are the throttle angle $\boldsymbol{\alpha_{thr}}$ and the braking pressure $\boldsymbol{P_{brh}}$. Its outputs are the longitudinal acceleration $\boldsymbol{a}$, vehicle velocity $\boldsymbol{v}$, as well as other measurable variables in the powertrain. When driving, the engine torque is amplified by the automatic transmission, final gear, and then acts on two frontal driving wheels. When braking, the braking torque acts on four wheels to dissipate the kinetic energy of vehicle body.

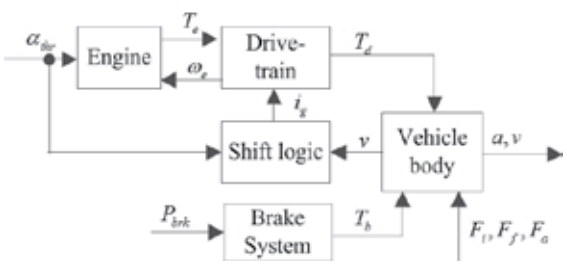

Figure 1. Vehicle longitudinal dynamics.

2.1. Vehicle longitudinal dynamics

For the sake of controller design, it is further assumed that (1) the dynamics of intake manifold and chamber combustion are neglected, and overall engine dynamics are lumped into a first-order inertial transfer function; (2) the vehicle runs on dry alphabet roads with high road-tyre friction, and so the slip of tire is neglected; (3) the vehicle body is considered to be rigid and symmetric, without vertical motion, yaw motion and pitching motion; (4) the hydraulic braking system is simplified to a first-order inertial transfer function without time delay. Then, the mathematical model of vehicle longitudinal dynamics is

$$
\begin{aligned}
&T_{es} = \mathbf{MAP}\left(\omega_e, \alpha_{thr}\right), T_e = \frac{1}{\tau_e s + 1} T_{es}, J_e \dot{\omega}_e = T_e - T_p, \\
&T_p = C_{TC} \omega_e^2, T_t = K_{TC} T_p, T_d = \eta_T i_g i_0 T_t, \omega_t = i_g i_0 \frac{v}{r_w}, \\
&M\dot{v} = \frac{T_d}{r_w} - \frac{T_b}{r_w} - F_i - F_a - F_f, T_b = \frac{K_b}{\tau_b s + 1} P_{brk}, F_i = Mg \cdot \sin(\varphi), \\
&F_a = \text{sign}\left(v + v_{wind}\right) C_A \left(v + v_{wind}\right)^2, F_f = Mg \cdot f,
\end{aligned}
\tag{1}
$$

where ω_e is the engine speed, T_{es} is the static engine torque, τ_e is the time constant of engine dynamics, T_e is the actual engine torque, $\mathbf{MAP}_{(.,.)}$ is a non-linear tabular function representing engine torque characteristics, T_p is the pump torque of torque converter (TC), J_e is the inertia of fly wheel, T_t is the turbine torque of TC, C_{Tc} is the TC capacity coefficient, K_{TC} is the torque ratio of TC, i_g is the gear ratio of transmission, i_o is the ratio of final gear, η_T is the mechanical efficiency of driveline, r_w is the rolling radius of wheels, M is the vehicle mass, T_d is the driving force on wheels, T_b is the braking force on wheels, v is the vehicle speed, F_i is the longitudinal component of vehicle gravity, F_a is the aerodynamic drag, F_f is the rolling resistance, K_b is the total braking gain of four wheels, τ_b is the time constant of braking system, C_A is the coefficient of aerodynamic drag, g is the gravity coefficient, f is the coefficient of rolling resistance, ϕ is the road slope and v_{wind} is the speed of environmental wind. The nominal values of vehicle parameters are shown in **Table 1**.

Symbol	Units	Nominal value
M	Kg	1300
J_e	kg·m^2	0.21
η_T	–	0.89
τ_e	Sec	0.3
i_o	–	4.43
i_g	–	[2.71, 1.44, 1, 0.74]
r_w	M	0.28
K_b	N·m/MPa	1185
τ_b	Sec	0.15
C_A	kg/m	0.2835
f	–	0.02
g	m/s^2	9.81

Table 1. Nominal parameters of vehicle model.

http://dx.doi.org/10.5772/63352

2.2. Inverse vehicle model

One major challenge of acceleration control is the salient non-linearities, including engine static non-linearity, torque converter coupling, discontinuous gear ratio, quadratic aerodynamic drag and the throttle/brake switching. These non-linearities can be compensated by an inverse vehicle model. The inverse models of engine and brake are described by Eqs. (2) and (3), respectively [22, 31]. The design of the inverse model assumes that (i) engine dynamics, torque converter coupling, etc. is neglected; (ii) vehicle runs on dry and flat road with no mass transfer; (iii) the inverse model uses nominal parameters in **Table 1**.

$$T_{\text{edes}} = \frac{r_w}{i_g i_0 \eta_T}\left(Ma_{\text{des}} + C_A v^2 + Mgf\right), \alpha_{\text{thrdes}} = \text{MAP}^{-1}\left(\omega_e, T_{\text{edes}}\right), \tag{2}$$

$$F_{\text{bdes}} = Ma_{\text{des}} + C_A v^2 + Mgf, P_{\text{brkdes}} = \frac{1}{K_b} F_{\text{bdes}}, \tag{3}$$

where a_{des} is the input for the inverse model, which is the command of acceleration control, T_{edes}, α_{thrdes}, F_{bdes} and P_{brkdes} are corresponding intermittent variables or actuator commands. Note that throttle and braking controls cannot be applied simultaneously. A switching logic with a hysteresis layer is required to determine which one is used. The switching line for separation is not simply to be zero, i.e. $a_{\text{des}} = 0$, because the engine braking and the aerodynamic drag are firstly used, and followed by hydraulic braking if necessary. Therefore, the switching line is actually equal to the deceleration when coasting, shown in **Figure 2**. The use of a hysteresis layer is to avoid frequent switching between throttle and brake controls.

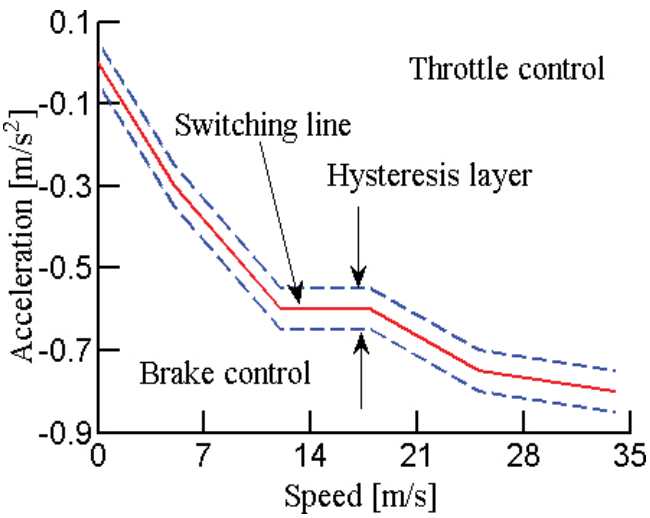

Figure 2. Switching between throttle and brake controls.

3. MMS-based acceleration control

The Multi Model Switching (MMS) control is an efficient way to control plants with large model uncertainties and linearization errors, especially sudden changes in plant dynamics [27–30]. The overall range of plant dynamics is covered by a set of models instead of a single one, and then a scheduling logic switches the most appropriate controller into the control loop. The speed of adaptation and transient performance can be significantly improved by the instantaneous switching among candidate controllers [29, 30]. Another benefit of MMS control is its potential to enclose the input-output behaviours to a required small range. **Figure 3** shows the MMS control structure for vehicle acceleration tracking, where $\boldsymbol{a}_{\mathbf{des}}$ and $\boldsymbol{a}$ are the desired and actual longitudinal acceleration respectively, $\boldsymbol{\alpha}_{thrdes}$ and $\boldsymbol{P}_{brkdes}$ are throttle angle and braking pressure respectively, which are the control inputs of a vehicle. It consists of the vehicle itself (**V**), the inverse model (**I**), a supervisor (**S**) and a controller set (**C**). The inverse model **I** is used to compensate for the non-linearities of powertrain; **I** and **V** together constructs the plant for MMS control. The combination of **I + V** tends to have large uncertainties, but is divided into small ones under the MMS structure. Such a configuration is able to maintain a more accurate and consistent input–output behaviour even under a large model mismatch.

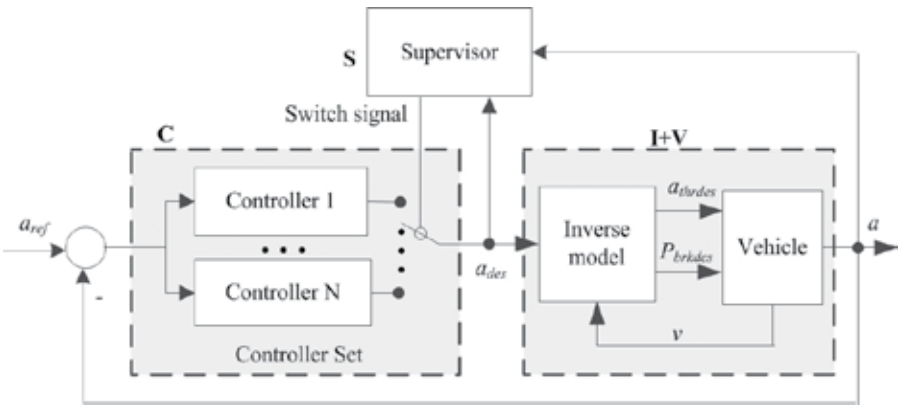

Figure 3. MMS control of vehicle acceleration.

3.1. Model set to separate large uncertainty

For the MMS control, **I** and **V** are combined together to form a new plant, whose input is desired acceleration and output is actual acceleration. Its major uncertainties arise from the change of operating speed, i.e. $v \in \mathbb{R}^1$, the parameter variation, i.e. $\theta = [M,\ \eta_T,\ \tau_e,\ K_b] \in \mathbb{R}^4$. and the external disturbance, i.e. $d = [\varphi,\ v_{\text{wind}}] \in \mathbb{R}^2$. Their uncertain range is $v \in [v_{\min},\ v_{\max}]$, $\theta \in [\theta_{\min},\ \theta_{\max}]$ and $d \in [d_{\min},\ d_{\max}]$. The main idea is to use multiple linear models, i.e. $P_i(s)$, $i = 1,\ \cdots,\ N$, to separate such large uncertainties into small ones, and accordingly design multiple feasible $\mathbf{H}_\infty$ controllers, i.e. $C_i(s)$, $i = 1,\ \cdots,\ N$, for each model with smaller uncertainty.

http://dx.doi.org/10.5772/63352

The range of vehicle speed, $v \in \mathbb{R}$, is equally divided into five points, i.e. $\left(v_{\min}, \frac{3v_{\min}+v_{\max}}{4}, \frac{2v_{\min}+2v_{\max}}{4}, \frac{v_{\min}+3v_{\max}}{4}, v_{\max}\right)$, and the range of $\theta \in \mathbb{R}^4$ and $d \in \mathbb{R}^2$ are each separated into three points, i.e. $\left(\theta_{\min}, \frac{\theta_{\min}+\theta_{\max}}{2}, \theta_{\max}\right)$, and $\left(d_{\min}, \frac{d_{\min}+d_{\max}}{2}, d_{\max}\right)$, respectively. Their combination is set as a candidate for model identification. Totally, there are $5\times3^{(4+2)}=3465$ candidate models. The 3465 models can be straightforwardly regarded as a multiple model set. Its shortcoming is that some of these models are quite closed to each other, which naturally leads to many redundant controllers (a waste of computing and storage resources). To reduce the model number, some close models are grouped and covered by an uncertain model. Hence, these 3465 models are clustered into four groups, which are covered with four uncertain models $P_i(s)$, $i=1, \cdots, N$, shown in **Figure 4**.

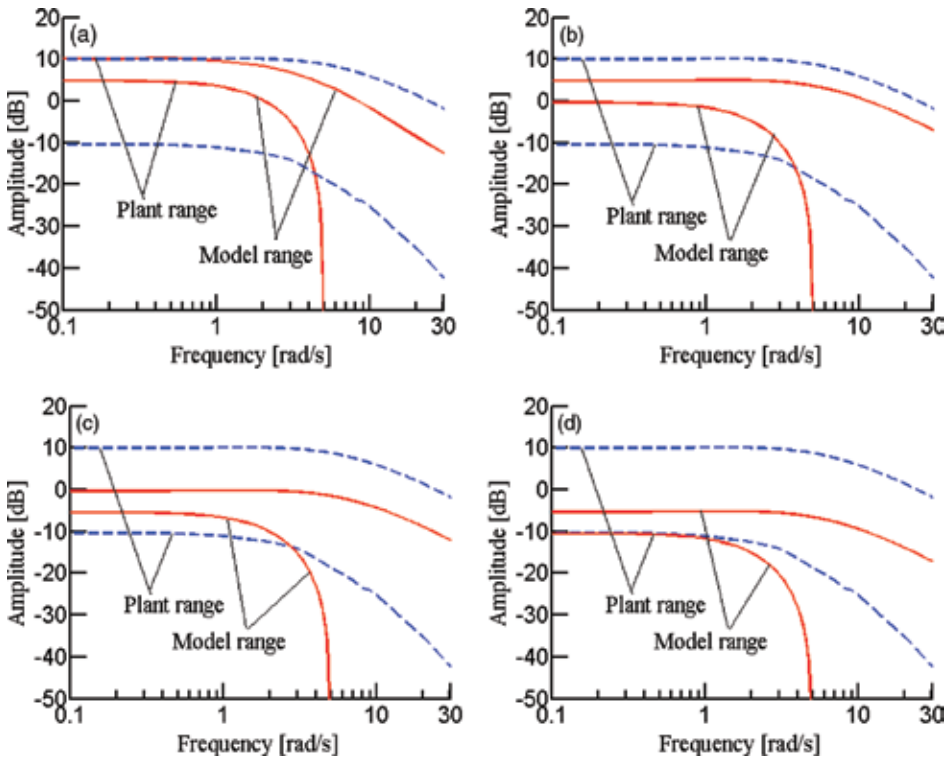

Figure 4. Frequency responses of four linear models. (a) Model $P_1(s)$, (b) Model $P_2(s)$, (c) Model $P_3(s)$ and (d) Model $P_4(s)$.

The model set $\mathbf{P}=\{P_i(s), i=1, \cdots, N\}$ is defined to have identical structure with a multiplicative uncertainty:

$$P_i(s) = G_i(s)\left[1+\Delta_i W(s)\right], G_i(s) = k_{Gi}\left(s+p_G\right)^{-1}, i=1\cdots N, \tag{4}$$

where $G_i(s)$ is the nominal models listed in **Table 2**, $W(s)$ is the weight function for uncertainty, Δ_i is the model uncertainty, satisfying:

$$\left\|\Delta_i\right\|_\infty^\delta < 1, i = 1 \cdots N, \tag{5}$$

where $\|\cdot\|_\infty^\delta$ is the induced norm of $\mathbf{L}_2^\delta$ norm of signals expressed as

$$\left\|\mathbf{x}(t)\right\|_2^\delta = \sqrt{\int_0^t \mathrm{e}^{-\delta(t-\tau)} \left|\mathbf{x}(t)\right|^2 d\tau}, \tag{6}$$

where $\delta > 0$ is a forgetting factor, and $\mathbf{x}(t)$ is a vector of signals.

No.	1	2	3	4
$G_i(s)$	$\frac{8.15}{s + 3.333}$	$\frac{4.5}{s + 3.333}$	$\frac{0.75}{s + 3.333}$	$\frac{0.22}{s + 3.333}$

Table 2. Nominal models of node dynamics.

3.2. Synthesis of the MMS controller

The main idea of this chapter is to use multiple uncertain models to cover overall plant dynamics, and so the large uncertainty is divided into smaller ones. Because the range of dynamics covered by each model is reduced using multiple models, this MMS control can greatly improve both robust stability and tracking performance of vehicle acceleration control. This MMS controller includes a scheduling logic **S**, multiple estimators **E** and multiple controllers **C**. The module **E** is a set of estimators, which is designed from model set **P** and to estimate signals a and z. Note that z is the disturbance signal arising from model uncertainty and it cannot be measured directly. The module **S** represents the scheduling logic. Its task is to calculate and compare the switching index of each model $J_i (i = 1, \cdots, N)$, which actually gives a measure of each model uncertainty compared with current vehicle dynamics. **S** chooses the most proper model (with smallest measure) and denoted as σ. The module **C** contains multiple robust controllers, also designed from **P**. The controller whose index equals σ will be switched into loop to control acceleration. The signal a_{ref} is the desired acceleration.

The scheduling logic is critical to the MMS controller, because it evaluates errors between current vehicle dynamics and each model in **P**, and determines which controller should be chosen. The controller index σ is determined by:

http://dx.doi.org/10.5772/63352

$$\sigma = \arg\min_{i=1,\cdots,4} J_i(t). \tag{7}$$

Intuitively, $J_i(t)$ is designed to measure the model uncertainty σ_i, and so the estimator set $\mathbf{E}=\{E_i,\ i=1,\ \cdots,\ N\}$ is designed to indirectly measure σ_i as follows:

$$\begin{aligned} &\hat{z}_i = -\frac{k_{Gi}}{\Lambda(s)} W(s) a_{\text{des}},\ \hat{a}_i = \\ &\frac{k_{Gi}}{\Lambda(s)} a_{\text{des}} + \frac{\Lambda(s) - (s + p_G)}{\Lambda(s)} a, i = 1, \cdots, 4, \end{aligned} \tag{8}$$

where $\Lambda(s)$ is the common characteristic polynomial of $\mathbf{E}$, $\hat{a}_i$ and $\hat{z}_i$ are the estimates of a and z using model P_i. It is easy to know that the stability of estimators can be ensured by properly selecting $\Lambda(S)$. Subtracting Eq. (8) with Eq. (4) yields the estimation error of a:

$$e_i = \hat{a}_i - a = -\frac{k_{Gi}}{\Lambda(s)} W(s) \Delta_i a_{\text{des}} = \Delta_i \hat{z}_i. \tag{9}$$

Then, the switching index $J_i(t)$ is designed to be

$$J_i(t) = \left(\left\| e_i(t) \right\|_2^{\delta} \right)^2 - \left(\left\| \hat{z}_i(t) \right\|_2^{\delta} \right)^2, i = 1, \cdots, 4. \tag{10}$$

Since the system gain from $\hat{z}_\sigma(t)$ to $e_\sigma(t)$ can be bounded by $\mathbf{S}$, $\hat{z}_\sigma(t)$ and $e_\sigma(t)$ can be treated as the input and output of an equivalent uncertainty. Considering Eq. (8), $\mathbf{E}$ is rewritten into

$$\begin{aligned} \dot{\mathbf{x}}_E &= \mathbf{A}_E \mathbf{x}_E + \mathbf{B}_{E1} a_{\text{des}} + \mathbf{B}_{E2} a \\ \hat{a}_i = \mathbf{C}_{E1i} \mathbf{x}_E, \hat{z}_i &= \mathbf{C}_{E2i} \mathbf{x}_E, \end{aligned} \tag{11}$$

where A_E, B_{E1}, B_{E2}, C_{E11}, C_{E12}, C_{E13}, C_{E14}, C_{E21}, C_{E22}, C_{E23}, C_{E24} are matrices with proper dimensions. By selecting weighting function as $W_p(s)=(0.1s+1.15)/s$, the required tracking performance becomes:

$$\left\|q(t)\right\|_2^{\delta} < \gamma \left\|a_{\text{ref}}(t)\right\|_2^{\delta}, \tag{12}$$

where a_{ref} is the reference acceleration, $q=W_{\text{p}}(s)e_{\text{a}}$ and $e_{\text{a}}=a_{\text{ref}}-a$, , which is expected to converge to zero. Substituting $a=\hat{a}_{\sigma}-e_{\sigma}$ and Eq. (12) to Eq. (11), we have,

$$\dot{\mathbf{x}} = \mathbf{A}_{\sigma}\mathbf{x} + \mathbf{B}_1 e_{\sigma} + \mathbf{B}_2 a_{\text{des}} + \mathbf{B}_3 a_{\text{ref}} \tag{13}$$

$$\hat{z}_{\sigma} = \mathbf{C}_{1\sigma}\mathbf{x}, q = \mathbf{C}_{2\sigma}\mathbf{x} + D_{\text{p}} e_{\sigma} + D_{\text{p}} a_{\text{ref}}, e_{\text{a}} = \mathbf{C}_{3\sigma}\mathbf{x} + e_{\sigma} + a_{\text{ref}},$$

where $\mathbf{A}_{\sigma}=\begin{bmatrix}\mathbf{A}_{\text{E}}+\mathbf{B}_{\text{E2}}\mathbf{C}_{\text{E1}\sigma} & 0\\ -\mathbf{C}_{\text{E1}\sigma} & 0\end{bmatrix}$, $\mathbf{B}_1=\begin{bmatrix}-\mathbf{B}_{\text{E2}}\\ -1\end{bmatrix}$, , $\mathbf{B}_2=\begin{bmatrix}\mathbf{B}_{\text{E1}}\\ 0\end{bmatrix}$, $\mathbf{B}_3=\begin{bmatrix}0\\ 1\end{bmatrix}$, $\mathbf{C}_{1\sigma}=[\mathbf{C}_{\text{E2}\sigma} \quad 0]$, $\mathbf{C}_{2\sigma}=[-0.1\mathbf{C}_{\text{E1}\sigma} \quad 1.15]$, $\mathbf{C}_{3\sigma}=[-\mathbf{C}_{\text{E1}\sigma} \quad 0]$, $\mathbf{D}_{31}=1$, $\mathbf{x}=\begin{bmatrix}\mathbf{x}_{\text{E}}\\ x_p\end{bmatrix}$ are system matrices with proper dimensions. The required robust controller set can be designed by numerically solving the following LMIs:

$$\begin{bmatrix}
\mathbf{A}_{\delta i}\mathbf{P}_1 + \mathbf{P}_1\mathbf{A}_{\delta i}^{\text{T}} + \mathbf{B}_2\tilde{\mathbf{C}}_i + \tilde{\mathbf{C}}_i^{\text{T}}\mathbf{B}_2^{\text{T}} & * \\
\left(\tilde{\mathbf{A}}_i^{\text{T}} + \mathbf{A}_{\delta i} + \mathbf{B}_2\tilde{\mathbf{D}}_i\mathbf{C}_{3i}\right)^{\text{T}} & \mathbf{P}_2\mathbf{A}_{\delta i} + \mathbf{A}_{\delta i}^{\text{T}}\mathbf{P}_2 + \tilde{\mathbf{B}}_i\mathbf{C}_{3i} + \mathbf{C}_{3i}^{\text{T}}\tilde{\mathbf{B}}_i^{\text{T}} \\
\left(\mathbf{B}_2\tilde{\mathbf{D}}_i + \mathbf{B}_1\right)^{\text{T}} & \left(\mathbf{P}_2\mathbf{B}_1 + \tilde{\mathbf{B}}_i\right)^{\text{T}} \\
\left(\mathbf{B}_2\tilde{\mathbf{D}}_i + \mathbf{B}_3\right)^{\text{T}} & \left(\mathbf{P}_2\mathbf{B}_3 + \tilde{\mathbf{B}}_i\right)^{\text{T}} \\
\mathbf{C}_{1i}\mathbf{P}_1 & \mathbf{C}_{1i} \\
\mathbf{C}_{2i}\mathbf{P}_1 & \mathbf{C}_{2i}
\end{bmatrix} \tag{14}$$

$$\begin{bmatrix}
* & * & ** \\
* & * & ** \\
-\beta^2\mathbf{I} & 0 & ** \\
0 & -\gamma^2\mathbf{I} & ** \\
0 & 0 & \mathbf{I}\,0 \\
D_p & D_p & 0\,\mathbf{I}
\end{bmatrix} < 0, i = 1, \cdots, 4, \begin{bmatrix}\mathbf{P}_1 & \mathbf{I}\\ \mathbf{I} & \mathbf{P}_2\end{bmatrix} > 0,$$

http://dx.doi.org/10.5772/63352

where $\beta < 1$ is a positive constant, $\mathbf{A}_{\delta i} = \mathbf{A}_i + 0.5\delta\mathbf{I}$, symbol "*" represents the symmetrical part. Then the controller set $\mathbf{C}$ is

$$\mathbf{C} = \left\{ K_i : \begin{array}{l} \dot{\mathbf{X}}_C = \mathbf{A}_{Ci}\mathbf{X}_C + \mathbf{B}_{Ci}e_{\mathrm{a}} \\ a_{des} = \mathbf{C}_{Ci}\mathbf{X}_C + \mathbf{D}_{Ci}e_{\mathrm{a}} \end{array}, i = 1, \cdots, N \right\}. \tag{15}$$

The matrices in Eq. (15) are calculated as:

$$\begin{aligned} \mathbf{D}_{Ci} = \tilde{\mathbf{D}}_i, \mathbf{C}_{Ci} &= \left(\tilde{\mathbf{C}}_i - \mathbf{D}_{Ci}\mathbf{C}_{3i}\mathbf{P}_1 \right) \left(\mathbf{M}^{\mathrm{T}} \right)^{-1}, \mathbf{B}_{Ci} \\ &= \mathbf{N}^{-1} \left(\tilde{\mathbf{B}}_i - \mathbf{P}_2\mathbf{B}_2\mathbf{D}_{Ci} \right), \end{aligned} \tag{16}$$

$$\begin{aligned} \mathbf{A}_{Ci} &= \mathbf{N}^{-1} \left[\tilde{\mathbf{A}}_i - \mathbf{P}_2 \left(\mathbf{A}_{\delta i} + \mathbf{B}_2\mathbf{D}_{Ci}\mathbf{C}_{3i} \right) \mathbf{P}_1 \right] \left(\mathbf{M}^{\mathrm{T}} \right)^{-1} \\ &-0.5\delta\mathbf{I} - \mathbf{B}_{Ci}\mathbf{C}_{3i}\mathbf{P}_1 \left(\mathbf{M}^{\mathrm{T}} \right)^{-1} - \mathbf{N}^{-1}\mathbf{P}_2\mathbf{B}_2\mathbf{C}_{Ci}, \; i = 1, \cdots, 4, \end{aligned}$$

where $\mathbf{M}$ and $\mathbf{N}$ are the singular value decomposition of $\mathbf{I} - \mathbf{P}_1\mathbf{P}_2$. The controller set $\mathbf{C}$, solved by LMIs Eq. (14), is listed as follows:

$$\mathbf{C} = \left\{ K_1(s), K_2(s), K_3(s), K_4(s) \right\}$$

$$\begin{aligned} K_1(\mathrm{s}) &= \frac{137.1(\mathrm{s} + 4.9)(\mathrm{s} + 3.133)}{s(\mathrm{s} + 41.85)(\mathrm{s} + 45.70)}, \; K_2(\mathrm{s}) \\ &= \frac{233.4(\mathrm{s} + 4.9)(\mathrm{s} + 3.133)}{\mathrm{s}(\mathrm{s} + 80.06)(\mathrm{s} + 21.42)}, \end{aligned} \tag{17}$$

$$\begin{aligned} K_3(\mathrm{s}) &= \frac{573.0(\mathrm{s} + 4.9)(\mathrm{s} + 3.133)}{\mathrm{s}(\mathrm{s} + 29.63)(\mathrm{s} + 99.30)}, \; K_4(\mathrm{s}) \\ &= \frac{283.4(\mathrm{s} + 4.9)(\mathrm{s} + 3.133)}{\mathrm{s}(\mathrm{s} + 54.15)(\mathrm{s} + 19.89)} \end{aligned}$$

4. Simulation results and analyses

To validate the improvements MMS controller for tracking of acceleration, two other controllers are designed, i.e. a sliding mode controller (SMC), and a single $\mathbf{H}_\infty$ controller.

4.1. Design of SMC and H_∞ controllers

It is known that SMC has high robustness to uncertainties. It is designed based on the nominal model $G_M(s)=0.33/(s+0.33)$. The sliding surface is selected to be

$$e(t)=a-a_{\text{ref}},\ s=\int_0^t e(t)dt+\lambda e(t), \tag{18}$$

where $\lambda>0$. The reaching law is designed to be $\dot{s}=-ks+\eta\text{sgn}(s)$, where $k<0$ and $\eta>0$. Then the sliding mode controller is

$$a_{\text{des}}=\frac{\tau_i}{\lambda k_i}\left[\lambda\dot{a}_{\text{ref}}+\lambda\frac{1}{\tau_i}a-e-ks+\eta\text{sgn}(s)\right] \tag{19}$$

$\mathbf{H}_\infty$ control is another widely used and effective approach to deal with model uncertainties. Here, a model matching control structure is applied to balance between robustness and fastness. The uncertain model of vehicle dynamics used for design of $\mathbf{H}_\infty$ controller is

$$P(s)=\frac{0.3s+1}{0.2s^2+0.6s+1}\left(1+\frac{5.2s+5}{2s+10}\Delta\right),\|\Delta\|_\infty<1 \tag{20}$$

The referenced acceleration response dynamics is $G_M(s)=1/(s+1)$. Then, the feed-forward controller designed by the model matching technique is

$$C_F(s)=\frac{0.2s^2+0.6s+1}{0.3s^2+1.3s+1} \tag{21}$$

The feedback controller designed by the $\mathbf{H}_\infty$ control method is

$$C_B(s)=\frac{6.5493(s+5)(s+6)(s^2+3s+5)}{s(s+10.39)(s+4.74)(s^2+7.049s+14.03)} \tag{22}$$

http://dx.doi.org/10.5772/63352

This $\mathbf{H}_\infty$ controller is numerically solved by the Matlab command *mixsyn*(), with the weighting function $W_p(s)=(0.1s+1.15)s^{-1}$.

4.2. Simulations and analyses

A naturalistic acceleration from real traffic flow is used as the reference acceleration. This naturalistic acceleration profile is from driver experiment data, which lasts around 50 min totally and is shown in **Figure 5**. The maximum and minimum desired acceleration is about 1.1 m/s^2 and −1.8 m/s^2, respectively and the vehicle speed varies in the range of 0–33 m/s. This condition can cover a wide range of vehicle dynamics.

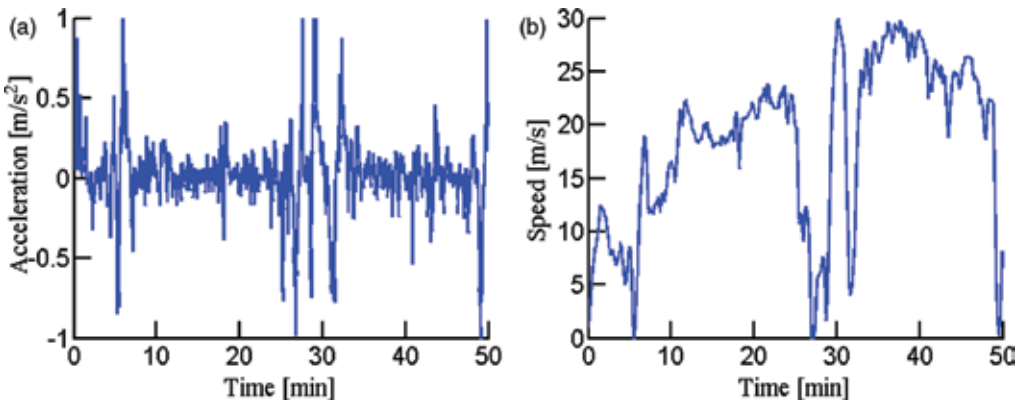

Figure 5. *Reference accele*ration and *speed*. (a) *Accele*ration a*nd* (b) *Veh*icle speed.

Two groups of simulations are conducted: (a) nominal condition; and (b) uncertain condition. Under the nominal condition, all vehicle parameters are shown in **Table 1** and there is no road slope and wind. Under the uncertain condition, the disturbed parameters are vehicle mass, road slope and wind. The maximum value of vehicle mass is used, i.e. M = 1600 kg. The disturbance of road slope is a sinusoidal signal:

$$\varphi = \varphi_{\max} \cdot \sin\left(\frac{2\pi}{T_{\text{slope}}} \cdot t\right) \tag{23}$$

where $\varphi_{\max}$ = 5 deg, and T_{slope} = 50 sec. The disturbance of wind is a periodic triangular signal:

$$v_{\text{wind}} = 2\frac{v_{\text{wmax}}}{T_{\text{wind}}}t - v_{\text{wmax}}, t \in \left[0, T_{\text{wind}}\right), \tag{24}$$

where v_{wmax} = 10 m/s, and T_{wind} = 40 sec.

The simulations results are shown in **Figures 6** and **7**, and to show clearly, only the responses from 0 to 500 sec are plotted as a demonstration. From **Figure 6(a)** and (**b**), under the nominal condition, all three controllers can track the reference acceleration accurately. With the uncertainties, it is found that from **Figure 7(a)** and (**b**) the tracking capability of SMC and H_∞ controller decreases obviously while MMS can still ensure acceptable tracking error. Though switching of controller occurs at both nominal and uncertain conditions (**Figure 6(e)** and **Figure 7(e)**), the control input of MMS behaves continuously and there is no obvious sudden change (**Figure 6(c)** and **Figure 7(c)**). Another concern that must be explained is the spike of acceleration shown in **Figure 6(b)** and **Figure 7(b)**. This is mainly caused by the impact of powertrain when gear switches. A more appropriately designed transmission model could improve the gear-shifting quality.

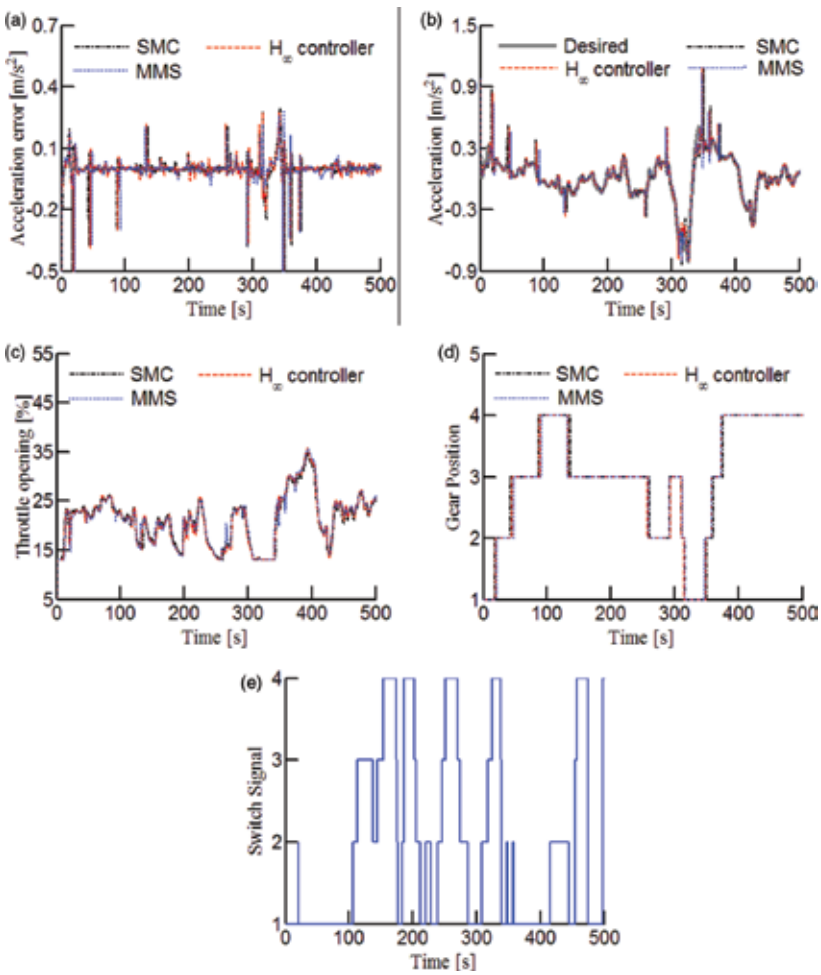

Figure 6. Results under normal condition. (a) Acceleration tracking error, (b) acceleration, (c) throttle control, (d) gear position and (e) switching signal.

http://dx.doi.org/10.5772/63352

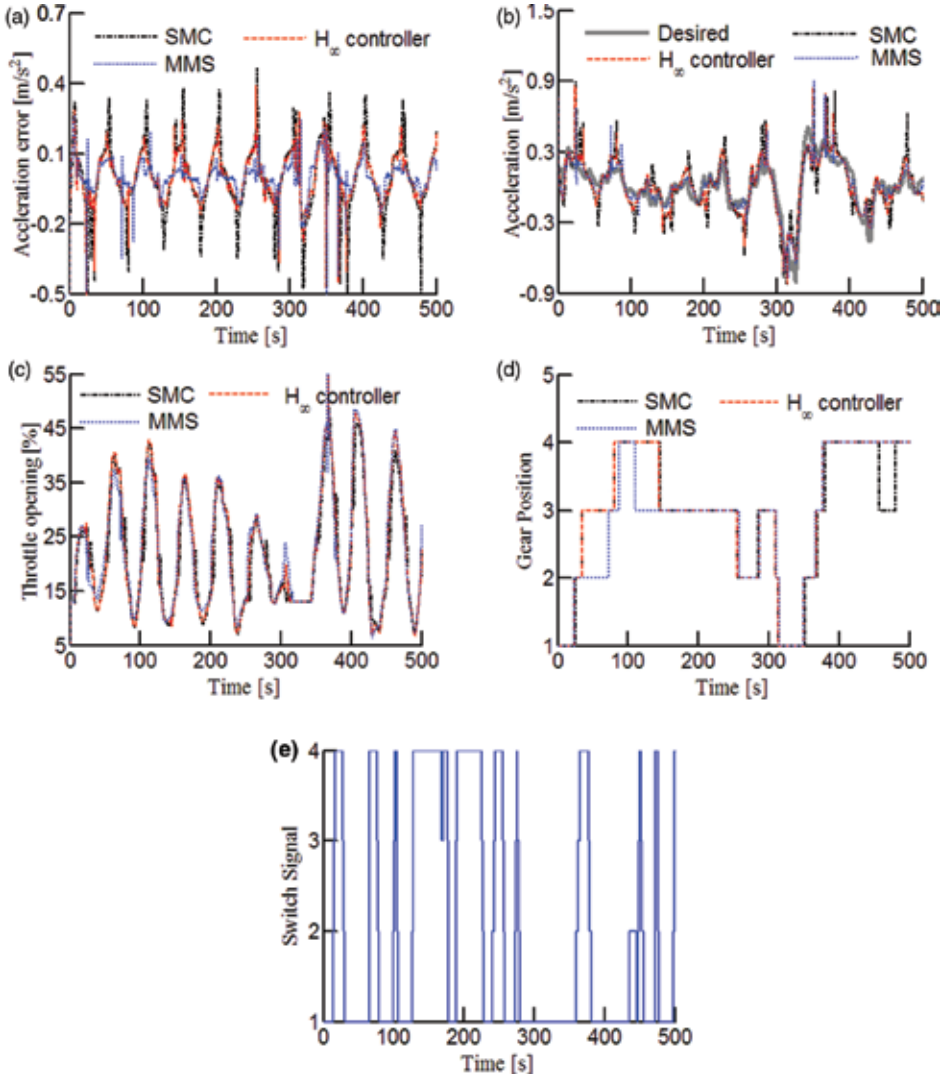

Figure 7. Results under disturbed condition. (a) Acceleration tracking error, (b) acceleration, (c) throttle control, (d) gear position and (e) switching signal.

A more deep simulation is conducted to analyse the influences of uncertain level on the tracking ability of acceleration and gear shifting behaviours. At this condition, the level of uncertainty is increased step by step and the relationship between the uncertain level and model uncertainties is described by:

$$\begin{aligned} M &= 1200\ \text{kg} + 40\text{kg} \cdot \varepsilon,\ \varphi_{\max} \\ &= 1\text{deg} \cdot \varepsilon, v_{\text{wmax}} = 2\frac{\text{m}}{\text{s}} \cdot \varepsilon, \end{aligned} \tag{25}$$

where ε represents the level of uncertainty, with maximum mass 1600 kg, maximum road slope 10 deg, and maximum wind speed 20 m/s (when $\varepsilon = 10$). $\varepsilon = 0$ implies that there is no model uncertainty. The root mean square error (RMSE) of acceleration is used to measure the capability of tracking. **Figure 8** presents the RMSE of acceleration error and the number of gear shifting per minute (denoted as N_{gear}/min). In nominal condition, the RMSE of acceleration error of the three robust controllers is almost the same. As the uncertainty level increases, the tracking capability of the SMC and H_∞ quickly drops, whereas the MMS still holds acceptable accuracy. **Figure 8(b)** is used to release the concern that the MMS might largely increase the number of gear shifting because of its switching structure.

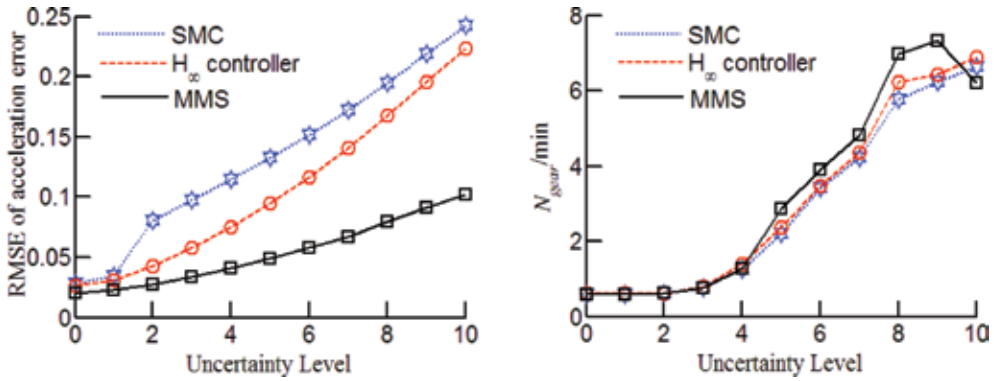

Figure 8. Performances under different uncertain levels.

5. Conclusions

This chapter proposes a robust acceleration control method for consistent node dynamics in a platoon of automated connected vehicles (CAVs). The design, which is based on multiple model switching (MMS) control structure, is able to offer more consistent and approximately linear node dynamics for upper level control design even under large uncertainties, including vehicle parametric variation, varying road slop and strong environmental wind. The following remarks are concluded:

(1) Homogeneous and linear node dynamics is important for platoon control. This requires the acceleration tracking performance to be accurate and consistent, and accordingly results in critical challenges because of the linearization error of powertrain dynamics and large model uncertainties in and around vehicles. The proposed MMS control structure can divide the large uncertainties of vehicle longitudinal dynamics into small ones. Accordingly, multiple robust controllers are designed from the multiple model set, and a scheduling logic is also presented to automatically select the most appropriate candidate controller into loop according to the errors between current vehicle dynamics and models.

(2) The designed switching index can measure the model error of vehicle longitudinal dynamics properly and the right acceleration controller is selected into the closed loop. The robust stability and performance of this acceleration tracking control system can be ensured. Both the simulation and experiment results demonstrate that this switching control system has better performances than that designed by either H_∞ control or sliding mode control approach in large uncertain conditions.

Acknowledgements

This was supported by the State Key Laboratory of Automotive Safety and Energy under Project No. KF16192 and NSF China with grant 51575293.

Author details

Feng Gao[1*], Shengbo Eben Li[2] and Keqiang Li[2]

*Address all correspondence to: gaofeng1@cqu.edu.cn

1 School of Electrical Engineering, Chongqing University, Chongqing, China

2 Department of Automotive Engineering, Tsinghua University, Beijing, China

References

[1] Luettel T, Himmelsbach M, Wuensche J. Autonomous ground vehicles—concepts and a path to the future. Proceedings of the IEEE 100. 2012; (Special Centennial Issue): 1831–1839. DOI: 10.1109/JPROC.2012.2189803.

[2] Shladover S. Longitudinal control of automotive vehicles in close-formation platoons. Journal of Dynamic Systems Measurement and Control. 1991; 113(2): 231–241. DOI: 10.1115/1.2896370.

[3] Sheikholeslam S, Desoer C. Longitudinal control of a platoon of vehicles with no communication of lead vehicle information: a system level study. IEEE Transactions on Vehicular Technology. 1993; 42(4): 546–554. DOI: 10.1109/25.260756.

[4] Hedrick J, Tomizuka M, Varaiya P. Control issues in automated highway systems. IEEE Transactions on Control System Technology. 1994; 14(6): 21–32. DOI: 10.1109/37.334412.

[5] Wang J, Rajamani R. Should adaptive cruise control systems be designed to maintain a constant time-gap between vehicles. IEEE Transactions on Vehicular Technology. 2004; 53(5): 1480–1490. DOI: 10.1109/TVT.2004.832386.

[6] Wang J, Longoria R. Coordinated and reconfigurable vehicle dynamics control. IEEE Transactions on Control System Technology. 2009; 17(3): 723–732. DOI: 10.1109/TCST.2008.2002264.

[7] Gao F, Dang DF, Li SB. Control of a heterogeneous vehicular platoon with uniform communication delay. In: IEEE International Conference on Information and Automation. 8–10 Aug: Lijiang. 8–10 Aug: IEEE; 2015. p. 2419–2424. DOI: 10.1109/ICInfA.2015.7279692.

[8] Stankovic S, Stanojevic M, Siljak D. Decentralized overlapping control of a platoon of vehicles. IEEE Transactions on Control System Technology. 2000; 8(5): 816–832. DOI: 10.1109/87.865854.

[9] Barooah P, Mehta P, Hespanha J. Mistuning-based control design to improve closed-loop stability margin of vehicular platoons. IEEE Transactions on Automatic Control. 2009; 54(9): 2100–2113. DOI: 10.1109/TAC.2009.2026934.

[10] Hao H, Barooah P. Stability and robustness of large platoons of vehicles with double-integrator models and nearest neighbor interaction. International Journal of Robust and Nonlinear Control. 2013; 23(18): 2097–2122. DOI: 1002/rnc.2872.

[11] Rajamani R, Shladover S. An experimental comparative study of autonomous and cooperative vehicle following control systems. Transportation Research Part C. 2001; 9(1): 15–31. DOI: 10.1016/S0968-090X(00)00021-8.

[12] Li ES, Li KJ, Wang JQ. Economy oriented vehicle adaptive cruise control with coordinating multiple objectives function. Vehicle System Dynamics. 2013; 51(1): 1–17. DOI: 10.1080/00423114.2012.708421.

[13] Gao F, Li XP, Ming GQ. Adaptive speed control under vehicle and road uncertainties using multiple model approach. In: American Control Conference; 4–6 June; Portland, OR. 4–6 June 2014: IEEE; 2014. p. 897–902. DOI: 10.1109/ACC.2014.6858598.

[14] Chen Z, Mi C, Xu J, Gong X, You C. Online energy management for a power-split plug-in hybrid electric vehicle based on dynamic programming and neural network. IEEE Transactions on Vehicular Technology. 2014; 63(4): 1567–1580. DOI: 10.1109/TVT.2013.2287102.

[15] Fritz A, Schiehlen W. Automatic cruise control of a mechatronically steered vehicle convoy. Vehicle System Dynamics. 1999; 32: 331–344. DOI: 10.1076/vesd.32.4.331.2077.

[16] Fritz A, Schiehlen W. Nonlinear ACC in simulation and measurement. Vehicle System Dynamics. 2001; 36(2): 159–177. DOI: 10.1076/vesd.36.2.159.3556.

[17] Hunt K, Johansen T, Kalkkuhl J. Speed control design for an experimental vehicle using a generalized gain scheduling approach. IEEE Transactions on Control System Technology. 2000; 8(3): 381–295. DOI: 10.1109/87.845870.

[18] Li SB, Gao F, Cao DP, Li KQ. Multiple model switching control of vehicle longitudinal dynamics for platoon level automation. IEEE Transactions on Vehicular Technology. Forthcoming. DOI: 10.1109/TVT.2016.2541219.

[19] Swaroop D, Hedrick J, Choi S. Direct adaptive longitudinal control of vehicle platoons. IEEE Transactions on Vehicular Technology. 2001; 17(1): 150–161. DOI: 10.1109/CDC.1994.410877.

[20] Higashimata A, Adachi K. Design of a headway distance control system for ACC. JSAE Review. 2001; 22(1): 15–22. DOI: 10.1016/S0389-4304(00)00091-6.

[21] Yamamura Y, Seto Y. An ACC design method for achieving both string stability and ride comfort. Journal of System Design and Dynamics. 2008; 2(4): 979–990. DOI: 10.1299/jsdd.2.979.

[22] Gao F, Li KQ. Hierarchical switching control of longitudinal acceleration with large uncertainties. International Journal of Automotive Technology. 2007; 8(3): 351–359. DOI: 10.1109/ICVES.2006.371597.

[23] Xu Z, Ioannou P. Adaptive throttle control for speed tracking. Vehicle System Dynamics. 1994; 23: 293–306. DOI: 10.1080/00423119408969063.

[24] Keneth J, Tor A, Jens K. Speed control design for an experimental vehicle using a generalized scheduling approach. IEEE Transactions on Control System Technology. 2008; 8(3): 381–395. DOI: 10.1109/87.845870.

[25] Naranjo J, Gonzalez C, Carcia R. ACC+stop&go maneuvers with throttle and brake fuzzy control. IEEE Transactions on Intelligent Transportation System. 2006; 7(2): 213–225. DOI: 10.1109/TITS.2006.874723.

[26] Dai X, Li C, Rad A. An approach to tune fuzzy controllers based on reinforcement learning for autonomous vehicle control. IEEE Transactions on Intelligent Transportation System. 2005; 6(3): 285–293. DOI: 10.1109/TITS.2005.853698.

[27] Hespanha J, Liberzon D, Morse A. Hysteresis-based switching algorithms for supervisory control of uncertain systems. Automatica. 2003; 39: 263–272. DOI: 10.1016/S0005-1098(02)00241-8.

[28] Hespanha J, Liberzon D, Morse A. Multiple model adaptive control. Part 2: switching. International Journal of Robust and Nonlinear Control. 2001; 11(5): 479–496. DOI: 10.1002/rnc.594.

[29] Gao F, Li SB, Kum D, Zhang H. Synthesis of multiple model switching controllers using H∞ theory for systems with large uncertainties. Neurocomputing. 2015; 157: 118–124. DOI: 10.1016/j.neucom.2015.01.029.

[30] Bashivan P, Fatehi A. Improved switching for multiple model adaptive controller in noisy environment. Journal of Process Control. 2012; 22: 390–396. DOI: 10.1016/j.jprocont.2011.12.010.

[31] Kianfar R, Augusto B, Ebadighajari A. Design and experimental validation of a cooperative driving system in the grand cooperative driving challenge. IEEE Transactions on Intelligent Transportation System. 2012; 13(3): 994–1007. DOI: 10.1109/TITS.2012.2186513.

Chapter 4

The Reliability of Autonomous Vehicles Under Collisions

Ibrahim Kutay Yilmazcoban

Additional information is available at the end of the chapter

http://dx.doi.org/10.5772/63974

Abstract

Unmanned autonomous vehicles (UAV) subject is one of the most conspicuous topics of the last decade ensures a better handling ability for more precision way of control of the system or the drive compared to the human. Focusing this issue causes the more computerized vehicles the less unacceptable mistakes. Notwithstanding the efficient drive parameters are increased, the collisions are still the worst scenarios for the vehicles that should be taken care of. The most reliable way to define the collision response of the vehicles and the occupants is crash tests, although it is time consuming. Except crash test is the most convenient procedure to define the details of the impact process; it is also the most expensive way even for the major companies and research centers. Considering the compelling pricey amount of the first investment of the crashworthiness facilities and the crash test costs, recently, computer-aided simulations with the finite element method (FEM) using an explicit dynamics approach is very convenient, especially for the transient dynamic analysis. This chapter characterizes some perspectives of the autonomous vehicles in a short glance of an enormous science of the collisions with the help of experimental and numerical approaches.

Keywords: crash worthiness (impact), vehicle reliability, occupant safety, FEM, explicit dynamics, LSDYNA

1. Introduction

Over the decades, safety standards of the vehicles have been raised from the demands of the automobile users and organizations like Federal Motor Vehicles Safety Standards and Regulations (FMVSS) [1], National Highway Traffic Safety Administration (NHTSA) [2], European New Car Assessment Program (Euro-NCAP) [3], Society of Automotive Engineers (SAE) [4], etc. Superior technology evolved vehicles, which need more resources, offer diverse facilities for the occupants. Respecting the autonomous systems, more interventions of the drivers are

starting to narrow. Although the yield of luxury and reliability, sometimes it operates against the occupants. During computer governing trips, individuals want to attain locations faster. In unexpected inaccuracy situations, automatic systems could cause fatal results.

However, the most common and important topic of vehicles is the crash-worthiness. Ensuring the reliability of the vehicles and safety of the occupants, the vehicle structure should be constructed in a way to absorb the impact effects and shock gradually, not to create a sudden deceleration which causes also injuries and fatalities. To decrease the failure risks, entire vehicle should be investigated, primarily starting from the basic structure of the vehicle under the perspectives of statics and strength of the materials. Then, the natural frequencies and the dynamic loading of the system should be incorporated into step by step. Generally for the dynamic loading, pre-captured dynamic road data also helps developing the vehicle structure. During the development period, beforehand defined systems like the concept design of the vehicle, and the shape should be protected, but the adaptation of the alterations should affect the design in minor.

Before determining the impact response and the behavior of the vehicle during a collision, the reasons of the accidents should be investigated. Serious amount of the accidents occur by the carelessness, negligence, and recklessness of the driver. The first one decreasing the risk of the collision is preventive driving techniques. This technique is a part of the education for the expert driving, although it refers time, patience, and talent. Yet, without any attention and enough reflexes, even this preventive method, results in frustration. In addition, if the all scenarios are considered the environmental and road conditions, and the faults of the other vehicles, including the drivers, effect the vehicles as other factors. Thence, the UAV technology becomes the redeemer of the system to solve the problems completely or decrease the errors to a sufficient level for a more reliable drive.

The most proper way to determine the causes is an experimental study, despite it is not a cost effective and time-consuming way. With the all other test methods such as positioning, loading, and calibrating, crash tests are the most significant ones. After the real-time collision tests, widely known experimental approach on the crash-worthiness researches is the sled test [2, 3, 5, 6]. The sled tests are more under-control when it is compared with the other methods. But again, the financial hassle is beyond the limits of the most companies and facilities.

Decreasing the expenses of the crash tests, many companies untangle their crash-worthiness difficulties after mandatory collision tests, with the computer-aided simulations. Consequently, computerized methods are immensely reliable, if almost, the last three decades are considered. To overcome the real-time simulations of the engineering problems, many developed computer-aided analysis softwares can be obtained from the market. Even though some of the softwares for an exact engineering solution such as structural analysis, impact analysis and thermal analysis remain part of the market is dealing with the multi discipline engineering solution packages serving for the finite element method (FEM). But for the general FEM and its solution methodology [7–9] is not focused on significant issues. Hence, the more applications in a software sometimes decreasing the expertise approach. According to our perspective, impact simulation codes indicate the prominent side of the vehicle collisions. Thereupon, for the impact procedures, explicit dynamics approach based on the FEM gets

http://dx.doi.org/10.5772/63974

through the formidable problems, satisfactorily [10]. In **Figure 1**, FEM model (a) and a crash simulation (b) of a wheelchair and a seating system via sled scenario are given using the human mass adaptation to understand the crash worthiness [11].

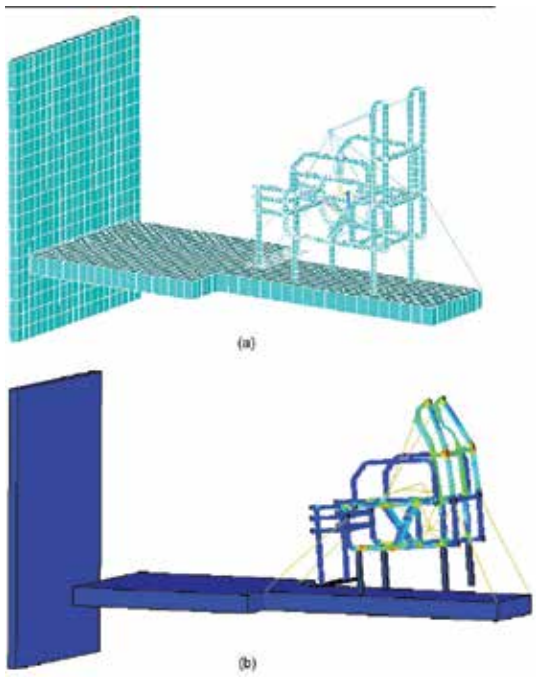

Figure 1. (a) Finite element model of a wheelchair crash simulation via sled test, (b) Finite element simulation result of the model for a defined specific time.

One of the most popular and extensively used software for the impacts is LSDYNA, the product of the Livermore Software Technology Corporation (LSTC) [12]. This code is used by some of the software companies as a fundamental explicit dynamics solver. With the help of the validated FEM results, reliable procedures will be determined to figure out the real vehicle crash scenarios in an inexpensive way, even for the UAV technology. During improvements invariably, reverse engineering applications are in the process from beginning till the end to mend the faults scores of times.

2. Autonomous vehicles: the perspective of collisions

Recently, the importance of the unmanned autonomous vehicles for every day, industrial and military applications are rapidly increasing, regarding the demand of the market. It is complex enough not to start the mass productions for today, especially manufacturing ability in excessive numbers of the automobile industry is considered. But, when the issue is saving a human being, we should reconsider everything referring the military developments against terrorism or wars. The defense industry focuses on the aerial vehicles to check the required

zones and decrease the threats by the enemies or the terrorists. An unmanned aerial vehicle (UAV) shown in **Figure 2** in Ref. [13], widely used as a drone, or an unmanned aircraft system (UAS), and also referred by several other names, defines an aircraft without a human pilot. Therefore, an aircraft without a pilot means, alive human, but in the right hands yet, this sophisticated technology will be so perilous against innocents. And also, the more professionally UAS requires the more trained and talented personnel in particular formidable and arduous duties. This can possibly cause unexpected mistakes during the tasks that provoke impacts and collisions.

Figure 2. Medium Altitude Long Endurance (MALE) UAV of Turkish Aerospace Industries, Inc.

Figure 3. Google self-driving car.

The technological improvements in numerous dissimilar segments are effecting the UAV technology too, like media and entertainment. With the help of the lately used drones are easily operated, simple and cheap widely used by the professionals likewise amateurs in various applications. This option introduces some hazardous results with the ease of the system. Although the price of the simple applications like drones less when it is compared with the complex vehicles, consequences could be analogous.

If we focus on the automobile industry some leading companies like Google have been paying attention for autonomous cars for a while. See **Figure 3** [14]. After spending many years to

http://dx.doi.org/10.5772/63974

research and development, the shown up products of UAV technology on the roads are a quite impressive story.

With regret, even for the finest tech. companies, some of the undesired incidents bring about the damaging results of the UAV. The self-driving car of the Google collided with a public transportation bus in California, USA (**Figure 4** in [15]) on February 14, 2016. In spite of the highly developed vehicle technology, it is indispensable to face with collisions for some cases.

Figure 4. Collided self-driving car of Google.

Whatever is done or planned for evolving the UAVs, sometimes these vehicles encounter with inevitable problems, and thus, it will be concluded with accidents as it was not planned. Under these circumstances, vehicle safety and crash worthiness should be taken care of in a comprehensive viewpoint.

3. Causes and prevention methods of collisions

Involuntary emerged incidents by the humans, vehicles, and environmental effects may cause accidents randomly. Sometimes, the reasons are known and the sufficient prevention methods can be created for the safety of the vehicles or the occupants or the both of the occupants and the vehicles. Although the vehicle is UAV, the opponents or the other vehicles could be driven by the humans. Thus, the human existence should be considered evermore, while the robustness of the vehicles is acceptable. With reference to known conversant reasons of the collisions, inaccurate parts of the mechanical, electronical, or software-based problems could be adjusted. However, the human originated mistakes which can differ from one being to another are much harder to fix with straightforward solution approaches. The psychological, physiological, behavioral potential, capability, and carefulness of the humans will alter the results of the happenings. Sometimes, the reasons are known, but it is not able be figured out by anything

else the events like the several natural disasters. Otherwise, if the reasons are not specified or estimated for the collisions, the new methodologies must be evaluated to diminish the odds of failures for both humans and the vehicles.

Considering the vehicle, which is not a UAV, can be also investigated for the safety of the pedestrians, occupants, regular vehicles, and the autonomous vehicles. The idea of preventive driving technique or expert skills will come into the minds for the human driver. Initially, validity of this opinion could be reasonable with the existence of the natural aptitude alongside the education of the preventive driving. Although the careful driving is very important, the reflex of a human body is a prominent factor of the innate talent effecting throughout the trip. Sometimes, this gained time in milliseconds can save lives when the human body reacts against an unexpected incident. Reflexes can be improved with the help of the practice, while we can assume this, as a learned or educated reflex.

Otherwise, if the reflex response is not satisfying the sudden handling situations, preventive driving education avails to avert the collisions during or before the accidents. This education covers primarily the calm driving in contrast with the aggressive and fast driving, refraining from the instantaneous movements of the steering wheel conducts the vehicle, sudden acceleration and decelerations in particular in tough weather and environmental conditions. To ensure a safe trip, an admissible space between the vehicles is a necessary approach to acquiring an enough time along the duration of the collision. Subsequently, scanning all around the vehicle with eyes and computerized systems for every single threat is the key factor for a reliable trip, like a radar system to perceive the risky ventures which could be possibly induced by anything else.

Afterward, the driver will face with the most critical phase: *Decision*! And the worst scenario is *Uncertainty* as an opposite situation signifying that "the worst decision is better than a hesitant behaviour." If we consider the options for the decision:

- Deceleration,
- Pull over,
- Suddenly stop,
- Acceleration,
- Return,
- U turn,
- Slide,
- Skid,
- Drift,
- Changing lanes,
- Manage to do both of the selected ones or more, simultaneously or consecutively.

http://dx.doi.org/10.5772/63974

If there is no chance avoiding from the accident, try to be in the safe zone or select the least hazardous way via changing the speed and maneuvering the vehicle to save the lives and minimize the collision effects. Doing nothing and being petrified is not an option, it is just an ambivalent condition eventuating with an undesirable result.

Considering the hassle of the situation during collisions, these types of behaviors and applications are so difficult for a human to apply and need some expertise. It is not for everyone! Thus, if the computerized UAV system is capable to handle all of these situations at the same time, except some uncommon incidents, it will be much more robust and reliable for everyone, although we consider that sometimes human mind and body can create metaphysical and exceptional solutions.

4. Vehicle safety standards

When we talk about the Unmanned Autonomous Vehicles, it comprises the ground, aerospace, and even the naval vehicles. If we try to clarify the safety standards for all conditions, it will be in the detail redundantly. Ordinarily when the crash-worthiness and accidents are on the carpet, extensively known portrayal is covering the automobiles followed up by the aircrafts and the other vehicles.

For determining the vehicle safety standards of the automobiles, some major organizations take place in the decisive position in the industry and the market. However, the most important role in framing the ideology of the crash testing is in the hands of the Federal Motor Vehicle Safety Standards and Regulations (FMVSS) and the National Highway Traffic Safety Administration (NHTSA) in the USA as one of the leading countries for the vehicle safety. In the NHTSA internet site [16] of the US Department of Transportation for the Federal Motor Vehicle Safety Standards and Regulations, safety assurance defined in four major topics given below:

1. Crash avoidance: Standards between 101 and 135 (Part 571),
2. Crashworthiness: Standards between 201 and 224 (Part 571),
3. Post-crash standards: Standards as 301, 302, 303, 304 and 500 (Part 571),
4. Other regulations: Standards between 531 and 595.

It is very important to point out, especially the contents of the crashworthiness for our point of view:

- Occupant Protection in Interior Impact,
- Head Restraints,
- Impact Protection for the Driver from the Steering Control System,
- Steering Control Rearward Displacement,
- Glazing Materials,

- Door Locks and Door Retention Components,
- Seating Systems,
- Occupant Crash Protection,
- Seat Belt Assemblies,
- Seat Belt Assembly Anchorages,
- Windshield Mounting,
- Child Restraint Systems,
- Side Impact Protection,
- Roof Crush Resistance,
- Bus Emergency Exits and Window Retention and Release,
- Motorcycle Helmets,
- Windshield Zone Intrusion,
- School Bus Rollover Protection,
- School Bus Body Joint Strength,
- School Bus Passenger Seating and Crash Protection,
- Rear Impact Guards,
- Rear Impact Protection.

In another perspective for the crash testing, in the internet site of the crash network [17] expresses the headings in different groups: interior testing, dash board, frontal impact, side impact, steering wheel, seats, seat belts, rear impact, rollover, head rests, and roof crush. Considering the developments in the vehicle industry including automobiles and aircrafts, etc., especially the UAVs, many countries trying to improve new methodologies against the collisions comprising hundreds of standards. The major idea for the crash worthiness is protect the occupants or all beings, and eliminate or diminish the damages caused by the collisions.

5. Crash worthiness and crash tests

The occupant safety and vehicle reliability are the fundamental topics that should be developed against collisions for the crash worthiness. Although the technology is evolved in many fields especially for the materials science comprehending composite materials and withal super collapsible beams to absorb impact energy, again if we are not able to provide a safe drive for the occupant or the vehicle it is going to be a fact that can be concluded with the injuries or fatality for the driver, passengers or the people outside while the vehicle face with the physical damage like self-destruction as a result of collision to the wall, barrier or a structure; accident

http://dx.doi.org/10.5772/63974

with another vehicle via front, behind or side impacts; and maybe a rollover incident by some other effects. These are by definition may differ from one incident to another defining the accidents of vehicles even for the autonomous systems. Whatever happens, the engineers should design a structure that can able to absorb some of the energy by collapsing itself or deforming to an adequate level to protect the human beings. If the structure is too rigid, there is an amplification occurs and affect everything in a poor way that is transferring the accelerations to the occupants causing worse situation. Therefore, even for the safety and reliability, optimum way is better to protect lives against accidents.

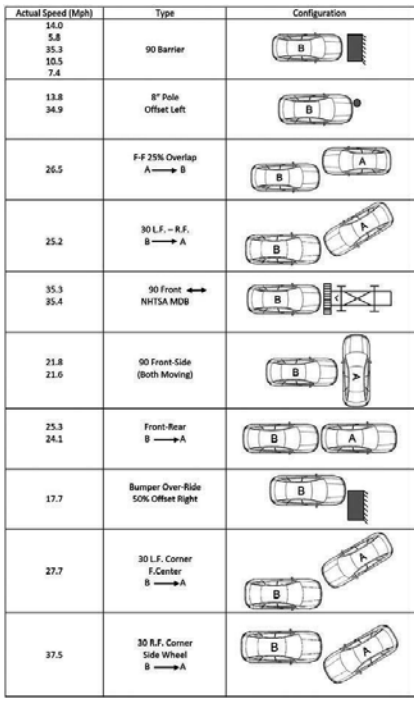

Figure 5. Crash test modes.

To determine the crash response, broad amount of tests have been carried out for many years by the validated official agencies for crash worthiness. During the collisions under the combined loading conditions, the application of the crash energy management is dependent to plenty of situations, starting with contact mechanics and collapse modes that could be in the axial and/or in bending way causing many other reactions. According to Huang [5], the crash tests were chosen after reviewing some previous works around the world, accident statistics, and experience with the Ford Tempo air bag fleet based on the real-world crash investigations. The tests consisted of car-to-car tests versus barrier and fixed pole tests. Crash data were accumulated from the 22 vehicles; the chosen tests representing a vast range of accidents at or near the expected threshold of air bag deployment. There are 22 vehicles in 16 tests, as shown in (**Figure 5**), were used to gather the crash pulse data. For every test, the

selected impact speed is a key factor to check the system performance of the air bag sensor will be activated or not during the incidents. Due to mentioned circumstances, we can define the types of the impacts [5]:

1. A perpendicular (90°) barrier,
2. A low- and high-speed rigid pole,
3. A front-to-front overlap,
4. An oblique front to front (three types),
5. A vehicle front to an moving deformable barrier (MDB) perpendicular,
6. A vehicle front-to-side,
7. A front-to-rear,
8. A bumper over-ride (or truck under-ride).

The tests can be classified in three categories: component tests, sled tests, and full-scale barrier impacts. Because of the complexity and many distinct test variables in full-scale tests, there is an acceptable reason in the reduction of the test's repeatability. The impact test depicted in (**Figure 6**) is representing a full-scale vehicle-to-vehicle impact test of Toyota Motor Company while they are developing a new safety system for their automobiles [18]. The dynamic and/or quasi-static response of an isolated component is defined by the component tests are exalted to detect the crush mode and energy absorbing ability. With the help of the component tests, it also gives the capability to the designers to develop prototype substructures and mathematical models. Moreover, the vehicle rear structure full-scale tests are governed either via a deformable barrier or a bullet car to state the integrity of the fuel tank. To evaluate roof strength according to FMVSS 216, a quasi-static load is applied on the "greenhouse," and providing that the roof deformation falls below a particular level for the applied load [6].

Figure 6. Vehicle-to-vehicle impact test of Totoya Motor Company.

http://dx.doi.org/10.5772/63974

For the sled test, engineers use a representation of a passenger compartment (buck) with all or some of the interior parts like seat, front panel, steering system, seat belts, and air bags. Anthropomorphic Test Devices or "Dummies" (ATD) or cadaver subjects are seated in the buck, utilized to simulate an occupant subjected to dynamic loads which is similar to a vehicle deceleration-time pulse, to determine the response in a frontal impact or side impact. To appraise the restraints of the system the sled test is a significant topic recorded by the high-speed cameras and photography applications for the dummy kinematics. It should also be stated that the performance of the ATD is determined at a higher impact speed of 35 mph in the NCAP test. Throughout the NCAP test, the restrain system is composed of three-point lap/shoulder belt system, and also additional restraint air bag. When we pay attention to the detail of the impact tests, numerous numbers of sensors as accelerometers, load cells, etc., located in the dummy and on the restraints, screen the forces and moments assisting to specify the impact reactions. Event data recorders have a very important role to understand the behavior of the system during accidents. However, when the recorded data will be analyzed digital filtering and reducing the noise (unwanted data) effect the results. Thus, it should be figured out cautiously.

Driving through the highways or freeways, the barriers are limiting the vehicles to get out of the road and protecting it, from crossings. During the barrier impact test there is a guided vehicle, canalized into a barrier with a predetermined initial velocity and angle. The purpose of the test is to maintain a structural integrity of the vehicle and adherence to the mandatory government regulations. The fully equipped vehicle collides a barrier at a 0°, +30°, and −30°, respectively, from an initial velocity of 30 mph.

The frontal offset impact test is another method acting with 40–50% overlap stating that the impact target could be rigid or deformable.

For the full-scale side impact test, a deformable barrier moving towards the left or right side of the vehicle with an initial speed at a certain angle (FMVSS 214). Especially for this test, side impact dummies ("SID" For the US and "EURO SID1" for Europe) which have different shape and properties, are used in the driver and outboard rear seat positions.

When the human parts are considered, the ATDs are widely used and capable enough to demonstrate the behaviors of the human nature in a fundamental way, even when it is indicating the spine, head, brain, organs, knee injuries, and whiplash incident in particular.

6. Explicit dynamics approach in FEM for the impact scenarios

The finite element method has been used by many scientists and engineers for decades to advance systems in different engineering applications for the validations, while reducing the experimental investments and the expenditure of the tests. This widely known method developed via the contributions of the researchers all around the world. While FEM problem is thriving, we will break the problem domain into a collection of 1D (dimensional), 2D and 3D shapes to form the discretization. Starting with the simplest way, $\{F\} = [K]\{D\}$ where F, K,

and *D*, are the nodal force vector, global stiffness matrix and nodal displacement vector, respectively, as usually known. The displacements in this equation are the unknowns which should be found and lead us to figure out the strains and stresses, etc. To solve the equations, generally, the direct stiffness method, variational technique, or weighted residual approaches are used. However, this fundamental technique is now capable enough to handle the issues lately popular like the fracture mechanics with an extended finite element method, cohesive modeling, contact algorithms, smoothed-particle hydrodynamics (SPH) and Arbitrary Lagrangian–Eulerian Method (ALE), etc. Regarding recent a few decades, requisition of a nonlinear mechanics or engineering plasticity, for the delicate and slightly designs which should be robust in tough conditions, induced the durability tests including impacts and crashes. Explicit dynamics approach in FEM emerges with this idea to untangle the difficulties of the impacts, drop tests, explosions, and collision scenarios.

Vehicle technology under the perspective of the crash worthiness and safety during the collisions via crash tests to explicit dynamics simulations of the FEM is a trustworthy way to follow up. If we have a dekko to the literature some valuable studies can be determined [5, 6, 19] about the vehicle crash worthiness and the safety, while some books [6, 10, 19] explain the details of explicit dynamics one of the most challenging nonlinear problems in structural mechanics.

The implicit FE solution technique delivers accurate results as long at the stress levels in the beam do not exceed the yield-stress value, thus remaining in the linear (elastic) region of the material curve. Because the implicit solver usually obtains a result with a single step, according to the slope of the material curve, which is represented by Young's modulus, for the plastic region of the material there will be an inaccuracy whereat the slope is changed up the plastic characteristics. It means that the implicit solver is very powerful for linear (static) finite element analysis (FEA); thence, it provides an unquestioningly stable solution methodology.

Unfortunately, the implicit solution approximation may have difficulties with the immensely nonlinear finite element models. Additionally, inverting extremely large stiffness matrices with the implicit solver might consume too much time and memory. Although this method is not logical to use in highly nonlinear problems, it can able to calculate the equations with the help of the iteration cycle, which is applying the load in minor increments called as "timesteps" [19].

During the accident, the vehicle body faces with the impact loads propagate localized plastic hinges and buckling. So the large deformations and rotations with contact and heaping between the many parts can be determined. One of the most important ideas for the explicit dynamics is the wave effects, primarily involved in the deformation stage, associated with the higher stress levels. When the stress level exceeds the yield strength and/or the critical buckling load and the localized structural deformations comprise throughout a few wave transits in the frame of the vehicle. The effects of the inertia will chase this step and also dominate the ensuing transient reaction. The collision could be considered as a less dynamic incident if there is a comparison between the ballistic impact and the vehicle crash. Closed-form analytical problems for the impact scenarios in structural mechanics offer tough times for everyone. Therefore, the numerical methods arise with the practical options to decipher the unknowns.

http://dx.doi.org/10.5772/63974

A set of nonlinear partial differential equations of motion in the space-time domain is solved numerically by the explicit dynamics approximation, related to the stress–strain properties of the material about the initial and boundary conditions. To obtain a set of second order differential equations in time, the equations in space are discretized by the solution in the course of formulating the problem in a weak variational form and supposing an acceptable displacement field. Subsequently, in the time domain, discretization calculates the system of equations. If the selected integration parameters deliver the equations coupled, the technique is defined as implicit, while the solution is unconditionally stable. Furthermore, if the solution will be defined as explicit, the equations should be decoupled by the selection of the integration parameters, and it is conditionally stable [6].

As Du Bois et al. [6] described, a set of hyperbolic wave equations in the region of effectiveness of the wave front is figured out via the explicit dynamics, even then it does not require coupling of large numbers of equations. Yet, the unconditionally stable implicit solvers requiring assembly of a global stiffness matrix provide a solution for all coupled equations of motion. Especially considering the impact and vehicle crash simulations, including the utilization of contact, several material models and withal a combination of non-conventional elements, the explicit solvers show up more potent and computationally more productive than the implicit solvers, while the timestep is about two to three orders of magnitude of the explicit timestep. "Explicit" defines an equilibrium at a moment in time that the displacements of the whole spatial points are known in advance. With the help of the equilibrium, we can determine the accelerations; moreover, the use of central differencing technique assures to establish the displacements at the next timestep and reiterate the process. And also, the only inversion of the mass matrix, M, is enough for this procedure.

There should be stated that if the lumped-mass approximation is utilized the mass matrix will be diagonal, so there is no obligation of the matrix inversion. When the uncoupled equation system is figured out, the results will be in a very fast algorithm. For the minimum memory exigency, the assembly of a global stiffness matrix should be avoided by using an element-by-element approach for the calculation of the internal forces. The explicit integration will be second order accurate when it is applied attentively. Utilization of the related nodal displacements and/or velocities, the stresses are calculated discretely for each element, causing the effect of the loads on one part of the element onto the opposite part which is simulated by each timestep. Accordingly, the stress wave propagation is demonstrated through the element clearly. The deficiencies of the explicit solution technique are the conditional stability and the weak approximation of treating the static problems. The meaning of the conditional stability of the explicit integration algorithm is the integration timestep must be smaller than or equal to an upper bound value known as the Courant condition,: $\Delta t \leq \frac{l_c}{c}$ explaining that the timestep must not pass over the smallest of all element timesteps identified by dividing the element characteristic length through the acoustic wave speed through the material from which origin the element is made like Du Bois et al. [6] mentioned. And they also said that the numerical timestep of the analysis must be smaller than, or equal to, the time required for the physical stress wave to pass by the element. If we try to explain it in a straightforward way, c of the mild steel elements is about 5000 m/s with a characteristic length of 5 mm for the automotive

field practices concluding with 1 μs for the analysis timestep. Consequently, incidents dealing with the short duration of time are appropriate for the explicit dynamics solution technique enclosed with superior nonlinear behaviors and loading velocities demanding small timesteps for more precision sequels.

The integration of the equations of motion defines the time integration:

$$[M]\{\ddot{x}\} + [C]\{\dot{x}\} + \{F_{\text{int}}\} = \{F_{ext}\} \tag{1}$$

or in a different representation,

$$M\ddot{x}_n + C\dot{x}_n + f_{n_{\text{int}}} = f_{n_{ext}} \tag{2}$$

The basic problem is to determine the displacement, x_{n+1}, at time t_{n+1}. We can also say that $[K]\{x\} = \{F_{int}\}$. By the way, the explicit direct time integration can in a conceptual form be written as:

$$x_{n+1} = f(x_n, \dot{x}_n, \ddot{x}_n, x_{n-1}, \ldots) \tag{3}$$

The equation shows that the solution depends on nodal displacements, velocities, and accelerations at state n, quantities which are known. Therefore, the equation can be solved directly. And for the implicit:

$$x_{n+1} = f(\dot{x}_{n+1}, \ddot{x}_{n+1}, x_n, \dot{x}_n, \ldots) \tag{4}$$

This equation represents the solution that depends on nodal velocities and accelerations at state $n + 1$, quantities which are unknown. This implies that an iterative procedure is needed to compute the equilibrium at time t_{n+1}.

If we try to define the time increments:

$$\Delta t_{n+1/2} = t_{n+1} - t_n \tag{5}$$

$$t_{n+1/2} = \frac{1}{2}\left(t_{n+1} + t_n\right) \tag{6}$$

$$\Delta t_n = t_{n+1/2} - t_{n-1/2} \tag{7}$$

http://dx.doi.org/10.5772/63974

$$t_{n+1} = t_n - \Delta t_{n+1/2} \tag{8}$$

Then, the central difference method is used for the velocity:

$$\dot{x}_{n+1/2} = \frac{x_{n+1} - x_n}{\Delta t_{n+1/2}} \tag{9}$$

and

$$x_{n+1} = \dot{x}_{n+1/2} \Delta t_{n+1/2} + x_n \tag{10}$$

When $\Delta t_{n+1/2} = t_{n+1} - t_n$ is used, we get:

$$x_{n+1} = \dot{x}_{n+1/2} \left(t_{n+1} - t_n \right) + x_n \tag{11}$$

With the help of the acceleration, velocity can be stated as:

$$\ddot{x}_n = \frac{\dot{x}_{n+1/2} - \dot{x}_{n-1/2}}{t_{n+1/2} - t_{n-1/2}} \tag{12}$$

With $\Delta t_n = t_{n+1/2} - t_{n-1/2}$, the velocity is given below:

$$\dot{x}_{n+1/2} = \dot{x}_{n-1/2} + \Delta t_n a_n \tag{13}$$

From the Eq. (2), the acceleration at a_{n+1} can be found like:

$$\ddot{x}_{n+1} = m^{-1} \left(f_{n+1_{ext}} - f_{n+1_{int}} - C\dot{x}_{n+1/2} \right) \tag{14}$$

Remember, the damping force is taken at $\dot{x}_{n+1/2}$. The new velocity will be calculated with the old velocity and acceleration by Eq. (13). From this result, displacement will be updated at Eq. (10). Consequently, the new internal and external forces help for determination of the new acceleration [Eq. (14)].

Considering the LSDYNA, the widely known commercial explicit solver, the procedure for the solution steps is given below:

When $t = 0$, it will be the beginning of the solution loop or cycle. Whereupon, the displacement will be updated at Eq. (10), while the velocity is also updated at Eq. (13). Then, the internal forces (strain rate, strain, stress, and force magnitude) will be computed looping over the elements. Subsequently, external forces will be calculated to reach the computation of the accelerations at Eq. (14) which is finalizing the initial loop. Thereafter, following loops will go through the process again and again, until the convergence criteria will be satisfied.

For the robust design, stress wave propagation, timestep adjustment, critical element length and finally, the mesh size and quality are the factors, will be considered carefully to affect the simulation performance in a better way.

Due to the reliable side of the explicit dynamics solution methodology, we indicated the differences between the implicit and explicit solver for the approximation of the vehicle crash simulations and safety of the occupants and vehicles. We can possibly say that, for the collision of the regular or autonomous vehicles the accident results will be similar that should be taken care of precisely.

6.1. Crash simulations of the vehicles

The studies about the crash worthiness and impact scenarios as explained in the previous section are based on the explicit dynamics solution technique resulting with the satisfactory approximations. Some of the commercial codes for the explicit dynamics simulations are embedded inside the multidiscipline FEA programs such as ABAQUS, ANSYS, and MSC softwares, even though some of them working alone for just these types of applications as LSDYNA, PAMCRASH, etc. As it was mentioned, before these softwares are auxiliary engineering applications for solving the problems with the numerical methods. The most important task is the prediction of the failures of the system or structure of the vehicle and the problems that occupants can be faced. When the prediction of the simulations is validated, it can be said that FEM code has done its job properly.

To comprehend the validation of the simulations with the real crash tests, numerous topics should be investigated before, during or after the simulations. We can simply name these steps like: before the process is pre-processing, during is processing or simulation, and after the processing is post-processing.

Pre-process section is dealing with the creation of the finite element model, starting from the Computer-Aided Design (CAD) of the structure or the system, material descriptions or modelling, element selections, defining the boundary conditions (describing the loads, displacements and support properties, etc.) and initial values like velocities, adjusting the contact algorithms, total time and timestep size definition. For more elaboration, mass scaling factor and/or hourglass controls can be adjusted. Considering the information given, the geometry should be meshed as smooth shapes as possible. During the mesh generation element, sizes are so prominent, will affect the simulation time, according to the number of the elements. If the mesh is coarse, there will be a weak approximation and short period of

http://dx.doi.org/10.5772/63974

processing time, notwithstanding if there is a finer meshed model exists, the convergence rate will be better, while the processing time is prolonged. Thus, there should be an optimum mesh size for the common structure; however, the significant zones are meshed with finer elements to increase the stability and for the better result.

When the simulation is processed, the finite element model is ready for the post-processing. The most considerable issue for the impact is absorb or get rid of the shock energy by different methods like geometrical change of the structure, material selection, and application. The second problem is the large deformation of the structural components. Additionally, changing the parameters of the simulation model will affect the results widely depending on the experience of the analyst. Because of dealing with the highly plastic problems and non-linearity during collisions, the analyst needs to possess deep knowledge about nonlinear finite element analysis for continuum mechanics [20–22]. It should be stated that the analyst can be faced with the geometrically nonlinear problems or material nonlinearities which is imported to be expressed.

Figure 7. The vehicle crash test and simulation.

Regarding the details of the post-processing, we will start to observe and evaluate the simulation outputs, step by step. While we are investigating the steps of the impact scenario, kinetic energy change, absorbed energy amount, deformations and displacements, strain and stress distribution, and some other major issues should be appraised attentively and the results should be validated with the real crash tests. Besides, the effects of the different components, deformation characteristics, and the changes of the parameters must be observed and the behavioral outcomes of the incident should be crosschecked with the real situation. The literature is replete with numerous of interesting researches about the crash-worthiness of the vehicles and the occupant safety including the Anthropomorphic Test Dummy (ATD) test and simulations [23–27]. Especially LSDYNA conferences are popular with the presentations of the explicit dynamics simulations and also most of the papers can be reachable from the internet

site of "DynaLook" [28]. For a better representation of an explicit dynamics simulation, **Figure 7** demonstrates the full vehicle crash scenario [29].

7. Conclusion

Whole crash-worthiness studies are remarkable starting with the elementary functions of the profound methods of NCAP tests considering despite the costs of the experiments are enormous, contribution of the test results is challenging.

For a robust vehicle, the engineers should design a structure that can able to absorb some of the energy by collapsing itself or deforming to an adequate level to protect the human beings. If the structure is too rigid, there is an amplification occurs and affect everything in a poor way that is transferring the accelerations to the occupants causing worse situation. Therefore, even for the safety and reliability, optimum way is better to protect lives against accidents.

Nevertheless, for diminishing the costs of the studies of FEM and explicit dynamics methods, which are proceeding under the supervision of the computers and codes verified by the long-term researches and applications, are competent to handle the complicated algorithms yielding with satisfactory results. The incidents dealing with the short duration of time are appropriate for the explicit dynamics solution technique enclosed with superior nonlinear behaviors and loading velocities demanding small timesteps for more precision sequels.

Take into account the results of the experiments, analytic solutions and computerized methods are mentioned as FEM codes are robust approximations to understand the behavior of the vehicle and occupants in the course of statics, dynamics, and collisions. Consequently, the finite element method and explicit dynamics solutions have been proven to validate the experiments and real life experiences in the range between 80 and 100%.

It should be clearly stated that the autonomous vehicles decreasing the risks of the collisions when it is compared to the human driver controlled vehicle.

8. Nomenclature

8.1. Symbols and descriptions

c Acoustic wave speed through the material of which the element is made

[C] Damping matrix

{D} Nodal displacement vector

{*F*} Nodal force vector or External load vector

$\{F_{ext}\}$ External forces

$\{F_{int}\}$ Internal forces

[*K*] Global stiffness matrix

l_c Element characteristic length

[M] Lumped-mass matrix

n Indicates step n

x Displacement

$\dot{x}$ Velocity

$\ddot{x}$ Acceleration

t Time

Δt Timestep size

Author details

Ibrahim Kutay Yilmazcoban*

Address all correspondence to: kyilmaz@sakarya.edu.tr and kyilmazcoban@berkeley.edu

Department of Mechanical Engineering, University of California, Berkeley, CA, USA

Department of Mechanical Engineering, Sakarya University, Serdivan, Turkey

References

[1] Federal Motor Vehicle Safety Standards (FMVSS). FMVSS.COM [Internet]. Available from: http://fmvss.com/. Accessed: 2.27.16

[2] National Highway Traffic Safety Administration (NHTSA). NHTSA [Internet]. Available from: http://www.nhtsa.gov/. Accessed: 2.27.16

[3] European New Car Assessment Program (Euro-NCAP). The Official Site of The European New Car Assessment Programme [Internet]. Available from: http://www.euroncap.com/en. Accessed: 2.27.16

[4] Society of Automotive Engineers (SAE). SAE International [Internet]. Available from: http://www.sae.org/. Accessed: 2.27.16

[5] Huang M. Vehicle Crash Mechanics. USA: CRC Press LLC; 2002. 504 p. doi: 10.1201/9781420041866.ch2

[6] Du Bois P, Chou C C, Fileta B B, Khalil T B, King A I, Mahmood H F, Mertz H J, Wismans J. Vehicle Crashworthiness and Occupant Protection. MIchigan, USA: American Iron and Steel Institute; 2004. 388 p.

[7] Logan D L. A First Course in the Finite Element Method. 5th ed. Stamford, CT, USA: Cengage Learning; 2012. 1000 p.

[8] Bathe K J. Finite Element Procedures in Engineering Analysis. New Jersey, USA: Prentice Hall; 1982. 735 p.

[9] Moaveni S. Finite Element Analysis Theory and Application with ANSYS. New Jersey, USA: Prentice Hall; 1999. 527 p.

[10] Wu S R, Gu L. Introduction to the Explicit Finite Element Method for Nonlinear Transient Dynamics. Hoboken, New Jersey, USA and Canada: WILEY, A John Wiley & Sons, Inc.; 2012. 352 p. doi:10.1002/9781118382011.ch1

[11] Yilmazcoban I K. Analysis of Wheelchairs' Frame Soundness under Environmental Conditions: Use of Finite Element Technique [thesis]. Sakarya, Turkey: Sakarya University; 2009. 162 p.

[12] Livermore Technology Software Corporation. Welcome to Livermore Software Technology Corp. [Internet]. 3.5.16 [Updated: 3.5.16]. Available from: http://www.lstc.com/. Accessed: 3.25.16

[13] TAI (Turkish Aerospace Industries, Inc.). Medium Altitude Long Endurance (MALE) UAV [Internet]. 3.31.2016 [Updated: 3.31.2016]. Available from: https://www.tai.com.tr/en. Accessed: 3.31.2016

[14] Google. Google Self-Driving Car Project [Internet]. 3.31.2016 [Updated: 3.31.2016]. Available from: https://www.google.com/selfdrivingcar/. Accessed: 3.31.2016

[15] HNGN (Headlines & Global News). Google Shares Blame For Autonomous Car Collision [VIDEO] [Internet]. 3.31.2016 [Updated: 3.31.2016]. Available from: http://www.hngn.com/articles/187103/20160310/google-shares-blame-v-day-autonomous-car-collision-video.htm. Accessed: 3.31.2016

[16] NHTSA. Federal Motor Vehicle Safety Standards and Regulations (Safety Assurance) [Internet]. 04.06.2016 [Updated: 04.06.2016]. Available from: http://www.nhtsa.gov/cars/rules/import/FMVSS/. Accessed: 04.06.2016

[17] Crash-Network (The web portal for the crash test engineer). FMVSS Standards related to Crash Testing [Internet]. 04.06.2016 [Updated: 04.06.2016]. Available from: http://www.crash-network.com/Regulations/FMVSS/fmvss.html. Accessed: 04.06.2016

[18] The Japan Times News. Imperial Family's car woes sparked Toyota whistleblower [Internet]. 04.17.2014 [Updated: 04.17.2014]. Available from: http://www.japan-times.co.jp/news/2013/06/09/business/corporate-business/imperial-familys-car-woes-sparked-toyota-whistleblower/#.VxPdUMJf2Ul. Accessed: 04.17.2014

[19] Christensen J, Bastien C. Nonlinear Optimization of Vehicle Safety Structures: Modeling of Structures Subjected to Large Deformations. 1st ed. US: Elsevier, Butterworth-Heinemann; 2016. 474 p.

[20] Belytschko T, Liu W K, Moran B, Elkhodary K I. Nonlinear Finite Elements for Continua and Structures. 2nd ed. UK: Wiley; 2014. 834 p.

[21] Reddy J N. An Introduction to Nonlinear Finite Element Analysis. 2nd ed. Great Britain: Oxford University Press; 2015. 687 p. doi:10.1093/acprof:oso/9780198525295.001.0001.

[22] Borst R, Crisfield M A, Remmers J J C, Verhoosel C V. Non-linear finite element analysis of solids and structures. 2nd ed. UK: Wiley; 2012. 542 p.

[23] Bambach M R. Fibre composite strengthening of thin-walled steel vehicle crush tubes for frontal collision energy absorption. Thin-Walled Structures. 2013;66:15–22. doi: 10.1016/j.tws.2013.02.006

[24] Golman A J, Danelson K A, Miller L E, Stitzel J D. Injury prediction in a side impact crash using human body model simulation. Accident Analysis and Prevention. 2014;64:1–8. doi:10.1016/j.aap.2013.10.026

[25] Al-Thairy H, Wang Y C. Simplified FE vehicle model for assessing the vulnerability of axially compressed steel columns against vehicle frontal impact. Journal of Constructional Steel Research. 2014;102:190–203. doi:10.1016/j.jcsr.2014.07.005

[26] Liu W, Zhao H, Li K, Su S, Fan X, Yin Z. Study on pedestrian thorax injury in vehicle-to-pedestrian collisions using finite element analysis. Chinese Journal of Traumatology. 2015;18:74–80. doi:10.1016/j.cjtee.2015.03.003

[27] Crocetta G, Piantini S, Pierini M, Simms C. The influence of vehicle front-end design on pedestrian ground impact. Accident Analysis and Prevention. 2015;79:56–69. doi: 10.1016/j.aap.2015.03.009

[28] DYNALook. Papers from European and International LS-DYNA User Conferences [Internet]. 04.14.2016 [Updated: 04.14.2016]. Available from: http://www.dynalook.com/. Accessed: 04.14.2016

[29] Structural crash. Esi-Get it right [Internet]. 04.17.2016 [Updated: 04.17.2016]. Available from: http://virtualperformance.esi-group.com/?q=applications-structural-crash. Accessed: 04.17.2016

Chapter 5

ADAS-Assisted Driver Behaviour in Near Missing Car-Pedestrian Accidents

Dario Vangi, Antonio Virga, Mattia Conigliaro,
Hermann Steffan and Ernst Tomasch

Additional information is available at the end of the chapter

http://dx.doi.org/10.5772/63705

Abstract

In intermediate steps on the way to full driving automation, the role of the driver will remain essential, and driver's behaviour when aided by Advanced Driver Assistance Systems (ADAS) must be allowed for, in order to obtain the maximum benefit. In the present study, a driving simulator experimentation was carried out. Sixty-nine volunteers were enrolled to face a simulated hazard situation involving a pedestrian; some of them were aided by ADAS, whereas others were not. The driving scenario was set up based on a statistical accident analysis and the thorough reconstruction of actual road accidents. By qualitative and quantitative analysis, some differences in drivers' behaviour were observed in relation to the presence of ADAS devices and their different modes of acting. The positive effect of ADAS was naturally confirmed, but some of the drivers were not fully able to benefit from it.

Keywords: driving simulation, avoidance strategy, road accident, driver model, automated driving

1. Introduction

It is commonly acknowledged that in the near future most of the road vehicles will travel, on almost the totality of the road network, in an automated way (autonomous driving). The reason for such a forecast is easily understood: the influence of the driver on safety, energy efficiency and traffic fluidity is very high [1]. In fact about 93% of road accidents are originated by some kind of driving error, as recognition errors, decision errors and performance errors [1]. Under such point of view, automated driving can bring dramatic improvements by eliminating the

influence of human factors, thus contributing to reduce serious and fatal road accidents, fuel waste and traffic congestion. The total elimination of road accidents, however, is not predictable at the moment, but their reduction to very little numbers is reasonably attainable. In the vision of many researchers, a roadmap to full automated vehicles can be defined; for instance, organisation like the Society of Automotive Engineers (SAE) has defined some steps (SAE Level of progressive automation, **Figure 1**), ranging from Level 0 (no automation) to Level 5 (full automation) [2].

SAE level	Name	Narrative Definition	Execution of Steering and Acceleration/ Deceleration	*Monitoring* of Driving Environment	Fallback Performance of *Dynamic Driving Task*	System Capability *(Driving Modes)*
***Human driver* monitors the driving environment**						
0	No Automation	the full-time performance by the *human driver* of all aspects of the *dynamic driving task*, even when enhanced by warning or intervention systems	Human driver	Human driver	Human driver	n/a
1	Driver Assistance	the *driving mode*-specific execution by a driver assistance system of either steering or acceleration/deceleration using information about the driving environment and with the expectation that the *human driver* perform all remaining aspects of the *dynamic driving task*	Human driver and system	Human driver	Human driver	Some driving modes
2	Partial Automation	the *driving mode*-specific execution by one or more driver assistance systems of both steering and acceleration/ deceleration using information about the driving environment and with the expectation that the *human driver* perform all remaining aspects of the *dynamic driving task*	**System**	Human driver	Human driver	Some driving modes
***Automated driving system* ("system") monitors the driving environment**						
3	Conditional Automation	the *driving mode*-specific performance by an *automated driving system* of all aspects of the dynamic driving task with the expectation that the *human driver* will respond appropriately to a *request to intervene*	System	**System**	Human driver	Some driving modes
4	High Automation	the *driving mode*-specific performance by an automated driving system of all aspects of the *dynamic driving task*, even if a *human driver* does not respond appropriately to a *request to intervene*	System	System	**System**	Some driving modes
5	Full Automation	the full-time performance by an *automated driving system* of all aspects of the *dynamic driving task* under all roadway and environmental conditions that can be managed by a *human driver*	System	System	System	**All driving modes**

Figure 1. SAE levels of progressive automation as defined in SAE International Standard J3016.

Levels 0–2 (partial automation) require that the human driver be responsible for monitoring the driving environment, whereas in Levels 3–5 such task is performed by the automated driving system. Unless having reached a condition of full automation (Level 5), the driver must be involved in car driving, that is to say that the driver must be kept "in the loop." In fact in any intermediate level of automation, several driving modes will include the possibility or the necessity that the control of the vehicle is shifted from the automated system to the driver, or that the driver is willing to keep the control back. As explained in Refs. [3, 4], such operation must be carefully designed. Such issue will be particularly important in the case of Level 3 (conditional automation) in which the driver, due to the increasing number of automated driving modes, will be often called to take the control back. The driving task can be

http://dx.doi.org/10.5772/63705

decomposed into three main activities: recognition, judgement and operation. In all of such activities errors are possible, likely to bring to some risks or even to accidents. Within SAE Level 0 (no automation), all of these tasks are performed by the driver, which can be defined as "conventional driving." If the implementation of Advanced Driver Assistance Systems (ADAS) is carried out, the driver can be assisted, or even substituted, by some automated or autonomous device or function, up to a level of full automation (SAE Level 5) in which recognition, judgement and operation are performed by the system taking full control. In intermediate levels of assistance (as, for instance, in SAE Levels 1 and 2) only recognition and/or judgement are assisted so that the responsibility for operation remains with the driver. Far from being infallible (at least at the present state of the art) such devices can be of great help to decrease the probability of errors and, consequently, of accidents.

1.1. Present advanced driver assistance systems

As regards the present state of the art of driving assistance devices, their functions can be divided into three main categories:

- Presentation of information about road environment and traffic conditions; the driver is helped during his recognition activity. Under this category, devices, such as road sign recognition (RSR), blind spot monitoring systems (BSM), and so on, can be included.
- Warning; the driver is helped as regards judgement. A timely and appropriate warning signal is issued when a possibly critical situation is detected (as forward collision warning (FCW)).
- Control (to help the driver in operation tasks); the system gets control over the vehicle.

Presently, two types of control can be considered:

- Control for normal driving conditions (as, for instance, lane keep assist (LKA), adaptive cruise control (ACC), etc.), mainly aimed at improving travelling comfort by reducing the workload on the driver.
- Control for pre-crash conditions (as autonomous emergency braking (AEB), often in combination with FCW) in which the driver may be overridden due to the lack of an effective response to some critical situation, aiming at avoiding or mitigating an imminent collision. In such cases, the system acts on the brakes but leaves the choice of steering to the driver.

Even if the control is took by the system, the driving responsibility remains to the driver: in the first case because the control is handed to the driver when conditions can become critical; in the second case, the driver is overridden only at pre-crash conditions (but only as regards braking) so that the accident consequences are mitigated.

In all of this assistance functions, it can be easily understood that a convenient interface (Human-Machine Interface (HMI)) between the generic device and the driver must be designed and implemented. HMI can be considered as the channel through which information are conveyed to a vehicle's occupant; HMI design is one of the main issues that must be

properly allowed for [5], addressing, for instance, the definition of the correct stimulus (type: visual, acoustic, haptic, etc.; sequence; timing; priority; etc.). In addition, since it is to be expected a different communication efficiency as a function of age, experience, education, etc., the interface must be properly tailored and some adaptation is certainly needed. The necessity of standardisation is to be expected, as well as the definition of human models capable to help interpreting correctly the situation and act accordingly.

During the progression towards full automation (especially when high levels of automation, such as SAE Levels 2, 3 and 4, will be implemented), several issues should be addressed in order to obtain a fast and successful path to SAE Level 5; three main topics can be identified as follows:

– Definition of suitable strategies for shifting control from the driver to the system and vice versa. Design of proper HMI systems will be of fundamental importance, also aiming at carrying out such operation in a seamless manner.

– Definition of procedures aimed at obtaining the functional assessment of the instrumental part of the automated system.

– Obtaining a wide user acceptance rate in order to accelerate the penetration in the market of automated systems.

The issues presented in the first two points are currently addressed by several standard practice and regulations (as, for instance, in [6, 7]).

Presently, most of the vehicles can be categorised as belonging to Level 0 of automation, but all the major car manufacturers (as well as tier one suppliers) offer, in their sales catalogues, devices that can be defined as Driver Assistance Systems (typical of SAE Level 1) and some of them show features that can be defined as partial automation.

In the Italian market, for instance, in the official sales catalogues of the end of 2015 as published by car magazines (basically Quattroruote, Italy), several automated assistance systems can be found, mainly belonging to the following categories:

– Adaptive cruise control (ACC),

– Blind spot monitoring systems (BSM),

– Lane departure warning systems (LDWS),

– Road sign recognition (RSR),

– Autonomous emergency braking/forward collision warning (AEB/FCW).

It can be easily recognised that such functions will certainly be part of a hypothetic future full automated system: even if the methods used to obtain such functions are hardly imaginable, the functions itself are necessary and the interaction with the driver must be allowed for. As can be seen in **Table 1**, the above-mentioned devices are offered by a good number of manufacturers on several models, both as standard equipment and as paid option; often they are included in a package together with other safety or comfort devices.

http://dx.doi.org/10.5772/63705

Device	No. of manufacturers	No. of models	No. of models with device as standard equipment	No. of models with device in package
ACC	27	136	26	59
BSM	27	134	32	57
LDWS	30	142	44	66
RSR	19	78	24	25
AEB	24	99	43	44

Table 1. Number of manufacturers and vehicle models offering ADAS devices in the Italian market in September 2015.

Table 2 shows average price and standard deviation (SD) for the same devices as **Table 1**, for the models offering such devices as paid option; as can be seen, when a device is included in a package, its price can be much higher. Price is a matter that can influence user acceptance and delay the diffusion of such safety devices.

Device	Overall		Single device		In-package	
	Average price	SD	Average price	SD	Average price	SD
ACC	1707	1096	1380	727	1989	1276
BSM	837	581	657	355	980	680
LDWS	929	714	540	93	1118	804
RSR	688	483	479	284	931	553
AEB	961	692	348	163	1128	688

Table 2. Average price (€) and standard deviation of some ADAS devices in the Italian market in September 2015.

1.2. User acceptance

Though many researchers are very optimistic on the large implementation of full automation in the near future [8], many factors can slow down the process. A survey conducted by IEEE among its members [8] revealed that in the vision of many experts in the field, six main obstacles to the rapid diffusion of autonomous vehicles can be identified, i.e., technology, cost, infrastructure, policy, liability and user acceptance. According to this source, the first three points should represent a minor problem; technology is rapidly improving as regards both efficiency and reliability, whereas cost is a problem that must be shared among private and public stakeholders, also taking into consideration the potential benefit of accidents reduction, as well as medical and social costs. The implementation of proper infrastructures is of the greatest importance (it is difficult to imagine an effective implementation of driving automation without, e. g., V2V and V2I communications) so that in relatively short terms it can be predicted that the largest diffusion of such systems will take place first in advanced geographical areas, such as North America, Europe and parts of Asia. The last three points, instead, will play a decisive role; policymakers can boost or slow down the process since many matters

require political decisions and a proper legislation will most probably be necessary, for instance as regards the realisation of the needed infrastructures and the settlement of issues related to legal liability. This last point can be particularly important: who will be responsible when an accident happens, as certainly will? It can be imagined that the involvement of car manufacturers and their suppliers will be greater, in a context that will also involve insurance companies, governments and customers [9–11]. User acceptance will play a fundamental role; in reference [12], for instance, a worldwide survey was carried out in order to understand how autonomous vehicles will be accepted, comparing all levels of automation (from conventional driving to full automation). In this study, the major concerns of future customers were indicated, including legal issues, cost (22% declared themselves unwilling to pay any additional sum for an automated vehicle), security (regarding especially software being subject to hacking), privacy concerns (vehicles are subject to be constantly monitored) and driving pleasantness, etc. Geographical differences were also pointed out. In reference [13], the intention of French drivers to use a partially or fully automated vehicle was investigated. In reference [14], the possible effect of motion sickness on user acceptance is investigated, and the necessity of considering such issue during the design and development phase is emphasised. Thus, if a fast and successful introduction in the global market is desired, such systems must be implemented in such a way as aiming at high performance and high user acceptance, and such steps require the most complete understanding of driving behaviour: in other words, a driver model (or better, driver models) must be set up.

1.3. The role of simulation

In the initial phase of the development of ADAS, it is a common practice to carry out testing in controlled environment, namely, by staged driving sessions or using driving simulators. Since their introduction, driving simulators have been widely used to study safety and human factor-related issues. Since the first appearance of advanced driving simulators they were extensively used to investigate over safety issues [15, 16] and also as an important tool in the design and assessment of advanced driving assistance systems [17, 18].

The use of simulators presents numerous advantages:

- Situations that normally reveal to be dangerous can be faced without any risk for the driver and for the researchers as well.
- A well-designed testing scenario allows a very good repeatability of the driving environment and control of all variables (traffic, course, road and weather condition, etc.).
- The situations through which the driver goes can be adapted to the driver behaviour itself.
- All testing parameters can be easily recorded and stored for successive elaboration.
- Experimentation can be speeded up.

On the other hand, the driving scenario must be carefully designed in order to obtain a sufficient representativeness of the results, and often a validation activity must be carried out, for instance by carrying out staged tests in controlled environments or by monitoring real-life driving. Moreover, not all the drivers are able to drive comfortably in a driving simulator.

http://dx.doi.org/10.5772/63705

Although some of the testing activities regarding ADAS development can be carried out using static simulators, the use of an advanced immersive driving simulator allows to have all the needed functionalities together with a sufficiently realistic testing condition.

In the present chapter, a simulator experimental study is presented, aimed at understanding drivers' behaviour when a sudden hazardous situation with pedestrians is presented; for such aim, 69 young drivers were submitted to different virtual driving scenarios. The experimentation, far to be definitive, will anyway provide useful information for setting up a driver model as well as for determining HMI requirements.

2. Definition of a reference accident scenario

Among road users pedestrians represent one of the weaker categories, and the percentage of accidents involving pedestrians is relatively high. According to WHO [19], in 2013, 22% of about 1.25 million worldwide road traffic deaths were pedestrians. In the USA, during 2012, 4743 pedestrians were killed (total casualties 33,561) and 76,000 were injured (total 2,362,000) [20]. It can be seen that the percentage of deaths with respect to injuries among pedestrians (6.2%) is much higher than the general one (1.4%), thus confirming the high level of danger. Pedestrian safety is expected to be highly boosted by the adoption of assistance systems as pedestrian detection system (PDS) and V2I communications, and for this reason it was chosen to study the drivers' behaviour in a situation with a high risk of being involved in an accident with a pedestrian.

Accident reconstruction is a powerful tool to explain the reasons of an accident and identify the main contributing factors. Thus, 26 accidents involving pedestrians actually happened in Austria were analysed using the CEDATU (Central Database for In-depth Accident Study) database [21, 22], by also using multi-body simulations (PC-Crash, DSD, 2015).

Following the indications collected during the preceding phase, a reference accident scenario was defined having, among others, the following features: low-density population urban environment, late evening (heavy darkness) with scarce electric lighting, good weather and road conditions, non-intersection, and pedestrian not using a crosswalk and walking without running from left to right; moreover, a car is coming from the opposite direction obstructing the visual.

3. Set-up of the simulation scenario

Sixty-nine young drivers were employed for the driving simulator testing, enrolled on a voluntary basis mainly among the students of the School of Engineering of the University of Florence. Each subject drove the test scenario once. Sixty-one tests were considered valid, whereas the remaining were discarded because of excessive simulator sickness or weird behaviour of drivers and simulator software; the main characteristics of the drivers of valid

tests (18 female, 43 male) are shown in **Table 3**. Age varied between 19 and 36 years and also driving experience was very different, ranging from few hundreds of kilometre per year to 50,000. Nineteen tests were actually used to tune the simulation scenario (set-up tests) and, in particular, to synchronise the behaviour of the other road users at the emergency situation. The remaining 42 drivers were used for the actual experimentation.

	Gender		**Age**		**km/year**		**Use of lenses**	
	F	M	Average	SD	Average	SD	Yes	No
Total	18	43	26.4	2.9	11688	9593	18	43
Set-up	5	14	26.6	2.2	10684	7558	3	16
Tests	13	29	26.3	3.2	11688	10453	15	27

Table 3. Subjects' characteristics.

For the experimentation, the driving simulator available at LaSIS (Laboratory for Road Safety and Accident Reconstruction, University of Florence, Italy) was used. It consists of a full-scale dynamic simulator (**Figure 2**) provided by AutoSIM (Norway, model AS 1200); the complete vehicle cabin and the 200 degrees wide cylindrical screen allow an immersive driving experience.

Figure 2. View of the simulator in use at LaSIS.

http://dx.doi.org/10.5772/63705

Following the indications obtained from the statistical analysis and the thorough reconstruction of typical road accidents, a generic scenario was defined, adapting one of the terrains available in the simulator database. In particular an environment with little population was chosen, in which the emergency situation described above was inserted (**Figure 3**). The driver reaches the point after having driven for about 5 minutes, encountering some vehicular traffic and pedestrians. Since the terrain contains several intersections and roundabouts, to be sure that the drivers reach the point of interest in a given time, indications by means of direction arrows were projected on the screen. The entire test was driven in night time conditions.

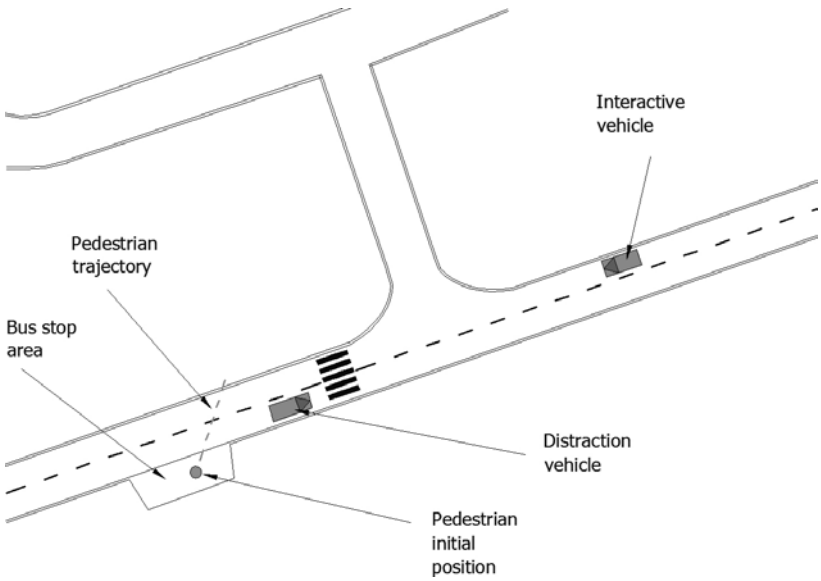

Figure 3. Map of the emergency situation area.

Before driving the test scenario, the subjects faced a training scenario in which, during about 10 minutes, they could get acquainted with the vehicle cabin and try the most common manoeuvres; the subjects began the drive under daylight and ended with dark condition in order to get gradually accustomed with night driving. In some of the tests, the presence of an ADAS was simulated, consisting in a pedestrian detection system. Those drivers who were going to drive in the scenario with the ADAS system also experienced it in the training scenario. Before and after the test, each subject was submitted a questionnaire in order to collect personal and driving information and record their impressions. Before the test, the subjects were informed about the aim of the test and were instructed on the basic functions of simulator and cabin; they were invited to drive in a normal way, respecting the normal traffic rules. No hints were given about the emergency situation they were going to meet. The emergency situation was designed as follows (**Figure 3**): when the interactive vehicle is at a given distance from the emergency area, a vehicle starts travelling in the opposite direction, interfering with the visual. When the interactive vehicle is at a distance that corresponds to a time to collision of about 4.5 s, a pedestrian starts walking from

the opposite side of the road, heading along an oblique direction, with a constant speed of 1.67 m/s; in the first part of his path, the pedestrian is hidden by the distraction vehicle (**Figure 4a**).

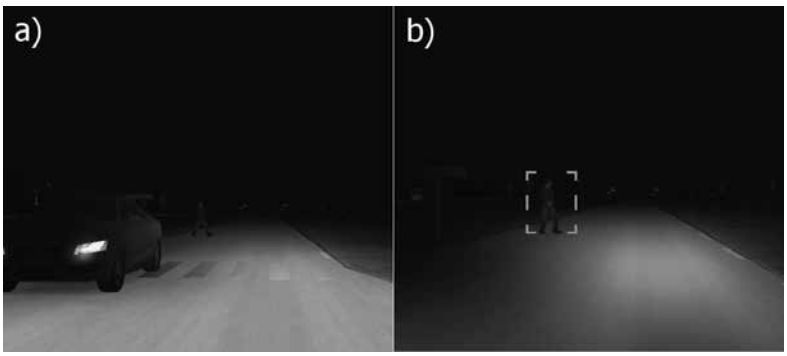

Figure 4. Scene of the emergency situation as seen by the subject driver: in scenarios A, B and C (a) and in scenario D (b).

Four different scenarios were set, one without ADAS and three in which the drivers were helped by a simulated PDS assistance system, characterised by different alert modes:

- Scenario A: no ADAS was simulated (12 drivers);
- Scenario B: a sound alarm (consisting of beeps with increasing frequency) is issued after 0.5 s the pedestrian start (10 drivers);
- Scenario C: as scenario B except that the sound is emitted after 1.5 s (10 drivers);
- Scenario D: as scenario C (10 drivers) with the addition of a visual warning, consisting in a self-lighted rectangular frame around the pedestrian (**Figure 4b**). The aim was to provide additional information to the driver about the position of the hazardous situation, simulating the use of a head-up display.

4. Data analysis

To obtain the results, data from three sources were analysed:

- Disk recording of several parameter of the vehicle, at the rate of 20 S/s, including position, speed, acceleration, pedals use, gear, steering wheel position, vehicle position in the lane, etc.
- Visual recording of the entire simulation, as performed by the simulator software.
- Information filled in questionnaires by the subjects.

From such data, besides a qualitative description of the driver's behaviour, the following values were calculated:

http://dx.doi.org/10.5772/63705

– Time, speed and position when a given event occurred (as reactions, actions, etc.).
– Time to collision (*ttc*) following a given event; time to collision is defined as the time needed to reach a given position (for instance an obstacle) if the speed is maintained constant; such value provides indications of the closeness of a danger situation, allowing for speed and distance; *ttc* of the vehicle relative to the pedestrian was calculated allowing for its actual position, since it can walk.
– Time between braking onset and maximum braking activation; it provides indications on how fast maximum braking action is obtained.
– Actual degree of emergency (ADE) shown in Eq. (1), combining speed (V), time to collision (ttc) and reaction time (t_R); it represents the constant deceleration that should be applied to stop just in front of the obstacle and is expressed as follows [15]:

$$ADE = \frac{V}{2 \cdot (ttc - t_R)} \tag{1}$$

In the present study, when *ttc* refers to the moment of braking onset, t_R is put equal to zero.

5. Results

All of the subjects had some reaction when approaching the pedestrian, but only 29 drivers out of 42 succeeded in carrying out a successful manoeuvre to avoid the collision. Usually, the drivers reacted by releasing the accelerator pedal and pressing the brake pedal; only two out of 29 successful drivers, after a short use of brakes, steered and avoided the obstacle (tests 31 and 34). None of the drivers chose to steer instead of braking. Thirteen drivers out of 42 hit the pedestrian (see **Table 4**): 50% in scenario A (without ADAS) and 23% in all the scenarios with ADAS. Of these only 4 out of 13 tried, while braking, to steer.

	Scenario A	Scenario B	Scenario C	Scenario D	Overall
Success	6	9	8	6	29
Failure	6	1	2	4	13
Total	12	10	10	10	42

Table 4. Number of failed and successful tests in different scenarios.

Tests without ADAS had higher speed at collision than those with ADAS, being in average 33.1 km/h (SD = 11.9 km/h) versus 22.4 km/h (SD = 9.4 km/h), with some statistical significance (P-value = 0.06 following the t-test [23]). As regards the functions of the simulated ADAS device, 4 out of 30 declared they did not hear the acoustic alarm, whereas 10 out of 10 saw the visual one.

5.1. Time of action and reaction

Time of action was determined by analysing the signal regarding pedals (brake and accelerator) and steering wheel. Every effort was put to identify the first action caused by the perception of a hazard. Approaching the obstacle an action on the brake was always detected; in the cases of scenarios with ADAS, sometimes the action on the accelerator was detected before the alarm was issued, mainly because the driver was prudently reducing the speed approaching an intersection with some traffic, so that the first action was considered braking; this happened 11 times out of 30.

Since the moment when the driver saw the pedestrian cannot be determined, it was not possible to obtain a reaction time following such event. In the cases of scenarios with ADAS, reaction time was here defined as the time interval between the alarm and the first successive action (on accelerator or brake); its mean value resulted to be 0.88 s.

An indication about the degree of emergency perceived by the driver can be the time difference between the first (releasing the accelerator) and the second action (pressing the brake pedal) $t_{A2} - t_{A1}$; the comparison between different scenarios, as well as the overall scenarios with ADAS, is shown in **Figure 5**. The *t*-test showed that there is no significant difference among the scenarios with ADAS (*P*-value > 0.5), whereas these last are significantly different from scenario A (no ADAS, *P*-value < 0.05).

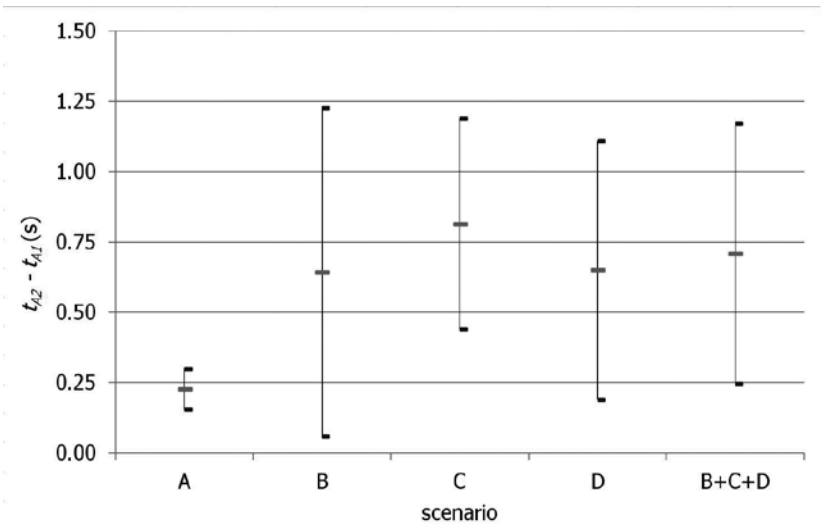

Figure 5. Mean values of $t_{A2} - t_{A1} \pm$ SD.

5.2. Time to collision

Time to collision [15] is the time at the end of which a collision will occur if speed does not change; in this study it was evaluated at the moment of the first action (release of accelerator) and the second action (braking). In **Figures 6** and **7**, mean values of both parameters are shown

http://dx.doi.org/10.5772/63705

together with their dispersion. Scenario A yielded a significantly lower value for ttc_{A1} (1.46 s vs. 2.52 s, *P*-value < 0.0001) as well for ttc_{A2} (1.34 s vs. 1.92 s, *P*-value < 0.01) in comparison to all the scenarios with ADAS.

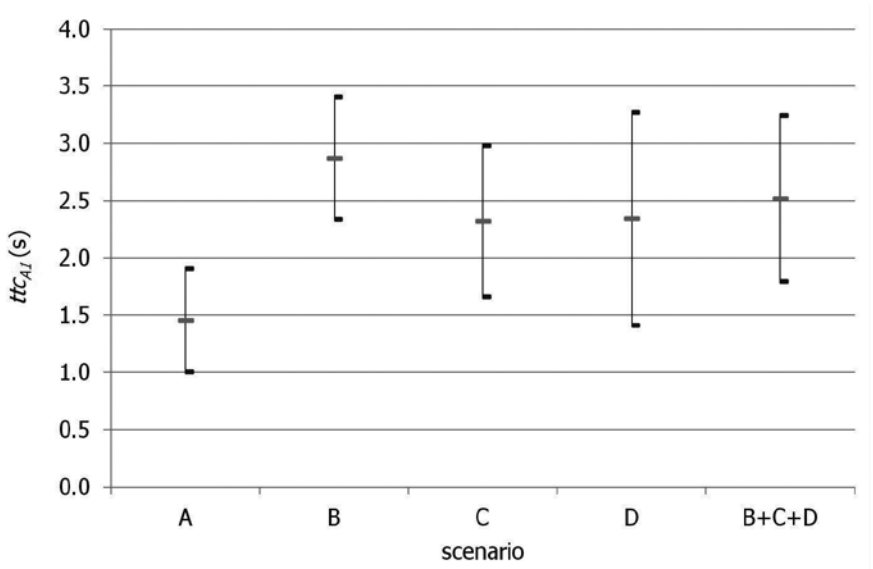

Figure 6. Mean values of ttc_{A1} ± SD.

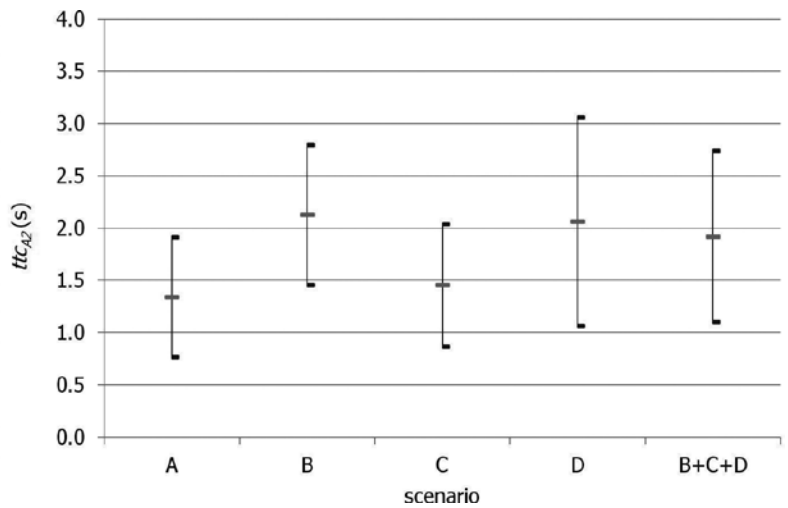

Figure 7. Mean values of ttc_{A2} ± SD.

Among the scenarios with ADAS, as expected, there were significantly higher values for scenario B as compared to scenario C as regards ttc_{A1} (2.87 vs. 2.32 s, *P*-value = 0.06) and above

all as regards ttc_{A2} (2.13 vs. 1.46 s, *P*-value = 0.03). No significant difference was found between scenarios C and D.

5.3. Braking

Braking represented, for 27 drivers out of 29, the first active actions attempted by successful drivers (as said, only two avoided the obstacle by steering only) since releasing the accelerator pedal, in itself, has a little effect on speed reduction. Braking is one of the actions that showed differences throughout the experimentation. In **Figure 8**, for instance, some typical modes of actions on the brake pedal are shown; they are related to the emergency braking approaching the pedestrian during four tests, two successful and two failed.

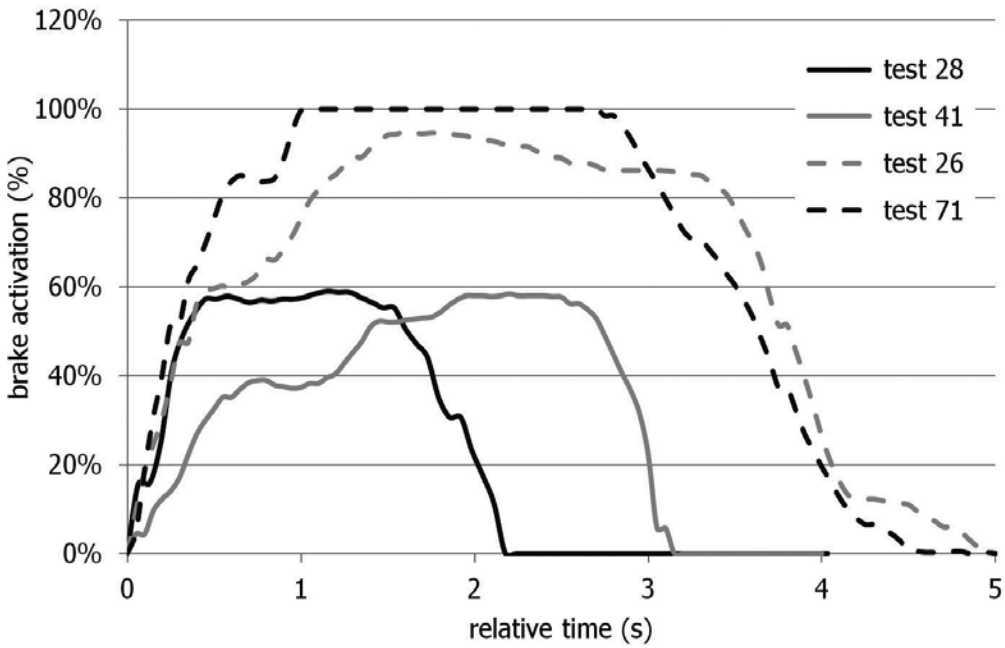

Figure 8. Typical emergency brake pedal activation; tests 28 and 41 were successful, and tests 26 and 71 were failed.

The main difference lies in the different time that the driver used to reach the maximum pedal activation. In order to characterise such difference, the parameter $t_{max} - t_{A2}$ is introduced, as the time difference between the beginning of the braking activation and the instant when the maximum action is reached. Such value could not be calculated for all the tests since in some failed tests the collision happened before the braking action reached a stabilised level. As shown in **Figure 9**, where $t_{max} - t_{A2}$ is plotted as a function of time to collision, a clear trend is visible, indicating that when *ttc* decreases, the action on the brake tends to be faster.

http://dx.doi.org/10.5772/63705

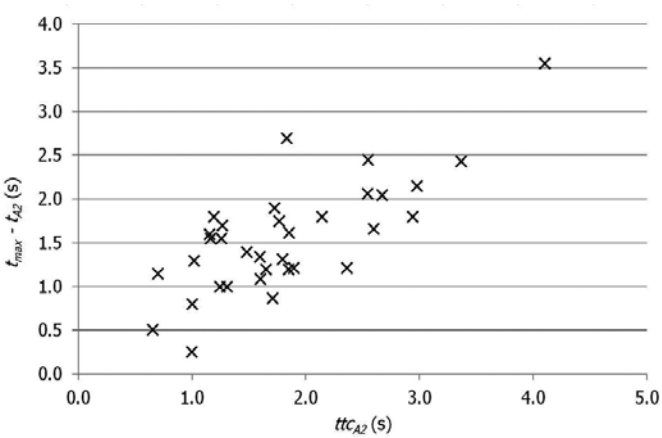

Figure 9. Trend of $t_{max} - t_{A2}$ as a function of time to collision.

As shown in **Figure 10**, $t_{max} - t_{A2}$ is also influenced by the presence of ADAS; scenarios with ADAS yielded significantly higher values than scenarios without ADAS (in average 2.03 s vs. 1.09 s, *P*-value < 0.001). As a consequence, part of the advantage afforded by ADAS devices (seen above, for instance, in terms of time to collision) is wasted because of a slower action on the brake pedal; trials that ended with a collision (indicated by a cross) are in some cases characterised by relatively high $t_{max} - t_{A2}$, indicating that a different braking approach could sometimes help avoiding the collision.

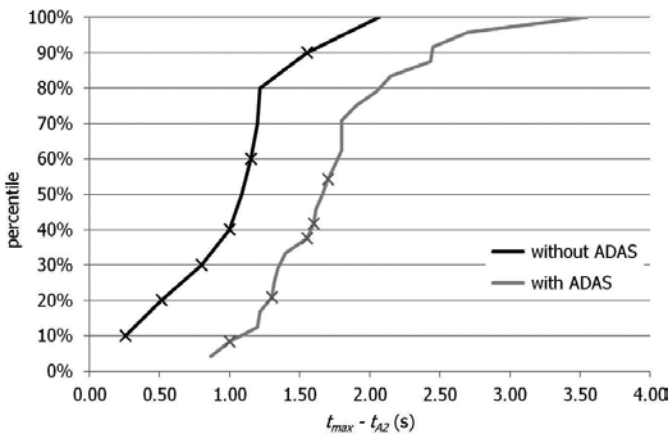

Figure 10. Cumulated distribution for $t_{max} - t_{A2}$ in tests with and without ADAS; the cross indicates a failed test.

5.4. Actual degree of emergency

The parameter *ADE* introduced above can provide indications on the degree of emergency (meant as the urgency to react) of a given hazardous situation, but also indicates if a manoeuvre

based on braking only can be successful, since the deceleration that a vehicle can experience is limited by the friction available.

In **Figure 11**, the cumulated distributions of actual degree of emergency corresponding to the action on the brake are shown, for failed and successful trials. A statistically relevant difference was identified between the two samples (in average 8.78 m/s^2 for the failed tests vs. 3.89 m/s^2 for the successful tests, *P*-value < 0.001). It is evident that it is impossible to stop before the collision when having *ADE* values near or greater than the maximum possible deceleration. Actually, the maximum value of ADE_{A2} that allowed a successful manoeuvre only acting on brakes was equal to 5.89 m/s^2; the cases with higher ADE (tests 31 and 34, highlighted in **Figure 11**) were successful only because a steering manoeuvre was performed.

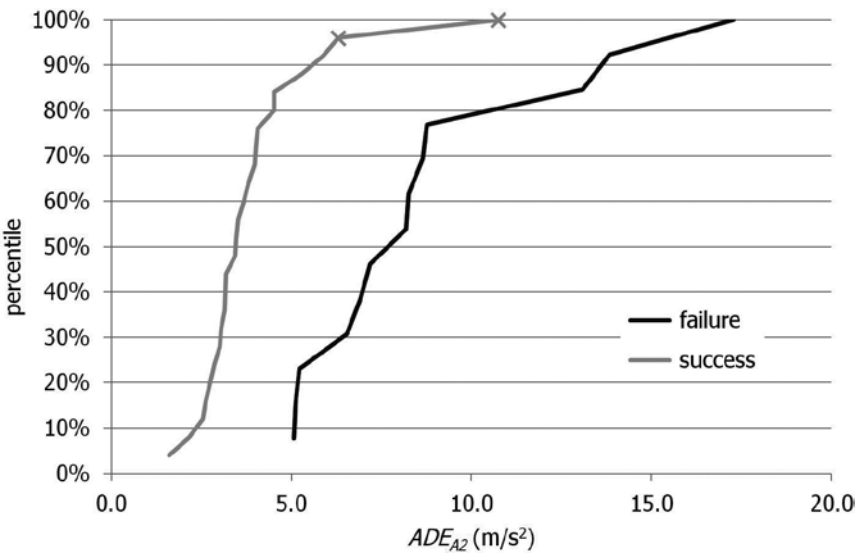

Figure 11. Cumulated distribution for ADE_{A2} in failed and successful tests. The cross indicates trials in which the driver avoided the obstacle by steering instead of braking (tests 31 and 34).

6. Conclusion

The effect of the presence of the ADAS was relevant since, for instance, it was capable to halve the percentage of collisions. Similarly, some of the other parameters that were examined showed clear advantages of using such device, as tt_{CA1}, tt_{CA2}, actual degree of emergency and speed at collision. Parameters as $t_{A2} - t_{A1}$ and $t_{max} - t_{A2}$, instead, showed that the presence of the ADAS could not prevent a slower execution of the required actions, perhaps caused by the anticipated perception of danger, so that sometimes it seemed that the driver was not capable of fully exploiting the advantages allowed by ADAS. In such cases, the use of further automation as autonomous braking or emergency brake assist (helping applying and maintaining the correct pressure on the brakes, already used by several manufacturers) will certainly help.

http://dx.doi.org/10.5772/63705

As regards the comparison between the different ADAS modes (scenarios B, C and D), the conclusions are less straightforward. Scenarios B and C have the same alert mode (a beep with increasing frequency), but in the latter it starts one second later. Consequently, in scenario C, time to collision is significantly lower, as well as $t_{max} - t_{A2}$, but no significant difference was identified as regards the other parameters, though always better. The advantage of an early alert seems, as expected, evident, and the risk of increasing the frequency of false positive in the attempt of anticipating the issue of the alarm must be carefully evaluated. As regards scenario D, in which a luminous rectangle framing the pedestrian was added to the same configuration of scenario C, no significant difference was noted, though all the drivers declared to have seen it but not everyone remembered to have heard the acoustic signal. Further experimentation and deeper comprehension is certainly necessary.

Author details

Dario Vangi[1], Antonio Virga[1*], Mattia Conigliaro[1], Hermann Steffan[2] and Ernst Tomasch[2]

*Address all correspondence to: antonio.virga@unifi.it

1 University of Florence, Florence, Italy

2 TU-Graz, Vehicle Safety Institute (VSI), Graz, Austria

References

[1] NHTSA. National Motor Vehicle Crash Causation Survey. 2008; DOT HS 811 059

[2] Society of Automotive Engineers. Taxonomy and Definitions for Terms Related to On-Road Motor Vehicle Automated Driving Systems. 2014; SAE International Standard J3016

[3] Merat N., Jamson A. H., Lai F. C. H., Daly M., Carsten O. M. J. Transition to manual: driver behaviour when resuming control from a highly automated vehicle. Transportation Research Part F. 2014;27:274–282. DOI: 10.1016/j.trf.2014.09.005

[4] Zeeb K., Buchner A., Schrauf M. What determines the take-over time? An integrated model approach of driver take-over after automated driving. Accident Analysis and Prevention. 2015;78:212–221. DOI: 10.1016/j.aap.2015.02.023

[5] Lewis B. A., Eisert J. L., Roberts D. M., Baldwin C. L. Designing Unambiguous Auditory Crash Warning Systems. Proceedings of the Human Factors and Ergonomics Society 58th Annual Meeting. 2014;58(1):2078–2082. DOI: 10.1177/1541931214581437

[6] Euro NCAP. TEST PROTOCOL—AEB systems, Version 1.0. 2013

[7] ISO. Intelligent transport systems—lane departure warning systems—performance requirements and test procedures. 2007; ISO International Standard No. 17361

[8] IEEE. IEEE Survey Reveals Mass-Produced Cars Will Not Have Steering Wheels, Gas/Brake Pedals, Horns, or Rearview Mirrors by 2035 [Internet]. 2014. Available from: http://www.ieee.org/about/news/2014/14_july_2014.html [Accessed: 2016-03-10]

[9] Fagnant D. J., Kockelman K. Preparing a nation for autonomous vehicles: opportunities, barriers and policy recommendations. Transportation Research Part A. 2015;77:167–181. DOI: 10.1016/j.tra.2015.04.003

[10] Schellekens M. Self-driving cars and the chilling effect of liability law. Computer Law & Security Review. 2015;31:506–517. DOI: 10.1016/j.tra.2015.04.003

[11] Čerka P., Grigiene J., Sirbikyte G. Liability for damages caused by artificial intelligence. Computer Law & Security Review. 2015;31:376–389. DOI: 10.1016/j.clsr.2015.03.008

[12] Kyriakidis M., Happee R., de Winter J. C. F. Public opinion on automated driving: results of an international questionnaire among 5000 respondents. Transportation Research Part F. 2015;32:127–140. DOI: 10.1016/j.trf.2015.04.014

[13] Payre W., Cestac J., Delhomme P. Intention to use a fully automated car: Attitudes and a priori acceptability. Transportation Research Part F. 2014;27:252–263. DOI: 10.1016/j.trf.2014.04.009

[14] Diels C., Bos J. E. Self-driving carsickness. Applied Ergonomics. 2016;53:374–382. DOI: 10.1016/j.apergo.2015.09.009

[15] Lechner D., Malaterre G. Emergency manuever experimentation using a driving simulator. SAE. 1991; SAE Paper 910016

[16] McGehee D. V., Mazzae E. N., Baldwin G. H. S. Driver reaction time in crash avoidance research: validation of a driving simulator study on a test track. In: Proceedings of the IEA/HFES 2000 Congress; 2000-07-29 to 2000-08-04; San Diego; 2000. pp. 320–323

[17] Schindler J., Cassani M. Using an integrated simulation environment for the risk based design of advanced driver assistance systems. Transportation Research Part F. 2013;21:269–277. DOI: 10.1016/j.trf.2013.09.018

[18] Belbachir A., Smal J.-C., Blosseville J.-M., Gruyer D. Simulation-driven validation of advanced driving-assistance systems. Procedia—Social and Behavioral Sciences. 2012;48:1205–1214. DOI: 10.1016/j.sbspro.2012.06.1096

[19] World Health Organization. Global status report on road safety 2015 [Internet]. 2015. Available from: http://www.who.int/violence_injury_prevention/road_safety_status/2015/en/ [Accessed: 2016-03-10]

[20] NHTSA. Traffic Safety Facts 2012. 2012; DOT HS 812 032

http://dx.doi.org/10.5772/63705

[21] Tomasch E., Steffan H. ZEDATU—Zentrale Datenbank tödlicher Unfälle in Österreich —A Central Database of Fatalities in Austria. In: ESAR—Expert Symposium on Accident Research; 2006; Hannover. 2006.

[22] Tomasch E., Steffan H. Retrospective accident investigation using information from court. In: TRA Transport Research Arena Europe; 2008; Ljubljana. 2008.

[23] Navidi W. Statistics for Engineers and Scientist. New York: McGraw-Hill; 2006.

Chapter 6

Flight Control Development and Test for an Unconventional VTOL UAV

Yang Wang, Changle Xiang, Yue Ma and Bin Xu

Additional information is available at the end of the chapter

http://dx.doi.org/10.5772/63355

Abstract

This chapter deals with the control system development and flight test for an unconventional flight vehicle, namely, a tandem ducted-fan experimental flying platform. The first-principle modeling approach combined with the frequency system identification has been adopted to obtain a high-fidelity dynamics model. It is inherently less stable and difficult to control. To accomplish the required practical flight tasks, the flying vehicle needs to work well even in windy conditions. Moreover, for flight control engineers, simple prescribed multi-loop controller structures are preferred. To handle the multiple problems, a structured velocity controller consisting of two feedback loops is developed, where inner loop provides stability augmentation and decoupling, and the outer loop guarantees desired velocity tracking performance. The simultaneous design of the two-loop controllers under multiple performance requirements in the usual H_∞ metrics can be cast as a nonsmooth optimization program. To compensate for changes in plant dynamics across the flight envelope, a smooth and compact polynomial scheduling formula is implemented as a function of the forward flight speed. Both simulations and flight test results have been presented in this work to showcase the potential for the proposed robust nonlinear control system to optimize the performance of UAV, specifically unconventional vehicles.

Keywords: unmanned ducted-fan aerial vehicle, system identification, robust flight control, nonsmooth optimization, gust alleviation

1. Introduction

Ducted-fan aerial vehicles (DFAVs) have attracted much more interest of the academic and industrial communities worldwide due to their compact layout and high-security applica-

tions in several tasks such as surveillance, data acquisition, and even physical interaction within unstructured environments. Among the different possible configurations, the vertical take-off and landing (VTOL) ducted-fan aircraft is well-suited for a variety of missions in environments cluttered with obstacles or close to infrastructures and humans. This fact is motivated mainly by the ducted-fan configuration in which the propeller is protected by an annular fuselage. In addition, a prominent advantage of ducted-fan system is better overall efficiency at low speeds [1]. In this respect, also inspired by the previous works considering test-fly methods in control [2, 3], the aircraft considered here is a tandem ducted-fan vehicle configuration characterized by a very simple mechanical structure, composed only of two tandem contra-rotating propellers inside the vehicle's fuselage, a number of control vanes which deviate the propeller's air flow in order to obtain full controllability of the attitude dynamics (see also [1, 4]) and a set of auxiliary "direct force control" with small lateral electric ducted fans (EDFs).

Drawing inspiration from the potential of the well-designed VTOL aircraft, the focus of this chapter is on the systematic modeling, flight control development, and implementation methods of the aerial vehicle named BIT-TDF at Beijing Institute of Technology (BIT). A number of contribution focuses on the problems of feedback control design for such a class of systems. In [5], a dynamic inversion controller is proposed to govern the nonlinear dynamics of a ducted-fan aircraft. In [6], a framework of nonlinear robust control based on a path following strategy is applied to a ducted-fan miniature UAV . A structured two-loop feedback controller combined with a static anti-windup compensator is proposed in [3] for a ducted-fan aircraft. However, few research laboratories are carrying out advanced theoretical and experimental works on the system; among others, to mention a few, the European Community under the 7th Framework Programme through collaborative projects AIRobots [7], the HoverEye project of autonomous ducted-fan aircraft [8], and the Martin Jetpack [9].

To actually show the potentials in a real application scenario, the overall system design of a fully functional UAV has to be validated experimentally using a real setup, especially the proposed control techniques. The object is to consider a robust flight control design for our small-scaled ducted-fan aircraft. The proposed methods have been tested either in simulation, experimental, or both frameworks where the implementation has been carried out using the ducted-fan UAV known as BIT-TDF.

Throughout the overall development of the UAV, deriving a high-fidelity nonlinear model has been a challenging issue due to their inherent instability and large amount of high-complexity aerodynamic parameters. After the hardware construction of the ducted-fan prototype, we first obtain a comprehensive flight dynamics model based on an elaborated approach which integrates first-principle and system identification techniques. The frequency-domain identification tool CIFER [10], which was developed by army/NASA Rotorcraft Division and is one of today's standard tools for identifying models of different aircraft configurations, has been used here to capture the key dynamics. With the identified model in hand, we then carry out to design a flight control system with two-loop architecture, in which an inner loop is for stabilization and decoupling the UAV dynamics and an outer loop is for desired velocity tracking performance. Specifically, we have combined (1) H_∞ technique; (2) nonsmooth

http://dx.doi.org/10.5772/63355

optimization algorithm; and (3) custom-defined gain-scheduling to design a nonlinear flight control law and successfully realized the automatic flight test.

2. Description and dynamics of the BIT-TDF system

The ducted-fan UAV of the Department of Mechanical Engineering of BIT is the BIT-TDF prototype (**Figure 1a**) developed by our team of researchers at Vehicle Research Centre (VRC). The front and aft propellers are enclosed within a protective carbon fiber duct to ensure safe operation of the vehicle in an indoor environment or close to building. The prototype uses a very simple, lightweight monocoque structure, producing an efficient and very durable design. The aerodynamic efficiency, in terms of additional thrust increase at the same power consumption, is improved by increasing the lip radius and decreasing the blade tip clearance. It uses eight 28-cm propellers for tandem ducted fans and standard RC motors and speed controllers. It is equipped with the COM Express Type 10 Mini Carrier Board CCG010, which is chosen as onboard flight control computer running at RT-Linux. The embedded computer system has a main processor running at 1.3 GHz, which can conveniently integrate all of necessary functions for data exchange with INS/GPS-based navigation system, servo-controller, and wireless modern, and a data acquisition board for RPM sensor. An 8-channel servo-controller (UAV100) is used to generate PWM signals necessary to drive the ducted-fan motors and the actuator servos. Custom-built real-time control software developed by the BIT VRC research group is used to real-time control the BIT-TDF.

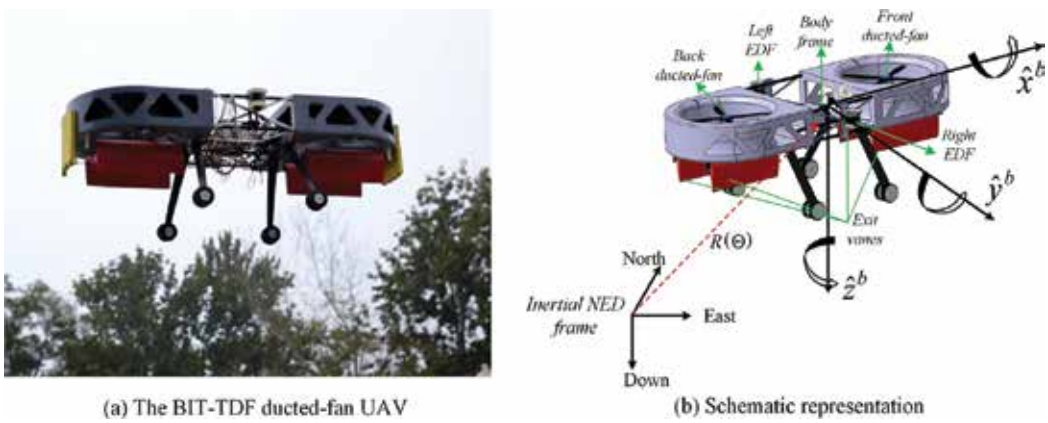

Figure 1. (a) The BIT-TDF ducted -fan UAV and (b) its schematic representation.

For ease of understanding, the block diagram of the entire UAV system is illustrated in **Figure 2**. From left to right, it is composed of three main parts:

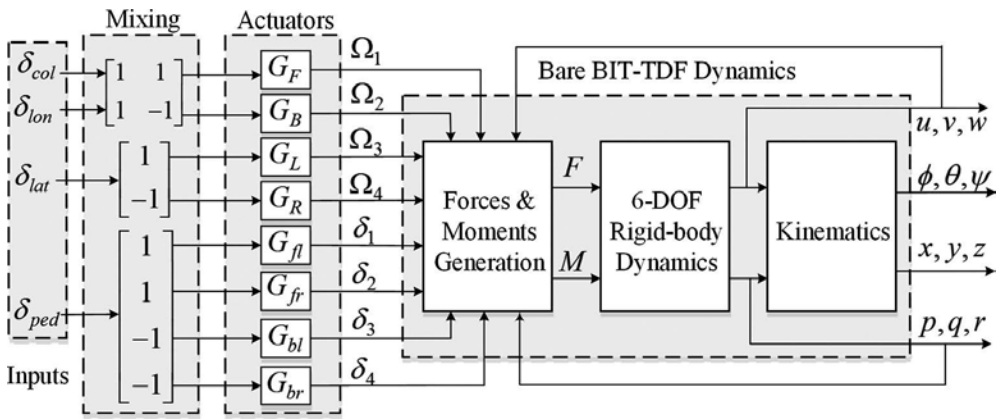

Figure 2. The system block diagram.

- The first part represents the actuators along with mixing function that converts conventional pilot inceptor inputs into a combination of exit vane deflections, and motor speed. The input to this part is $u = [\delta_{col}\ \delta_{lon}\ \delta_{lat}\ \delta_{ped}]^T$ which are pulse-width modulation (PWM) signals. The outputs are the vector $\Omega = [\Omega_1\Omega_2\Omega_3\Omega_4]^T$ representing the motor speed of front-aft ducted-fan propellers and left-right EDFs, in RPM, and the vector $\delta = [\delta_1\delta_2\delta_3\delta_4]^T$, representing the four exit vane deflections, in degrees.
- The second part is the force and moment generation mechanism block that relates the generated inputs to the applied lift, torques, and the aerodynamics acting on the system. This block corresponds to all the body components of the aircraft, that is, the tandem ducted-fan system, left-right EDFs thrust generation, vanes deflection system, and the fuselage drag part.
- The third part is the rigid-body dynamics that relates the applied force and moments to the attitude, velocity, and position of the BIT-TDF.

The subsequent sections present a comprehensive nonlinear flight model the ducted-fan aircraft.

2.1. Equations of motion for BIT-TDF

The following flight-dynamics equations of motion describes a general physical structure based on Newton-Euler formulism, and the reader is referred to any classical flight-mechanics references for a more complete development.

http://dx.doi.org/10.5772/63355

$$\begin{bmatrix}\dot{u}\\ \dot{v}\\ \dot{w}\end{bmatrix}=\begin{bmatrix}-wq+vr\\ -ur+wp\\ uq-vp\end{bmatrix}+\begin{bmatrix}-gsin\theta\\ gcos\theta sin\phi\\ gcos\theta cos\phi\end{bmatrix}+\frac{1}{m}\begin{bmatrix}F_{aero,x}\\ F_{aero,y}\\ F_{aero,z}\end{bmatrix}$$
$$\begin{bmatrix}\dot{p}\\ \dot{q}\\ \dot{r}\end{bmatrix}=J^{-1}\begin{bmatrix}qr(J_{yy}-J_{xx})\\ pr(J_{zz}-J_{xx})\\ pq(J_{xx}-J_{yy})\end{bmatrix}+J^{-1}\begin{bmatrix}M_{aero,x}\\ M_{aero,y}\\ M_{aero,z}\end{bmatrix} \quad (1)$$
$$\begin{bmatrix}\dot{\phi}\\ \dot{\theta}\\ \dot{\psi}\end{bmatrix}=\begin{bmatrix}1 & sin\phi tan\theta & cos\phi tan\theta\\ 0 & cos\phi & -sin\phi\\ 0 & sin\phi sec\theta & cos\phi sec\theta\end{bmatrix}\begin{bmatrix}p\\ q\\ r\end{bmatrix}$$

where u, v, and w are the velocities in the body frame, p, q, and r are the angular velocities in the body frame, m is the system mass, and J_{xx}, J_{yy} and J_{zz} are the moments of inertia along body-frame main axes. ϕ, θ, and ψ are the roll, pitch, and yaw Euler angles. F_{aero} and M_{aero} are the vector of external aerodynamic force and moments, respectively, which are given by

$$\begin{cases} F_{aero,x}=\sum_{i=1}^{2}\left(D_{mxi}-H_{xi}\right)+X_{fus}\\ F_{aero,y}=\sum_{i=1}^{2}\left(D_{myi}-H_{yi}\right)+Y_{fus}+\sum F_{vy}\\ F_{aero,z}=-\sum T_{f,a}+Z_{fus}+\sum F_{vz}-\sum T_{edf(l,r)}\\ M_{aero,x}=\sum_{i=1}^{2}PM_{xi}+\left(T_{edf(l)}-T_{edf(r)}\right)d_e+h_r\sum_{i=1}^{2}\left(D_{myi}-H_{yi}\right)+d_{zv}\sum F_{vy}+\sum_{i=1}^{2}(-1)^i R_{mx}\\ M_{aero,y}=\sum_{i=1}^{2}PM_{yi}+\left(T_f-T_a\right)d_r+h_r\sum_{i=1}^{2}\left(D_{mxi}-H_{xi}\right)+\sum_{i=1}^{2}(-1)^i R_{my}\\ M_{aero,z}=\sum_{i=1}^{2}(-1)^{i+1}Q_i+\sum F_{vy}d_{xv}+d_r\left(\sum_{i=1}^{2}(-1)^i H_{yi}\right)\end{cases} \quad (2)$$

where the index $i = 1$ for front ducted-fan, $i = 2$ for aft ducted-fan, D_m for the momentum drag, H for the hub force, $(\square)_{fus}$ for the fuselage, $\sum F_v$ for the exit vane, $T_{f,a}$ for the thrust of front and aft ducted-fan, $T_{ed(l)}$ and $T_{edf(r)}$ for the thrust of left and right EDF, PM for the duct pitching moment, R_m for the rolling moment of a propeller, Q for the propeller anti-torque moment, and the d_e, h_r, d_{zv} and d_{xv} are all the distance parameters related to torque. They are introduced in detail as follows.

2.1.1. Ducted-fan system forces and moments

The aerodynamic forces and moments are derived using a combination of ducted-fan inflow model and blade element theory. In ref. [1], one comprehensive and creative inflow model for computing ducted-fan thrust T and induced velocity v_i is proposed. Such procedure is based on some modifications of classic momentum theory inflow of an open propeller. For easier reference, we list the inflow model but there involves a revised derivation of the equation of conservation of energy.

An illustration of the inflow model is shown in **Figure 3**. The velocity vectors upstream of the propeller, at the disk of the propeller, and far downstream of the propeller are shown below.

$$\begin{cases} V_0 = V_0 cos\alpha i - V_0 sin\alpha j \\ V_R = V_0 \cos\left(\alpha^R\right) i - \left(V_0 \sin\left(\alpha^R\right) + v_i\right) j \\ V_\infty = V_0 \cos\left(\alpha^\infty\right) i - \left(V_0 \sin\left(\alpha^\infty\right) + v_\infty\right) j \end{cases} \tag{3}$$

The affected angles of attack, α^R and α^∞, are modeled as a function of the flow turning efficiency factors $k_{\chi R}$ and $k_{\chi\infty}$, which are given by

$$\begin{cases} \alpha^R = \alpha + k_{\chi R}\left(\dfrac{\pi}{2} - \alpha\right) \\ \alpha^\infty = \alpha + k_{\chi\infty}\left(\dfrac{\pi}{2} - \alpha\right) \end{cases} \tag{4}$$

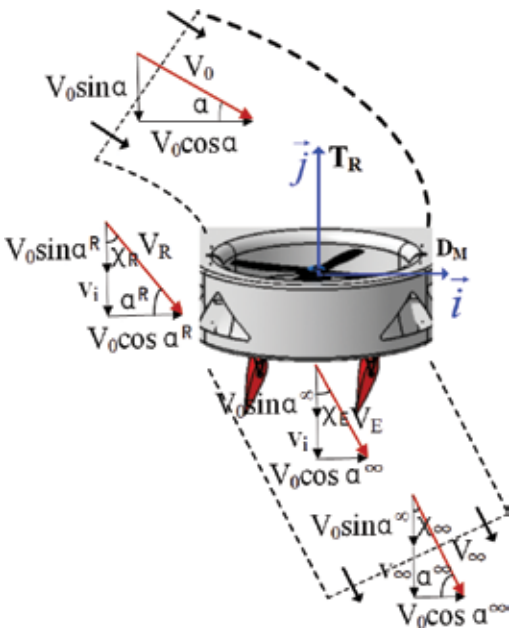

Figure 3. Inflow model illustration.

The thrust of ducted-fan system is a combination of propeller thrust T_R, and duct thrust T_D,

$$T = T_R + T_D = (1 + k_{aug})T_R \tag{5}$$

http://dx.doi.org/10.5772/63355

where k_{aug} is the thrust augmentation factor.

The mass flow rate of air through the duct is given by

$$\dot{m} = \rho A_D |V_R| \tag{6}$$

where ρ is the local air density and A_D is the duct area at the plane of the propeller.

By considering only the vertical component of conservation of momentum from free-stream flow to the far-wake flow, the expression for thrust is given by

$$T = \dot{m}((-\sin\alpha + \sin\alpha^{\infty})V_0 + v_{\infty}) \tag{7}$$

Similarly, considering only the horizontal component, the expression for momentum drag is found to be

$$D_m = \dot{m}(\cos\alpha - \cos\alpha^{\infty})V_0 \tag{8}$$

It is assumed that energy enters the ducted-fan system through the propeller thrust and the momentum drag. Therefore, a revised equation of increment in kinetic energy is formulated here that accounts for the contribution of the propeller thrust.

$$T_R\left(V_0 \sin\alpha^R + v_i\right) = \frac{1}{2}\dot{m}\left[\left(V_0 \sin\alpha^{\infty} + v_{\infty}\right)^2 - \left(V_0 sin\alpha\right)^2\right] \tag{9}$$

Substituting the Eq. (6) into (7), an expression is derived for the velocity v_{∞}. Another expression for the velocity v_{∞} is found by substituting the Eqs. (5) and (7) into (9). The final result after joint solution of the velocity v_{∞} is given as the newly formulated inflow equation.

$$T = 2\rho A_D\left[\frac{1}{1+k_{aug}}(V_0 \sin\alpha^R + v_i) - V_0 \sin\alpha\right]\sqrt{V_0^2 + 2V_0 V_i \sin a^R + v_i^2} \tag{10}$$

Based on the work of Gary Fay in Mesicopter project [10, 11], the aerodynamic forces and moments of rotating propeller are resolved using classic blade element theory. For convenience of the reader, we recall some symbols. σ: solidity ratio, $c_{l\alpha}$: lift slope, λ: inflow ratio, μ: advance ratio, R: propeller radius, $\overline{C_d}$: averaged drag coefficient, θ_0: pitch of incidence, θ_{tw}: twist pitch. Thrust force T_R is the resultant of the vertical forces acting on all the blade elements.

$$\begin{cases} T_R = C_T \rho A_D (\Omega R)^2 \\ \dfrac{C_T}{\sigma C_{l\alpha}} = \left(\dfrac{1}{6} + \dfrac{1}{4}\mu^2\right)\theta_0 - \left(1+\mu^2\right)\dfrac{\theta_{tw}}{8} - \dfrac{1}{4}\lambda \end{cases} \tag{11}$$

Hub force H is the resultant of horizontal forces acting on all the blade elements.

$$\begin{cases} H = C_H \rho A_D (\Omega R)^2 \\ \dfrac{C_H}{\sigma C_{l\alpha}} = \dfrac{1}{4a}\mu\overline{C_d} + \dfrac{1}{4}\lambda\mu\left(\theta_0 - \dfrac{\theta_{tw}}{2}\right) \end{cases} \tag{12}$$

The propeller anti-torque moment Q is caused by the horizontal forces acting on the propeller that are multiplied by the moment arm and integrated over the propeller.

$$\begin{cases} Q = C_Q \rho A_D (\Omega R)^2 R \\ \dfrac{C_Q}{\sigma C_{l\alpha}} = \dfrac{1}{8a}\left(1+\mu^2\right)\overline{C}_d + \lambda\left(\dfrac{1}{6}\theta_0 - \dfrac{1}{8}\theta_{tw} - \dfrac{1}{4}\lambda\right) \end{cases} \tag{13}$$

Rolling moment R_m of a propeller exists in forward flight when the advancing blade is producing more lift than the retreating one.

$$\begin{cases} R_m = C_{R_m} \rho A_D (\Omega R)^2 R \\ \dfrac{C_{R_m}}{\sigma C_{l\alpha}} = \mu\left(\dfrac{1}{6}\theta_0 - \dfrac{1}{8}\theta_{tw} - \dfrac{1}{8}\lambda\right) \end{cases} \tag{14}$$

Once the thrust created by the ducted-fan system is determined from (11), the quasi-steady induced velocity is found by iterating the inflow Eq. (10), and vice versa. A simple bisection algorithm is implemented here to obtain the thrust and induced velocity. Consequently, all the forces and moments of ducted-fan system are solvable.

2.1.2. Control vanes forces and moments

The exit control vanes are modeled as all-moving control surfaces that operate in the wake generated by the propellers, and provide yaw attitude control and thrust augmentation. To model those forces and moments, we refer to our mixing schematic shown in **Figure 4** (also shown in the "mixing" block of **Figure 2**). First, we will consider all the forces generated by each vane, and then, we will consider the resultant contributions that affect the yaw dynamics. Let us denote by $i = 1, \ldots 4$ the each vane. There resulting force F_v and an induced moment Γ_v are given by

http://dx.doi.org/10.5772/63355

$$\begin{cases} F_v = \sum_{i=1}^{4}\left(F_{vyi} + F_{vzi}\right), \Gamma_v = \sum_{i=1}^{4} d_i \times F_{vi} \\ F_{vy} = L\cos\alpha_0 + D\sin\alpha_0, F_{vz} = -L\sin\alpha_0 + D\cos\alpha_0 \\ L = \frac{1}{2}\rho V_E^2 S_v C_{lv}\left(\alpha_v\right), D = \frac{1}{2}\rho V_E^2 S_v D_{lv}\left(\alpha_v\right) \end{cases} \tag{15}$$

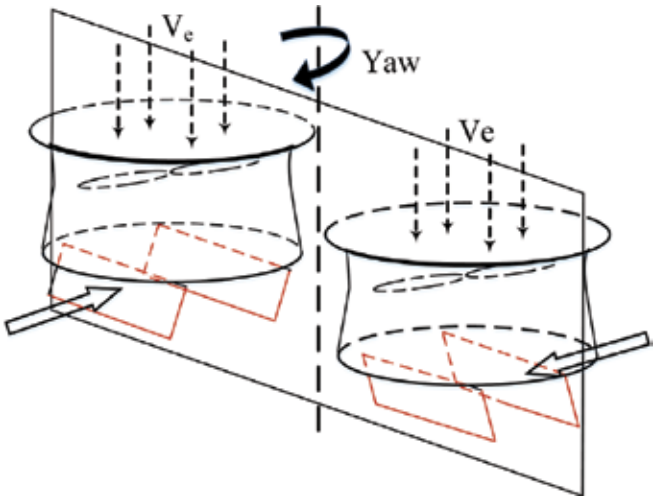

Figure 4. Exit vanes used to govern yaw attitude.

where F_{vy} and F_{vz} are the aerodynamic forces projected into the body-fixed frame, α_0 is the flow deflection angle and the induced moment Γ_v can be decomposed into the components $d_{zv}\,\Sigma\,F_{vy}$ and $\Sigma\,F_{vy}\,d_{xv}$ in (2).

2.1.3. Fuselage forces

There are always drag forces caused by the fuselage and have to be modeled. The fuselage drag model is a key element in the correlation with flight-test data. A function is integrated into the simulation model that calculates the fuselage drag forces along three body frame axes, which is given by

$$\begin{cases} X_{fus} = \frac{-1}{2}\rho S_{fx}\left|u_a\right|u_a \\ Y_{fus} = \frac{-1}{2}\rho S_{fy}\left|v_a\right|v_a \\ Z_{fus} = \frac{-1}{2}\rho S_{fz}\left|w_a\right|w_a \end{cases} \tag{16}$$

where S_{fx}, S_{fy}, and S_{fz} are the effective drag area in the x_b, y_b, and z_b direction.

2.1.4. Lateral EDF thrust

The two lateral small electric ducted-fans are responsible of controlling the roll attitude dynamics, regulating differential thrust on the EDFs. Specifically, a positive control input results in increased thrust on the left EDF and a decrease thrust on the right one. It should be mentioned that the previous prototype BIT-TDF in [12, 13] is a vane control mixing version, which means roll and yaw control are all achieved by deflecting the exit vanes in a mixing way. This compact VTOL vehicle was tested extensively by our research group. Although it realized basic stabilization flight, it exhibited some serious operational limitations, the most notable being its poor stability and controllability in windy conditions. Therefore, a set of auxiliary "direct force control" with small EDFs are mounted on the current prototype (see **Figure 1**) to optimize the system's maneuverability. Controllability analysis and recent flight-test demonstrate that the overall performance of the newly constructed configuration has been significantly improved.

The generated thrust T_{edf} of the EDF is related to the PWM input u_{pwm} by a first-order linear transfer function:

$$T_{edf} = \frac{K_{edf}}{\tau_e s + 1} u_{pwm} \tag{17}$$

where K_{edf} is a positive gain and τ_e is the time constant of EDF.

2.1.5. Duct pitching moment

Perhaps the most challenging issue of ducted-fan system over conventional configuration is the strong nose-up pitching moment produced by the duct in edgewise flight or in presence of cross-wind. The duct pitching moment is caused by the dissymmetry lift of the duct due to the unequal flow experienced by the front and aft sections of the duct. This moment makes the vehicle so unstable that even an experienced pilot would not be able to hold it steady in flight without a stability and control augmentation system (SCAS). A meaningful observation by [1] stated that the pitching moment may be a function of airspeed, angle of attack, advance ratio, and inflow velocity. According to the experimental data in [8], the pitching moment model is implemented solely as a parabolic function of the relative airspeed for simplicity, which can be written as

$$PM = \varepsilon_c V_0 + \varepsilon_x V_0^2 \tag{18}$$

where V_0 is the relative airspeed, ε_c and ε_x are the constant coefficients to be determined.

2.1.6. Actuator dynamics

Four linear servo-actuators are used to control the vane deflections, while the front and aft electronic speed controllers (ESCs) are used to control the speed of motor-propellers. The

http://dx.doi.org/10.5772/63355

lateral EDF dynamics has been addressed in Section 2.1.4. The dynamics of all actuators can be identified in ground tests with an input of the actuator command and an output of the actuator response or the control surface deflection. However, in our case, an artificial control mixing function was used and we would like to explicitly account for this block. After examination of the respective frequency responses of the four control input channels, we see that a first-order system should adequately capture the dynamics. The corresponding differential equations are as follows:

$$\begin{cases} \dot{m}_f = \dfrac{-1}{\tau_m} m_f + Z_{col}\delta_{col} + M_{lon}\delta_{lon} \\ \dot{m}_r = \dfrac{-1}{\tau_m} m_r + Z_{col}\delta_{col} - M_{lon}\delta_{lon} \\ \dot{\alpha}_v = \dfrac{-1}{\tau_v} \alpha_v + N_{ped}\delta_{ped} \\ \dot{\beta}_e = \dfrac{-1}{\tau_e} \beta_e + L_{lat}\delta_{lat} \end{cases} \tag{19}$$

where the states m_f and m_r are the speed of front and aft motor-propellers, α_v is the vane deflection command that is converted into a combination of four exit vane deflections, and the last state β_e denotes the thrust of lateral EDF, and the corresponding time constants are τ_m, τ_v, and τ_e. The effective linkage gains of four input channels (Z_{col}, M_{lon}, N_{ped}, and L_{lat}) completely depend on the defined usable range of physical inputs that correspond to the normalized inputs in the range [−1, 1]. The equations for the effective linkage gains are as follows:

$$\begin{cases} \delta_{col} \in [-1,1] \Leftrightarrow [-1,1] * Z_{col}\tau_m * \pi / 30(rpm) \\ \delta_{lon} \in [-1,1] \Leftrightarrow [-1,1] * M_{lon}\tau_m * \pi / 30(rpm) \\ \delta_{ped} \in [-1,1] \Leftrightarrow [-1,1] * N_{ped}\tau_v(\deg) \\ \delta_{lat} \in [-1,1] \Leftrightarrow [-1,1] * L_{lat}\tau_e(N) \end{cases} \tag{20}$$

2.2. Identification of model parameters

From the above analysis, a full 15th-order nonlinear dynamic model can be obtained and a linear model of the BIT-TDF at the prescribed flight condition can also be extracted. We have implemented an integrated identification procedure to identify all the physical parameters. Using global optimization methods, the extracted lineal models can be utilized to tune the unknown physical parameters of the nonlinear model to match frequency responses from flight tests, which delivers a very accurate nonlinear model suitable for flight simulations, and linear models adequate for control design.

The focus of this section is on the identification results obtained by the particular CIFER tool. The frequency-domain system identification method allows for rapid updating of the vehicle

response model as changes are made to the unconventional UAV designs by repeating flight tests. At first, the description of the experimental setup is given. The parameterized model with the associated stability derivatives is also provided. Then, the final results of the identification procedure follow. Finally, the accuracy of the extracted model is validated in the time domain.

2.2.1. Experimental platform

The experimental platform, as depicted in **Figure 5**, includes an onboard flight control computer, an INS/GPS module, a sonar sensor, four high-speed brushless DC ESCs, a servo-controller, a pair of free-wave wireless data transceivers, and a ground station. The pair of transceivers establish communication between the onboard system and the ground station. The onboard system is to collect sensor data, process and fuse them, feed to the control law, send the servo-driving signals to realize desired control mode. The C code is programmed, complied, and then downloaded to the onboard system and ground system to perform specific tasks.

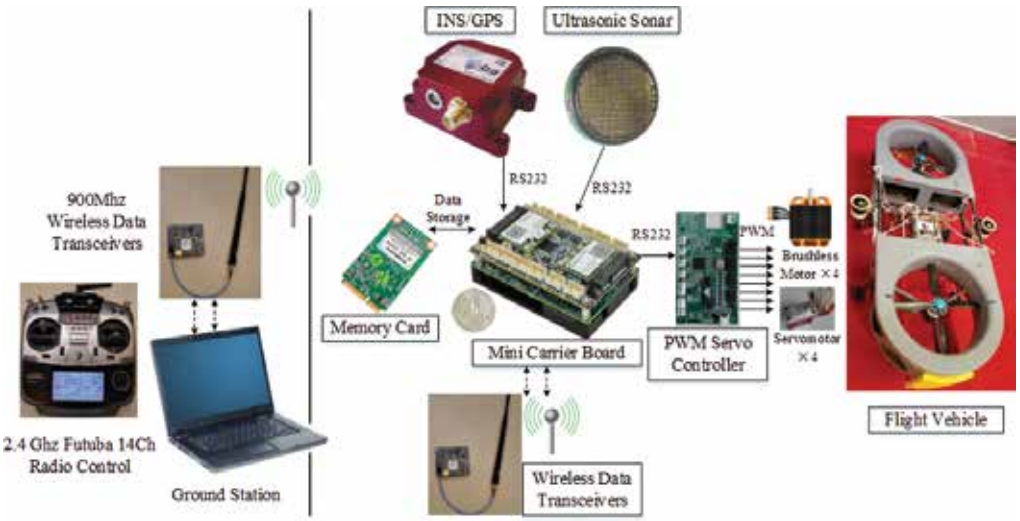

Figure 5. Block diagram of the experimental platform.

2.2.2. Parameterized state-space model

The model structure of the BIT-TDF consists of 12 states. These states include eight rigid-body states and four explicit states for the actuator dynamics. The final structure is obtained first systematically eliminating the derivatives that have high insensitivity and/or high Cramer-Rao bound and then refining the model in a similar process in [14]. **Figure 6** shows the system matrix A and the input matrix B of the minimum parameterized model structure.

http://dx.doi.org/10.5772/63355

$$A=\begin{bmatrix} X_u & 0 & 0 & 0 & X_q & 0 & 0 & -g & 0 & 0 & 0 & 0 \\ 0 & Y_v & 0 & Y_p & 0 & 0 & g & 0 & 0 & 0 & 0 & 0 \\ Z_u & Z_v & Z_w & Z_p & Z_q & Z_r & Z_\phi & Z_\theta & Z_{m_f} & Z_{m_r} & Z_{\alpha_v} & 0 \\ 0 & L_v & 0 & L_p & 0 & 0 & 0 & 0 & 0 & 0 & 0 & L_{\beta_e} \\ M_u & 0 & 0 & 0 & M_q & 0 & 0 & 0 & M_{m_f} & M_{m_r} & 0 & 0 \\ 0 & 0 & 0 & 0 & N_q & N_r & 0 & 0 & N_{m_f} & N_{m_r} & N_{\alpha_v} & 0 \\ 0 & 0 & 0 & 1 & 0 & 0 & 0 & 0 & 0 & 0 & 0 & 0 \\ 0 & 0 & 0 & 0 & 1 & 0 & 0 & 0 & 0 & 0 & 0 & 0 \\ 0 & 0 & 0 & 0 & 0 & 0 & 0 & 0 & -1/\tau_m & 0 & 0 & 0 \\ 0 & 0 & 0 & 0 & 0 & 0 & 0 & 0 & 0 & -1/\tau_m & 0 & 0 \\ 0 & 0 & 0 & 0 & 0 & 0 & 0 & 0 & 0 & 0 & -1/\tau_v & 0 \\ 0 & 0 & 0 & 0 & 0 & 0 & 0 & 0 & 0 & 0 & 0 & -1/\tau_e \end{bmatrix} \quad B=\begin{bmatrix} 0 & 0 & 0 & 0 \\ 0 & 0 & 0 & 0 \\ 0 & 0 & 0 & 0 \\ 0 & 0 & 0 & 0 \\ 0 & 0 & 0 & 0 \\ 0 & 0 & 0 & 0 \\ 0 & 0 & 0 & 0 \\ 0 & 0 & 0 & 0 \\ Z_{col} & 0 & M_{lon} & 0 \\ Z_{col} & 0 & -M_{lon} & 0 \\ 0 & 0 & 0 & N_{ped} \\ 0 & L_{lat} & 0 & 0 \end{bmatrix}$$

Figure 6. System and input matrix for the state-space model.

The above-parameterized model provides a physically meaningful description of the system dynamics. All stability derivatives included in this model are related to kinematic and aerodynamic effects of the ducted fans, exit vanes and the fuselage. The challenge is the determination of their arithmetic values.

2.2.3. Identification setup

As shown in **Figure 7**, the data-collection experiment is performed in closed-loop with an external SCAS engaged. The reason for the closed-loop experiment arises from that the BIT-TDF is lightly damped and inherently unstable. When the ducted-fan vehicle is set to hover, we inject a set of computerized frequency sweep excitation signal to one of the four control inputs. The resulting control signals along with their corresponding output responses are inserted into the CIFER software which processes the time domain experimental data to produce a high quality multi-input multi-output (MIMO) frequency response pairs. For our BIT-TDF vehicle, the selected frequency responses and their frequency ranges are depicted in **Table 1**.

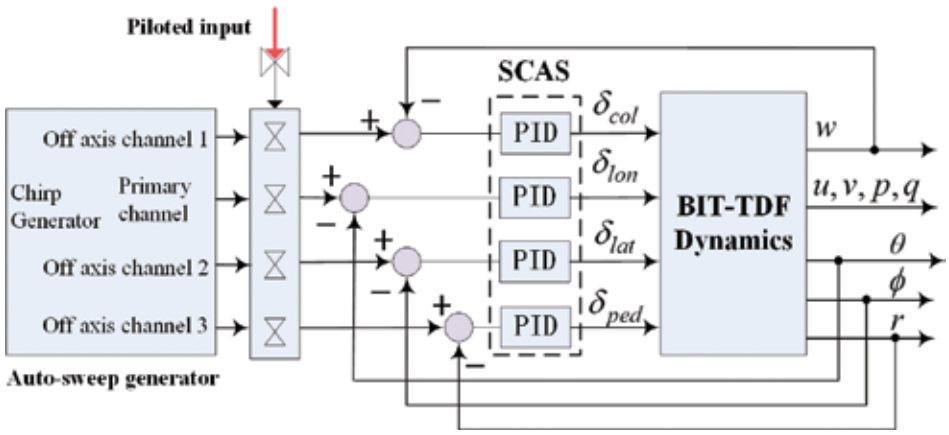

Figure 7. Schematic diagram of data collection in the closed-loop setting.

	δ_{col}	δ_{lon}	δ_{lat}	δ_{ped}
u	—	0.3–15	—	—
v	—	—	0.3–26	—
w	0.3–28	—	—	—
p	—	—	0.3–28	—
q	—	0.3–26	—	—
r	—	0.3–24	—	0.3–28
ϕ	—	—	0.3–28	—
θ	—	0.3–28	0	—

Table 1. Selected frequency-response ranges (rad/s).

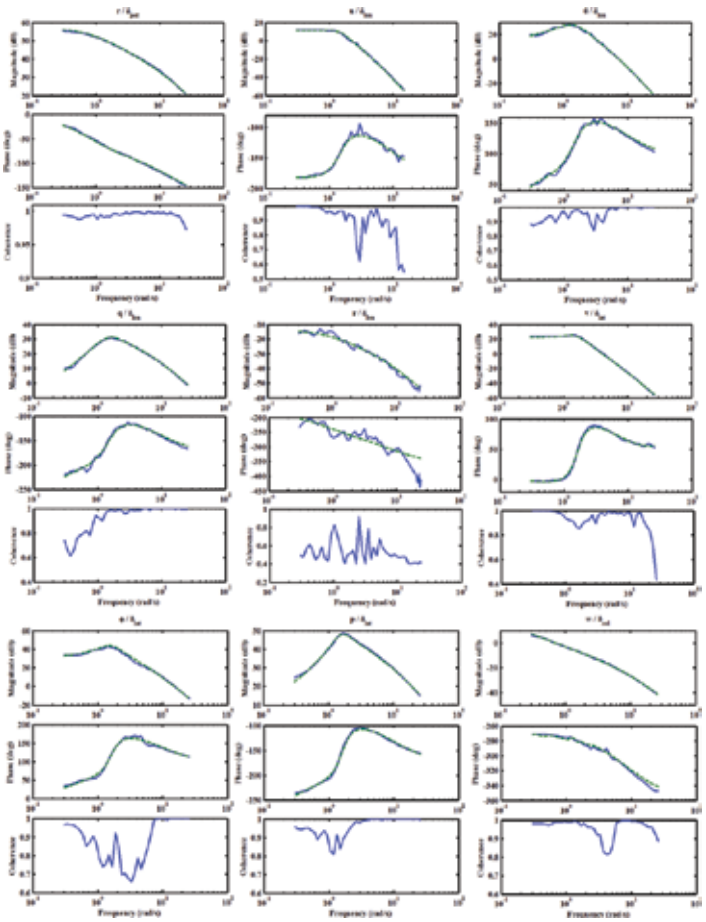

Figure 8. Frequency responses for the flight data (solid line) and frequency responses predicted by the state-space model (dashed line).

http://dx.doi.org/10.5772/63355

The extraction of the parametric model is an iterative procedure, which continues until difference between the actual and simulation frequency responses is minimized as shown in **Figure 8**. The identification results illustrate the system can be well characterized as a linear process in the interested frequency range. Note that the parameters in the model structure have been designated as the following four categories:

- Fixed parameters known as a priori;
- Constrained parameters with constraint equations to enforce commonality and kinematic interrelationship;
- Isolated parameters that is difficult to achieve a satisfactory identification;
- Free parameters to be determined in the course of the identification.

CIFER results	Descriptions	CR bound (%)	Insensitivity (%)
X_u =−0.2752	Longitudinal speed-damping derivative	2.069	2.033
Y_v =−0.4710	Lateral speed-damping derivative	8.905	3.491
Y_p = 0.246	Roll rate damping derivative	26.17	11.45
Z_ϕ = −0.5	Vertical stability derivative of roll attitude	10.09	9.07
$Z_{m_f} = -0.0025$	Vertical stability derivative of propeller speed	5.413	4.7034
$L_v = -0.5452$	Lateral speed stability derivative	7.189	3.525
L_p =−0.7955	Roll rate stability derivative	23.29	8.404
L_{β_e} = 0.8231	Stability derivative of lateral EDF thrust	7.507	3.104
M_u =0.3410	Longitudinal speed stability derivative	2.072	2.031
M_q =0.1275	Pitch rate stability derivative	7.084	5.038
M_{m_f} = 0.0065	Longitudinal stability derivative of propeller speed	8.094	6.039
N_r =−0.7941	Yaw rate stability derivative	8.322	3.348
N_{m_f} = 0.0005	Yaw stability derivative of propeller speed	5.964	3.819
N_{α_v} = 0.4257	Yaw stability derivative of vane deflection	10.64	2.829

Table 2. Parameters identified using CIFER.

Some physical parameters, such as gravity and actuators-related parameters (determined from input-output ground tests), are known as a priori and should be fixed. Some stability derivatives in system matrix exist constrained relationships due to the symmetrical configuration, such as $Z_{m_f} = Z_{m_r}$, $M_{m_f} = -M_{m_r}$. There are also some parameters difficult to identify due to poor low-frequency excitation and they can be obtained based on the static trim estimation. The

remaining free parameters for our vehicle are listed in **Table 2**, from which it is clear that all the parameters identified using CIFER are highly accurate.

2.2.4. Time-domain validation

Time-domain is more straightforward for evaluating the predictive capability of the identified model for test inputs, such as steps or doublets that are dissimilar with the ones used in the identification process. Four individual flight records are collected, each corresponding to one of the test inputs. The recorded inputs are used as inputs to the identified model, and the ducted-fan vehicle's responses predicted by the model are compared to the responses recorded during the flight tests. The comparison results are depicted in **Figure 9**, which indicates an excellent fit between the predicted values from the identified model and the flight data.

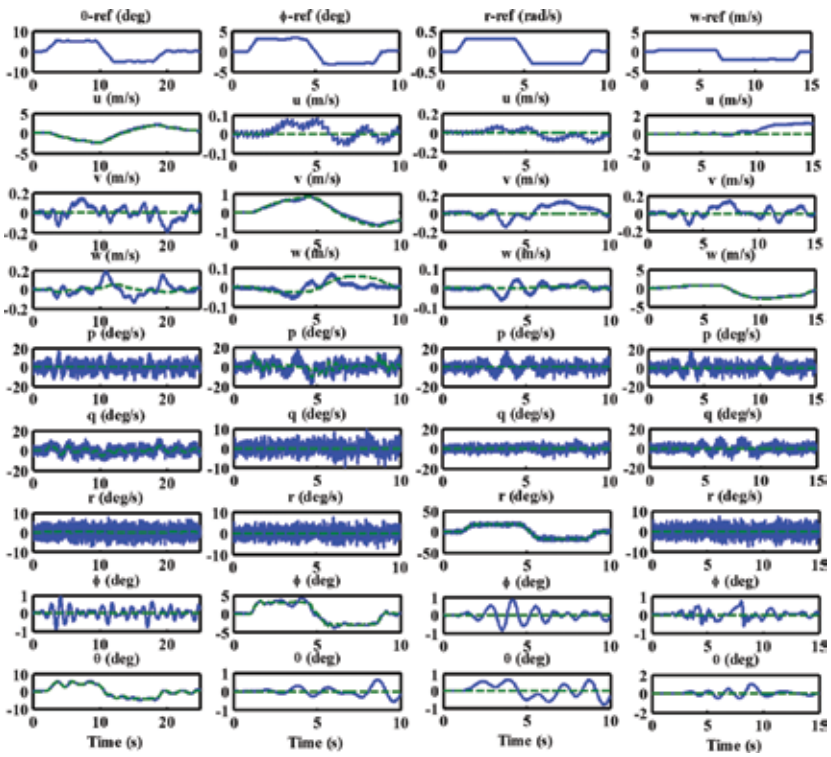

Figure 9. Time-domain validation.

3. Robust flight control system design

During the BIT-TDF project, we explored several control approaches from theoretical development to final experiments. After the evaluation of all the control approaches tested in this

http://dx.doi.org/10.5772/63355

project, it becomes clear that the way to follow is the systematic application of the structured robust control based on nonsmooth optimization algorithm. In fact, the newly developed nonsmooth optimization algorithm in [15] is well suited for robust control synthesis of the cascaded structure of the ducted-fan dynamics. Moreover, the fixed-structure controller is easy to implement and fine-tune within a standard flight control infrastructure based on PID feedback terms or low-order terms. In addition, the robust framework is able to elegantly reject strong disturbances and easily extended to robust gain scheduling control. After a phase of extensive simulation and experimentation, the structured robust control was proposed as a single approach for flight control system design.

3.1. Feedback control configuration

The key task of the control system is to regulate the flight velocity of the vehicle to a desired value and keep it irrespectively of the exogenous wind disturbances. However, as a matter of fact, there is a potentially countless kinds of control structure to achieve the control task. From the perspective of engineering implementation, decentralized collections of simple control elements such as PIDs, static gains, structured, or limited-complexity controllers are preferred. Moreover, it is known that most practical problems can be controlled by low-order controllers with good performance. In this context, we chose the very simple control architecture, shown in **Figure 10**, which consists of two feedback loops. The inner loop (static output feedback), being fully actuated, provides stability augmentation and channel decoupling. The outer loop (four PI controllers), cascaded with inner loop, is in charge of regulating the inner loop in such a way that provides proper attitude variables as virtual inputs to velocity outer loop to asymptotically approach the desired velocity references.

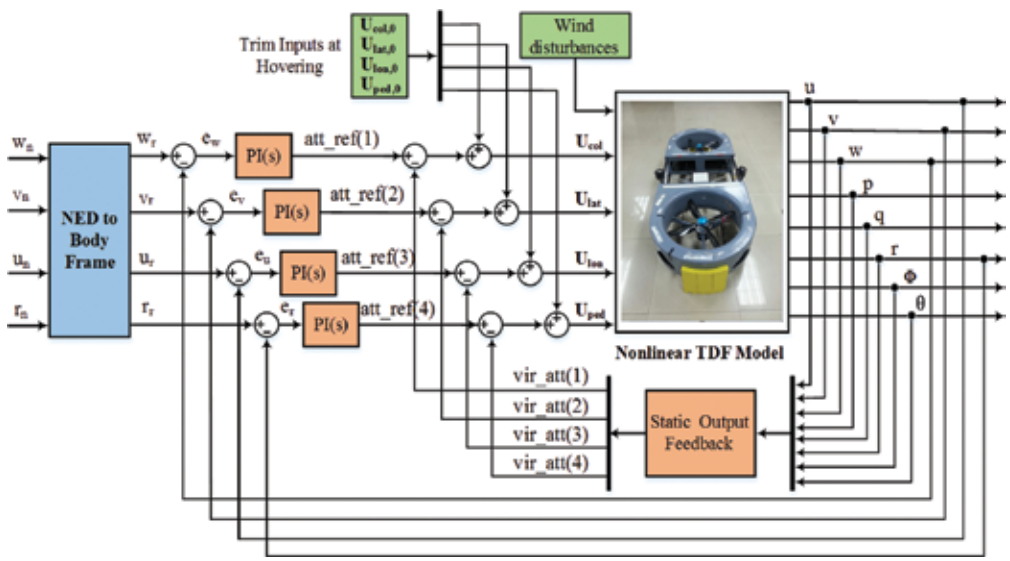

Figure 10. Feedback control configuration.

3.2. Gain scheduling compensation

The control task is complicated by the fact that the plant dynamics are nonlinear throughout the flight envelope, so the flight controllers must be adjusted as a function of flight speed, which is also called the scheduling variable. As for TDF, we have selected the equilibrium conditions for five flight conditions which are corresponding to the forward flight speed u = 0, 2.5, 5, 7.5, and 10 m/s, respectively, and linearized the flight dynamics around each equilibrium. Motivated by [16], we combine the linear controllers design and the scheduled process by parameterizing the controller gains as low-order polynomials in forward flight speed and directly tuning the polynomial coefficients for the desired envelope. This approach results in a compact scheduling formula and guarantees smooth gain variations. More specifically, we use a quadratic polynomials for the four PI gains

$$K_j(V) = K_{j0} + K_{j1}V + K_{j2}V^2 \tag{21}$$

where the three coefficients K_{j0}, K_{j1} and K_{j2} are tunable parameters, and V is the forward flight speed. We use a simple first-order polynomials for the static output feedback matrix

$$SF(V) = SF_0 + SF_1V \tag{22}$$

3.3. Design of the structured controller

Using simple block diagram manipulations, we can transfer the initial control architecture of **Figure 10** into a design-oriented form as illustrated by **Figure 11**, which is known as the standard lower linear fractional transformation (LFT). Two exogenous inputs, wind disturbances and reference signals, are gathered in W, and exogenous performance-related outputs,

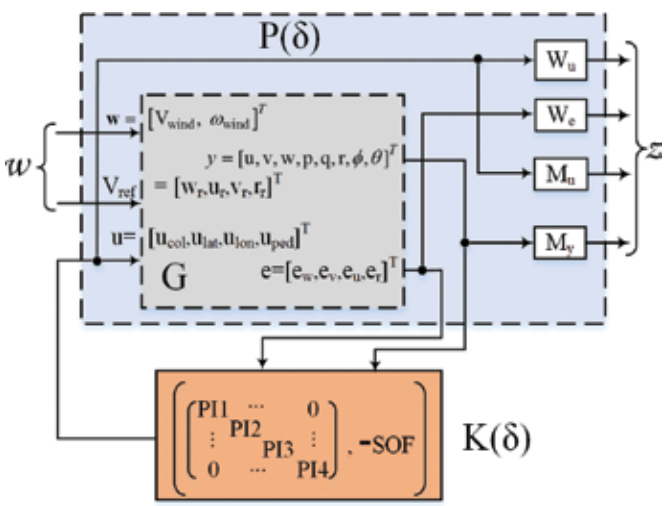

Figure 11. LFT of an augmented system and a structured controller.

http://dx.doi.org/10.5772/63355

the weighted error signals and actuator effort signals, are gathered in *Z*. δ denotes the gain scheduling variable, which is the forward flight speed in our design case. *P* is the augmented linear parameter-varying plant composed of the original plant dynamics and the weight filters used to express the control objectives. K is the controller to be designed and scheduled as a function of δ. The structured controller K is just a reformulation of the architecture described in **Figure 10**. That is, the outer-loop PIs and inner-loop static output feedback form the components 4-by-4 diagonal PI block and the negative constant matrix-SOF, respectively, of the compound controller K.

The H_∞ control problem is formulated as the following program

$$\begin{gathered} minimize \| F_l(P,K) \|_\infty \\ subject\ to\ K\ stabilizes\ P\ internally \\ K \in a\ controller\ space\ \mathsf{K} \end{gathered} \tag{23}$$

It should be emphasized that when smaller and more practical controller space *K* are chosen as in the compound controller K, the problem (23) is much harder to solve and this is exactly the reason for adoption of nonsmooth optimization techniques.

For good tracking accuracy, the weights associated with each outputs should include integral action at low-frequency range and a finite gain at high frequencies is useful in reducing overshoot. Therefore, the following high-gain low-pass filters are selected

$$W_e = diag\left\{\frac{0.1}{s+10^{-4}}, \frac{0.01}{s+10^{-4}}, \frac{0.01}{0.05s+10^{-4}}, \frac{0.21}{0.4s+10^{-4}}\right\} \tag{24}$$

For attenuating noise, increasing robustness to unmodeled dynamics, and preventing high-frequency control activity that would saturate the actuator physical limits, the following high-pass filters W_u are selected

$$W_u = diag\left\{\frac{10^{-4}s}{2s+1}, \frac{0.5s}{2s+1}, \frac{0.02s}{s+1}, \frac{0.05s}{s+1}\right\} \tag{25}$$

We also consider the multivariable stability margins also called disk margins discussed in [17], which can be viewed as robustness against simultaneous gain and phase variations at both the plant inputs and outputs. The target gain and phase margin values are converted into a normalized scalar function to be minimized

$$\min_D \max \| \alpha D^{-1} X(j\omega) D \|_\infty < 1 \tag{26}$$

where $x(s) = (1 + L)(1 - L)^{-1}$, D is a diagonal scaling matrix to be computed during the iteration process, L is the corresponding open-loop response to be shaped, and the parameter α is the minimum distance between the open-loop response and the critical point. Here, we impose a minimum distance of 0.6, which guarantees margins of nearly 5dB and 40°. Note that the weighted function blocks M_u and M_y (see **Figure 11**) are exactly used to express the stability margins requirement.

The resulting control problem of (23) is concretely rewritten as the following nonsmooth program

$$\min_{x} \max_{m} f_m(x) \, subject \max_{m} g_m(x) < 1 \tag{27}$$

where x is the decision variable in the space formed by collecting all tunable entries in the structured controller, m denotes a given operating point of the objective flight envelope, the function $f_m(x)$ and $g_m(x)$ are of the following form

$$\begin{cases} g_m(x) = \left\| \begin{matrix} W_e S_R \\ W_u K S_R \end{matrix} \right\|_\infty \\ f_m(x) = \| \alpha D^{-1} X(j\omega) D \|_\infty \end{cases} \tag{28}$$

where S_R is the closed-loop sensitivity function from setpoints to tracking errors.

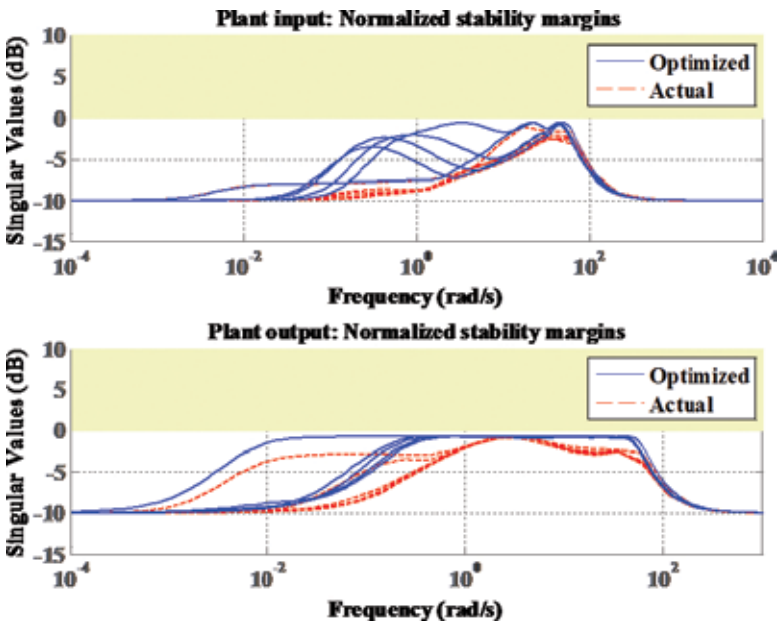

Figure 12. Multivariable stability margins.

http://dx.doi.org/10.5772/63355

The structured robust controller synthesis is carried out in the framework of the nonsmooth H_∞ optimization algorithm using the MATLAB ***Hinfstruct*** solvers. After some trail-and-error iterations and design repetitions, the smallest values of L_2 gain of hard constraint $g_m(x)$ and soft constraint $f_m(x)$ are found to be 0.9994 and 0.935, which indicates the resulting design satisfy all the design requirements. A visual inspection of the multivariable stability margins can be seen in **Figure 12**. The yellow region denotes margins that violate the requirements. The blue plot represents the margin objectives to be optimized in the calculation process, which is an upper bound on the actual margin. Note that the five different curves represent the five discrete operating points. The actual stability we obtained in the red dotted lines indicate that the stability margin requirements are satisfied at all frequencies in the designed fight envelope. The frequency responses related to the hard constraints are shown in **Figure 13**, which indicates the disturbance rejection and tracking errors at low frequencies are expected to perform well and fast actuator movement can be effectively suppressed inside the closed-loop bandwidth.

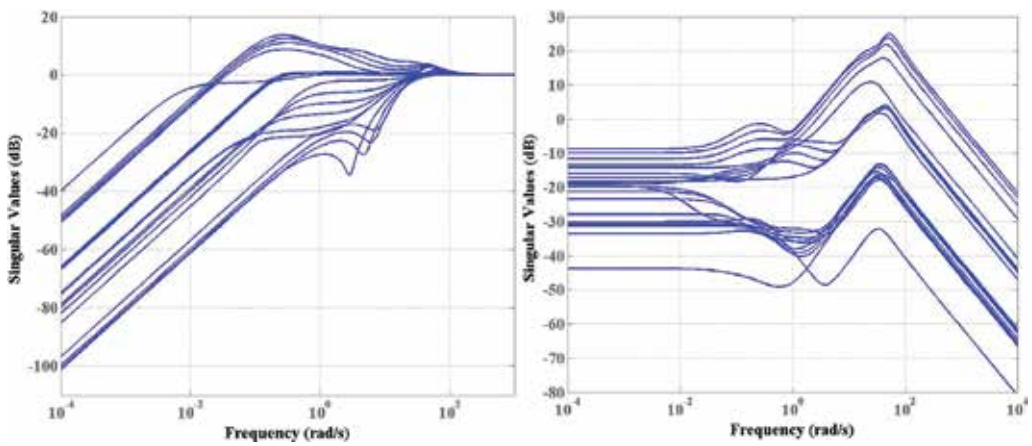

Figure 13. Singular value plots for the closed-loop transfer functions (left for S and right for KS).

4. Simulation and flight test results

The simulation and experimental tests have been carried out in the ARC flight arena at Beijing Institute of Technology. The employed hardware architecture for the experimental validation is briefly introduced in Section 2.1.1. A variety of simulation tests have been conducted before actual flight experimentation. As a representative example show in **Figure 14**, we present the gust alleviation effects of the closed-loop system for hovering flight. The strong wind gust has been intentionally injected into the x-, z-, and y-axis of the body frame, with the peaking amplitude of 9, 3, and 7 m/s, respectively. The system response clearly demonstrates that the wind gust effect has been effectively attenuated.

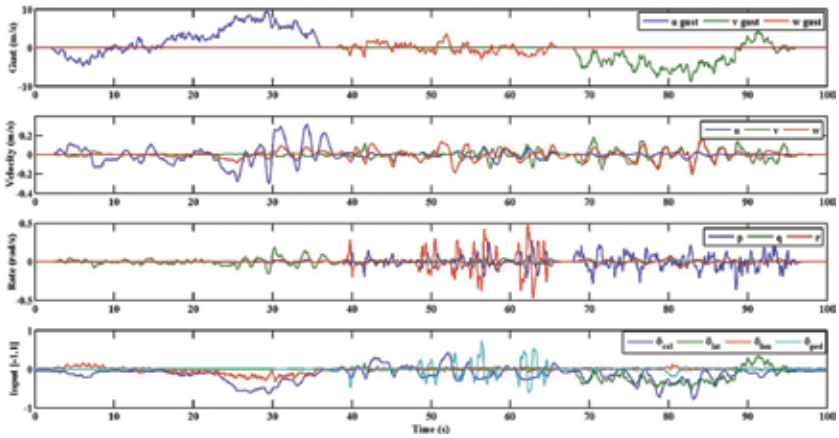

Figure 14. Simulation results of wind gust alleviation effect at hovering.

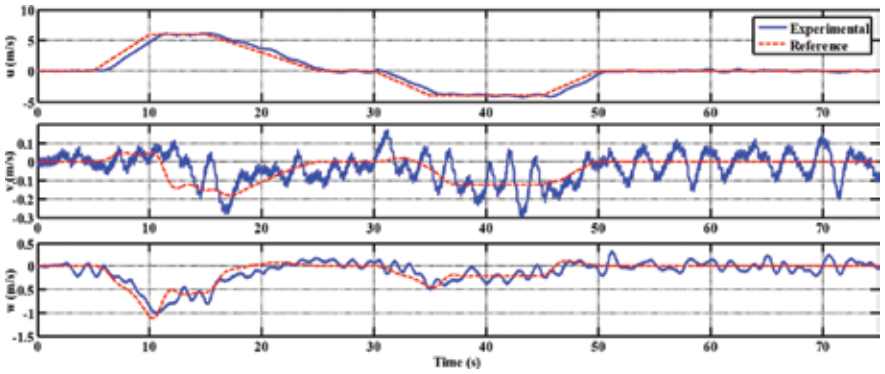

Figure 15. Flight test-velocities.

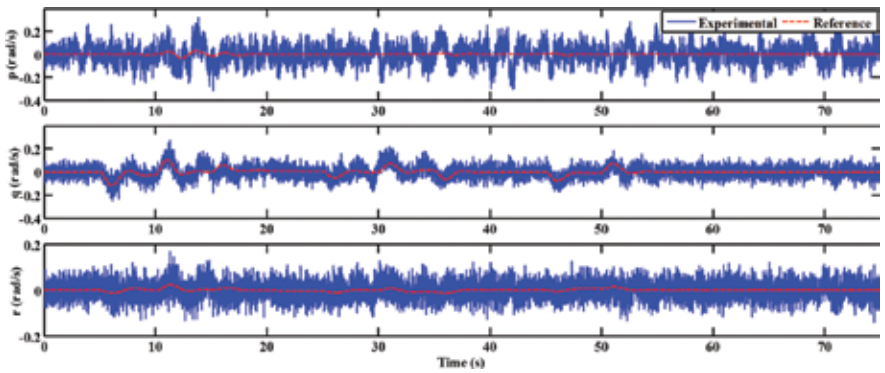

Figure 16. Flight test-angular rates.

http://dx.doi.org/10.5772/63355

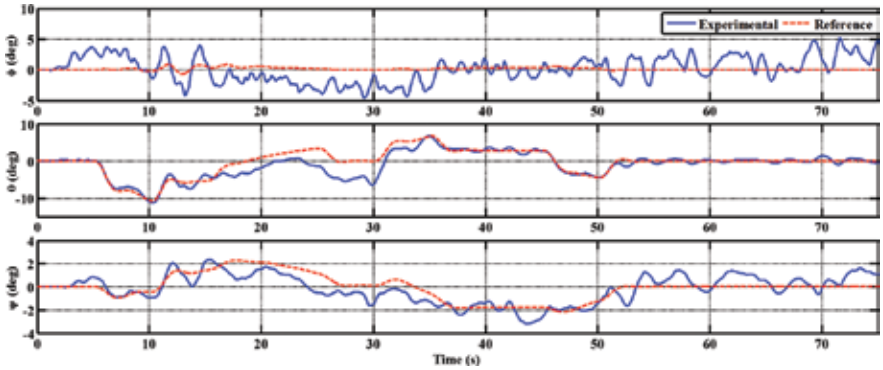

Figure 17. Flight test-Euler angles.

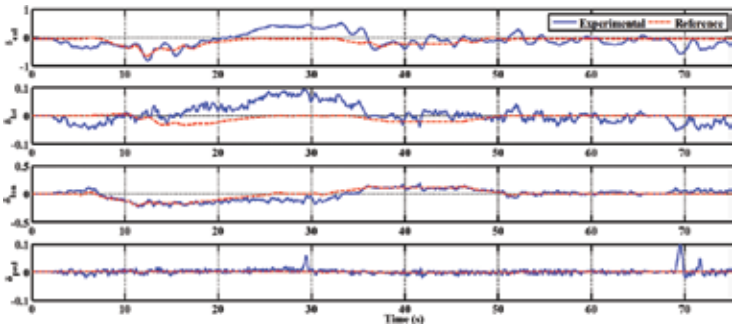

Figure 18. Flight test-control inputs.

The experiment proposed in this part consists of an accelerated flight maneuver after a short-time hovering flight. The desired maneuver is a horizontal forward and inverted flight with a trapezoidal velocity in the longitudinal direction of the inertial frame. Throughout the maneuver the desired heading rate remains constant with the value $r_d = 0$. The resulting responses versus the reference signals are illustrated in **Figures 15–18**. The test results show that the predefined flight maneuver can be well achieved with small fluctuation of the actual responses from the reference signals. Such fluctuations are within an acceptable range, which is mainly caused by the limited accuracy of the output feedback measurement signals. A certain degree of deviations between the control input signals are due to both the model uncertainties and the gust disturbances during the flight test.

5. Conclusion

Summarizing, it can be stated that, following systematic design and implementation of BIT-TDF, including unconventional configuration design, hardware and software development, frequency-domain identification as well as navigation and control algorithms, it is expected

that flight control development described in this chapter would have successful application in support of Unmanned Aerial Vehicle UAV development. The main concern is to propose approaches that can be effective, easy to implement and to run onboard the UAVs. The proposed flight control law has been implemented and tested with the BIT-TDF ducted-fan vehicle and current work aims to propose and implement more advanced and practical techniques. Considering the requirements on various practical implementations, extensive contributions could be achieved by extending the BIT-TDF research in physical interactions with the environment in terms of desired or even unpredictable contacts.

Acknowledgements

Financial support of this work by the National Nature Science Foundation of China under Grants 51505031, as well as BIT National Key Laboratory for VRC Basic Research Foundation is highly acknowledged. Acknowledgments go also to the colleagues at the Department of Mechanical Engineering of Beijing Institute of Technology and all Postdoctoral Fellows/ Research Associates, Ph.D., MASc/MEng students who contributed to this work.

Author details

Yang Wang*, Changle Xiang, Yue Ma and Bin Xu

*Address all correspondence to: yangwangeducn@gmail.com

School of Mechanical Engineering, Beijing Institute of Technology, Beijing, China

References

[1] Tobias EL, Joseph F. Horn. Simulation Analysis of the Controllability of a Tandem Ducted Fan Aircraft. In: AIAA Atmospheric Flight Mechanics Conference, Honolulu; 18–21 August 2008; Honolulu, Hawaii. AIAA; 2008. pp. 1–24.

[2] Wang Y, Xiang C, Ma Y. Modelling and hovering attitude control of a prototype tandem ducted fan vehicle. Journal of Intelligent & Robotic Systems. 2015;79(1):155–172. doi: 10.1007/s10846-014-0126-6

[3] Xiang C, Wang Y, Ma Y, Xu B. Structured Robust Control-Loop Design with Input Saturations for Tandem Ducted Fan Vehicle. In: International Conference on Unmanned Aircraft Systems (ICUAS '15); 9–12 June 2015; Denver. Colorado: IEEE; 2015. pp. 914–919.

[4] Marconi L, Naldi R. Control of aerial robots: hybrid force and position feedback for a ducted fan. IEEE Control Systems. 2012;32(4):43–65. doi:10.1109/MCS.2012.2194841

[5] Ozdemir GT, Horn JF. Control of Ducted Fan Aircraft using Redundant Effectors. In: AIAA Atmospheric Flight Mechanics Conference; 10–13 August 2009; Chicago. Illinois: AIAA; 2009. pp. 1–15.

[6] Marconi L, Naldi R, Gentili L. Modelling and control of a flying robot interacting with the environment. Automatica. 2011;47(12):2571–2583. doi:10.1016/j.automatica.2011.09.020

[7] Naldi R, Torre A, Marconi L. Robust control of a miniature ducted-fan aerial robot for blind navigation in unknown populated environments. IEEE Transactions on Control Systems Technology. 2015;23(1):64–79. doi:10.1109/TCST.2014.2312929

[8] Pflimlin J-M, Binetti P, Soueres P, Hamel T, Trouchet D. Modeling and attitude control analysis of a ducted-fan micro aerial vehicle. Control Engineering Practice. 2010;18(3):209–218. doi:10.1016/j.conengprac.2009.09.009

[9] Grant OL, Stol KA, Swain A. Handling qualities of a twin ducted-fan aircraft: an analytical evaluation. Journal of Guidance, Control, and Dynamics. 2015;38(6):1126–1131. doi:10.2514/1.G000826

[10] Tischler MB, Remple RK. Aircraft and rotorcraft system identification. Reston, VA: AIAA; 2006. 523 p. doi:10.2514/4.861352

[11] Gary F. Derivation of the aerodynamic forces for the mesicopter simulation. Stanford:Stanford University. 2001

[12] Wang Y, Xiang C, Ma Y, Xu B. Comprehensive Nonlinear Modeling and Simulation Analysis of a Tandem Ducted Fan Aircraft. In: Proceedings of 2014 IEEE Chinese Guidance, Navigation and Control Conference; 8–10 August 2014; Yantai, China: IEEE; 2014. pp. 255–261.

[13] Xiang C, Wang Y, Ma Y, Xu B. Robust flight control using nonsmooth optimization for a tandem ducted fan vehicle. Asian Journal of Control. Forthcoming. doi:10.1002/asjc.1295.

[14] Mettler B, Tischler MB, Kanade T. System identification modeling of a small-scale unmanned rotorcraft for flight control design. Journal of the American Helicopter Society. 2002;47(1):50–63. doi:10.4050/JAHS.47.50

[15] Apkarian P, Noll D. Nonsmooth H_∞ synthesis. IEEE Transactions onAutomatic Control. 2006;51(1):71–86. doi:10.1109/TAC.2005.860290

[16] Gahinet P, Apkarian P. Automated tuning of gain-scheduled control systems. In: Decision and Control (CDC), editors. 2013 IEEE 52nd Annual Conference on; 10–13 December 2013; Firenze. IEEE; 2013. pp. 2740–2745. doi:10.1109/CDC.2013.6760297

[17] Blight JD, Lane Dailey R, Gangsaas D. Practical control law design for aircraft using multivariable techniques. International Journal of Control. 1994;59(1):93–137. doi: 10.1080/00207179408923071

Chapter 7

Design of Large Diameter Mine Countermeasure Hybrid Power Unmanned Underwater Vehicle

Kwang Sub Song

Additional information is available at the end of the chapter

http://dx.doi.org/10.5772/63795

Abstract

Mines are one of the most cost-effective and moderated weapon systems that are easy to deploy, but difficult to clear. Not only has the development of the mine countermeasure (MCM) underwater unmanned vehicle (UUV) improved cost- and time-effectiveness in operation, but also it has avoided unnecessary human casualties.

In MCM UUV operations, technical challenges, such as detection, classification and neutralization of mines, and vehicle management operations, arise from the incapacity of detection sensors, data-processing power. Due to the small volume capacity, decision-making processing and mine-clearing operations are insufficient for safe mine countermeasure warfare operations. Larger displacement UUVs must be integrated into new platform designs so that they can be a viable organic asset.

Realization of the full potential of the UUV as a truly autonomous undersea vehicle (AUV) in warfare will begin with a transition to a large displacement vehicle. In case we try to make a larger and heavy UUV system, we still encounter various problems, including vehicle operational time and speed at sea, in addition to vehicle and mission management algorithms with appropriate hardware configurations. In this work, we suggest a larger diameter of the MCM UUV with hybrid power, including the basics of artificial intelligence applied expert systems integrated into the MCM mission management systems.

Keywords: mine countermeasure warfare, large diameter unmanned underwater vehicle, artificial intelligence, hybrid power operation, mission management

1. Introduction

The naval mine is one of the most cost-effective weapons in the naval arsenal and have many synergetic effects in the maritime warfare. Mines are relatively simple, cheap and can be laid from any type of sea and air platform. Combat effectiveness of naval mines covers from defending important and high-valued targets at sea, ports, and offshore structures to denying hostile forces access to the coastal zone [1]. Mines can quickly stop, or seriously impair surface, submarine forces and amphibious or seaborne attack. Their flexibility and cost-effectiveness make mines attractive to the less powerful belligerent in asymmetric warfare and maritime warfare.

Mines can be used as both offensive, defensive weapons and tools of psychological warfare in rivers, lakes and oceans. As offensive weapons, mine are placed in enemy waters and across important shipping routes to destroy or damage both civilian and military vessels [2]. Defensive minefields protect tactical areas of coast from enemy ships and submarines, or keeping them away from sensitive and high-valued targets. Threats of mines are increasing due to recent technology development, such as autonomous systems and computer systems with artificial intelligent capability. There are many solutions to solve MCM problems so far as difficulties to detect identify and classification. Unmanned systems also cleared the way to sweep and naturalize mine safely without involvement of human beings.

Mine countermeasure (MCM) is a tactical measure to clear or neutralize mine threat. Tactical MCM operations can be preceded with both passive and active operations. Passive MCM relies on minimizing the influence of the ship's physical signature such as emitted acoustic and magnetic and electric signals to be sensed by mines. Active MCM operations are minesweeping, neutralization and mine hunting, which are trying to sweep or destroy mines. Influence minesweeping uses acoustic, magnetic and pressure signals to detonate targeted mines [1]. Mechanical sweeping uses a towed minesweeping tools to cut the cables of moored mines. After mines are floated to the surface, they are detonated by shooting or explosives.

Mine hunting is getting difficulties in most parts of the littoral regions near enemy territory. Access to these tactically important areas by the sea requires minesweeping or neutralization operations. Keeping the man out of dangerous minefield requires various unmanned autonomous MCM systems as a potential attractive option [3]. Many of developed high technologies that are operated in manned mine warfare operations could be transformed into an effort to develop unmanned and autonomous MCM vehicle systems.

Unmanned systems integrated with emerging technologies are the minesweepers and hunters of the future MCM operations. A focused technology effort is needed to incorporate unmanned systems into the mine countermeasure ship and other related MCM fleet forces. It is time to press ahead with establishing fleet requirements for unmanned MCM systems that lead to programming decisions allowing mine hunting and minesweeping missions to be performed without a man onboard, eliminating the risk to personnel.

The physical and operational capacity of small displacement UUVs will greatly limit what UUVs can provide as multimission assets and effective autonomy at a real combat situation.

http://dx.doi.org/10.5772/63795

New platform designs that are true viable organized intelligent assets should be incorporated with large diameter UUVs [4]. Realization of the full potential of UUV system as a truly autonomous undersea vehicle (AUV) in MCM warfare will have sufficient energy system for super long combat endurance and intelligent mission management capability and mine disposal weapons.

Since current technology is available to deactivate or eliminate mines, an effort to make a larger and heavier UUV system should be discussed, in order to produce an unmanned system to integrate complete MCM UUV systems. With a larger diameter UUV system, however, there are still problems with vehicle's operation time and speed at sea, vehicle and mission management systems with appropriate hardware configurations. Larger displacement UUVs must be integrated into a new platform design so that they can be a viable organic asset. Realization of the full potential of the UUV as a truly autonomous undersea vehicle (AUV) in warfare will begin with a transition to a large displacement vehicle.

We investigate strategy and threat of mine warfare and recommend optimal concepts of operation of their mine countermeasure operation of future maritime warfare. In this chapter, we provide CONOPs developments of future large diameter MCM UUV in Section 2, specifications of the MCM UUV system configurations in Section 3, system effectiveness discussions in Section 4, and the conclusion in Section 5.

2. Concepts of operation establishment of mine countermeasure UUV

2.1. Importance of information, surveillance and reconnaissance (ISR)

The intelligence, surveillance and reconnaissance (ISR) aspects of mine warfare are of particular importance, since that is where mine warfare really starts, regardless of the specific purposes for using this collected information. As with most complex military operations, mine warfare operations are inherently joint operation between theater forces. The tactical commands from theater headquarters actually operate the mine warfare forces in theater. The intelligence agencies provide vital ISR information [5], and Marine Corps units must work closely with the navy in any amphibious operations, as well as interface with army mine warfare in addition to other operations ashore. Navy and Coast guard units must work together closely in inshore mine warfare operations to secure good communication.

Battlefield reconnaissance data are essential for both safe far- and near-shore operations. Mine warfare is the strategic, operational and tactical use of sea mines, and the countermeasures to defeat them [6]. Undersea physical characteristics, ocean climate variations and environment are considered before an operation is initiated. Ocean environmental characteristics are very important to determine where mines should be placed and how many and how to deliver the mine to the position. Oceanographic parameters have greatest impact on mine warfare operations and need the most enhanced predictive modeling capabilities for a wide range of oceanic processes. They will greatly enhance the war fighter's ability to turn vast amounts of oceanographic information into knowledge, which is used to control battlefield operations [7].

Major physical oceanographic data for the mine warfare consist of current patterns, salinity, temperature, bottom status and clarity of water of the area [8].

Bathymetry forms the boundary condition for all fluid motions and can extend beyond the local region. Ocean currents are long-time-scale fluid flows arising from a wide variety of processes, such as direct wind forcing and tides. The complexities of forces driving current flow require to work together with meteorological and oceanographic analysis. They also determine how these forces are interacting with each other, understand the time scale of variability driving current flow and understand how this may affect the mission [5].

Mine laying and mine countermeasure operations are parts of the main subsystem of mine warfare operations [6]. Better priority weight should be given to the technical exploitation of threat mines, mine warfare indications and warning (I&W) tasking. There are several points of consideration in mine warfare at the combat zone or landing assault area. Thus, currently, both near-term and long-term mine reconnaissance systems (NMRS and LMRS) are developed to expand organic and dedicated MCM capabilities. The MCM command center should disseminate them at all command levels and provide rules of engagement (ROE) to counter hostile miners and relevant environmental databases, such as the mine warfare environmental decision aids library (MEDAL) and the contingency planning tool [2].

2.2. Communication and control (C2) in MCM operations

Naval ISR group is collecting and processing any potential data and information in order to develop optimized mine detection procedure and clearance capabilities, organic to carrier and surface battle groups (CV). With those ISR information and operational procedures, naval forces can identify, avoid or neutralize mines within tactically acceptable time limit and with minimum operational risk [9]. On-scene MCM capabilities, through introduction of organic capabilities into all carrier battle group (CVBGs) and surface battle groups, would be completed with completion of MCM communication and control network systems.

Major MIW capabilities include intelligence collection and surveillance, notification of imminent mining, interdiction, postinterdiction intelligence evaluation and dissemination and passive MCM threat awareness and signature control. With wide dissemination and availability of the battle space information, the MCM control center has to communicate frequently as the real-time development changes so far.

Communication systems related to the mission operations are data communication links where tactical maneuvering information on MCM missions is exchanged. Each division on communication links is evaluated through communication quality of data, security and interoperability. As organized supporting systems, and command, control, communications, computers, intelligence (C4I) are introduced into the naval forces. Effective C4I systems must allow MCM functions to be performed from variety of platforms with highly dynamic environment. Database systems for mine identifications will include such features as high-resolution environmental mapping data and explicit simulations. It can be used for doing detailed operational planning, training and rehearsing [8].

http://dx.doi.org/10.5772/63795

In the future MCM operations, the decision-making software, and combat information display systems will be driven by data from extensive multi-source collections. The C4I architecture will be networked to ensure the existence of communication paths between platform and detachment despite uncertain point-to-point links. Shared awareness of combat scene information, such as analysis efforts, off-board forecasts and historical environmental database, is critical, robust, real time and cooperated. With all these doctrinal evolvements, up to dated technologies, hardware (H/W) with appropriate operating software (S/W) should be accompanied for smart and safe MCM operations in the future [2]. Fundamental issues for evaluating communication systems for MCM are bandwidth, range, covertness and required infrastructure [3]. The combined C4I system architecture will be central for the coordinated and multiplatform operations.

2.3. Mine hunting, sweeping and neutralization [10]

In the MCM operations, there is many data sensed and produced to detect, identify, classify mines and start sweeping and neutralization operations. Active countermeasures are ways to clear a path through a minefield or remove it completely. This is one of the most important tasks of any MCM fleets and task forces. Minesweeping is either a contact sweep, a wire dragged through the water by one or two ships to cut the mooring wire of floating mines, or a distance sweep that mimics a ship to detonate the mines.

Mine hunting is different concepts and operations from minesweeping, although some mine hunters can do both operations. Mines are hunted using sonar, side scan sonar or synthetic aperture sonar, then inspected, classified and destroyed either by remote controlled or by divers unmanned vehicle systems. Mine hunting started as mine was used, but it was only after the Second World War that it became truly effective [11].

A more drastic MCM method is mine breaking which is simply to load a cargo ship with cargo that makes her less vulnerable to sinking and drive her through the minefield, letting the ship to be protected follow the same path. An updated form of mine breaking is application of small unmanned systems that simulate the acoustic and magnetic signatures of larger ships and are built to neutralize mines. In future, more autonomous unmanned systems are involved in every step of minesweeping and neutralization operations due to safety of human beings and effectiveness of MCM operations. Applications of RF and laser optic technology are considered as potential alternative methods of efficient underwater communication systems [3].

2.4. Data processing and decision making AI logic system

All data processing in intelligent MCM operations is carried through a systematic data fusion approach. AI machine learning and perception, feature extraction via real-time image or intelligent navigation and mine-clearing operation sequences are integrated with mission management processes. Main control center will support and coordinate automatic classification of mines and other ordnance, as well as intelligence obstacle avoidance navigations using data from navigation sensors. The image and pattern identification-processing techniques, which have been adapted from video image and sensor signal, focus on classification of mines

by the recovery of explicit feature-based descriptions of man-made objects [12]. Silhouette descriptions and classification are used to support the dynamic view positioning and automatic object classification.

The algorithmic partitioning in a front-end digital signal processing (DSP) dedicates image acquisition, dynamic range equalization, image segmentation and region-of-interest identification [13]. The parallel processing engine supporting applications of a statistical evaluation of linearity or regular curvature have gradient extraction, edge thinning and threshold algorithms [14]. All the data from traditional navy data base, mine warfare environmental decision aid library (MEDAL) systems on MIW, MCM and tactical oceanography also could be accessed in main processing unit in the MCM UUV system and fed into the identification and classification processors [15]. A typical MCM data-processing flow of MCM UUV systems is shown in **Figure 1**.

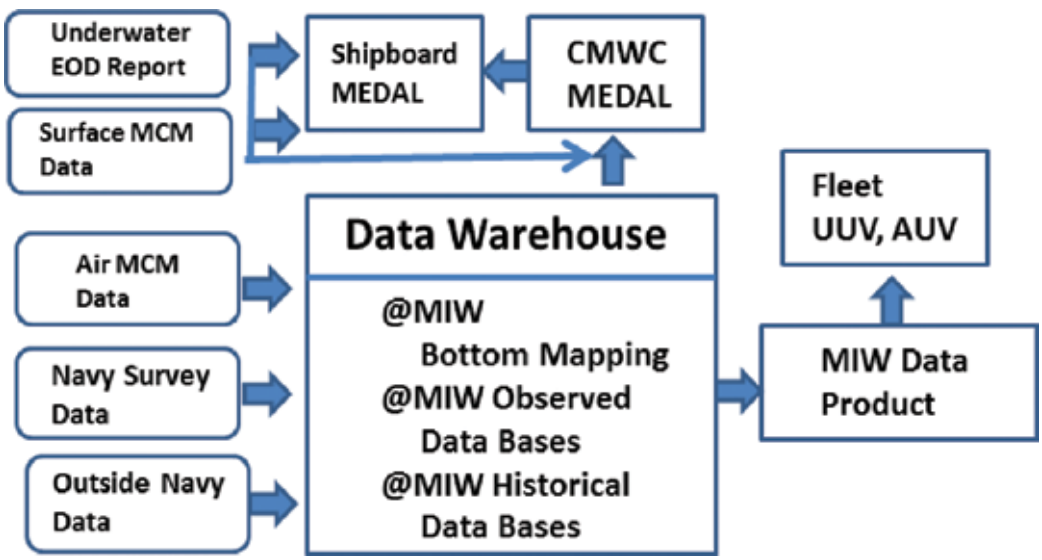

Figure 1. Mine warfare environmental data flow.

Reacquisition and relocalization of predesignated mine or mine fields need huge amount of signal, communications and data packages from various sensor systems. Data sets for reconstructing three-dimensional (3D) and two-dimensional (2D) modeling are very big and very difficult to transfer through current acoustic carrier in underwater environments [5]. Some other information comes from distance oriented and directional angle of illumination of light source, which gives some incentive in the reconstruction of 3D or 2D model of mines.

Identification, reconfirmation of mines and mine-like objects (MLO) classifications are critical factors for mine disposal operations. Efficient and different bandwidth characteristics of communication careers are critically needed at the main control center of MCM operations to

http://dx.doi.org/10.5772/63795

gain access to high-quality mine detection sensor data from a remote area, due to the lack of computational capabilities of the existing sensor data-processing systems [16, 17].

2.5. Mission management system

If the duration of MCM operations at sea is expanded to more than 50 days, it is necessary to maintain the clandestine nature of the MCM operation at enemy littoral zone; therefore, in these cases, mission management is critical to autonomous MCM operations. With the introduction of system autonomy of mission goals, which is a relatively new area of research, this system will retain clandestine operations and power system requirements for functionality [18]. Coordinated MCM mission management systems optimize available sensors and systems, regardless of the host platform, to ensure that the most effective is used when and where it is most needed.

Fundamentals to the MCM operational concept are to locate minefields, identify no-mine areas accurately and clear mines efficiently as soon as possible [19]. This area focuses primarily on unmanned autonomous vehicles intelligence since these often have the greatest redundancy, and because they have the most intricate machine-readable, autonomous mission plans. Models of the vehicle including their planning/control systems, and operating environment can be linked together to form an assessment tool [16]. This tool helps to verify interface compatibility and basic functionalities, as well as to facilitate exploration of control options and evaluation of potential benefits.

The mission control data, which are required to define current mission objective, the vehicle's dynamic characteristics and the environmental data are collected from external sensors and provided by the user, as they are specific to the effective MCM operations. The autonomous mission-planning algorithm translates the mission requirements into a mission plan, a set of constraints and execution sequences. An integrated mission planner and power management algorithm would combine to this intelligent system with motion and power control subsystem [10].

MCM mission management configuration [17] of MCM UUV consists of degrees of perception, intelligent control and management to define sense-plan-act or sense-react behavior doctrine. Functional limitations of vehicle sensor systems imposed by the combat environment require alternative course of vehicle control, which defined mission goals to be factored in the control system appropriately. A common approach to mission implementation process is to develop functions, which are grouped and sequenced to perform overall tasks through artificial intelligent (AI) expert system architecture [12].

It is based on a traditional perception-action loop, allows low-level sensor signal processing and does feature extraction to assist mine classification, MCM mission planner and vehicle control system. MCM UUV mission management system focuses on mine classification and dynamic repositioning, which optimizes the aspect relative to the designated mine target and clearing mine. Obstacle avoidance navigations require relatively sparse sensor data in the dynamic construction of world models for environment [12]. In the main control block, the perception/classification processor is combining with dynamical position sensors via a highly

maneuverable platform. MCM expert system has the capability to perceive the object of interest from multiple perspectives, which then increases the probability of classification for the mine targets. A key concept in data fusions of expert system includes the employment of heuristic knowledge, which incorporates constraint knowledge associated with target characteristics, environment and attitude of vehicle.

This provides basis for interaction with the object of interest, and dynamic perceptions that provide active sensor management and vehicle path planning in the navigation and guidance [16]. A second unique aspect of the AI expert system architecture is the implementation of sensing, evaluation and action encapsulated as subordinate tasks under the integrated mission control system. It optimizes machine-generated direction of task-organized approach and initiates signal for the course of action [6]. The MCM AI expert system architecture and its relationships between the executors, and the data/signal processing are shown in **Figure 2**.

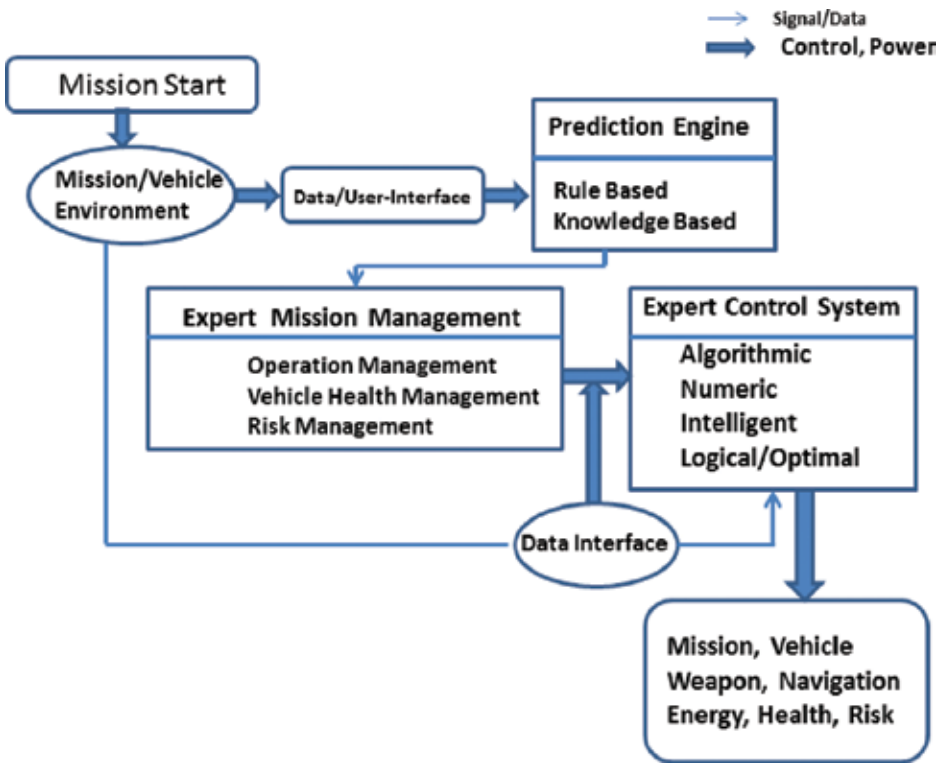

Figure 2. Operations of MCM mission management expert system.

2.6. Vehicle management system

The system capability of precise navigation and operational data collection is critical to ensure safe navigation of the vehicle and in the achievement of system objectives. To resolve the vehicle position at the submeter level, a compact low-power solid state inertial measurement

http://dx.doi.org/10.5772/63795

unit (IMU) has been incorporated [20]. This unit measures the change of 3D velocity, angular velocity and temperature as well as performs corrections of thermally induced drift. The IMU is augmented by a compact Doppler Sonar System using the Kalman filter or other processing techniques. A precise navigational compass and clinometers provide heading information and navigation frame correction data for noises [21].

Simultaneous localization and mapping (SLAM) techniques [22] are utilized as a navigational tool and are adapted for reconfirmation of designated mine localizations with autonomous navigation for obstacle avoidance to a safe margin. All the information are filtered and processed in a data processing and distribution unit and distributed for navigation, SLAM processing and mine neutralization procedures. With updated environmental 3D map and obstacle information, the MCM UUV navigation system can be guided and controlled within guided optimal paths to the targets with a degree of accuracy [22].

2.7. Operational endurance and available power system alternatives

System endurance in unmanned underwater vehicle (UUV) operations consists of available total energy sources, vehicle system objectives, maneuvering path plan and design parameter characteristics. In general, the more the endurance is desired for UUV operations, the more the coordinated efforts are required during the vehicle design stage regarding the structural design, energy systems and power management. UUV endurance with respect to UUV system activities is characterized by range of missions, operation time and kinds of energy systems and is controlled by the capacity of on-board energy, hull structure of the vehicle, optimal propulsion and energy management system [23]. Until now days, these properties were investigated separately with system endurance as an individual component. In this study, we integrate all these components and make overall suggestions to the system endurance with respect to hull shape, power systems, propulsion efficiencies and respective activities of missions.

2.8. Energy sources for MCM UUVs

Power system considerations dominate the design of UUVs, due to the fact that usually the energy source is the most limiting factor for mission operations of autonomous vehicles. The energy system of UUVs has been a major issue due to its impact on the ultimate performance and extension of UUV missions [24]. There are strong desires to minimize the size, cost and energy consumption rate for all aspects of UUV operations. In the operation of unmanned vehicles, missions with high speed and longer endurance, such as mine countermeasure (MCM), antisubmarine warfare (ASW), and intelligence, surveillance, and reconnaissance (ISR), need more powerful and sophisticated energy systems, such as fuel cells and hybrid systems in addition to battery power [23].

Since the power required to propel an underwater vehicle is roughly proportional to its surface area, and cubic of forward velocity, the stored energy capacity is proportional to its volume, the mission duration or range achievable at a given velocity varies directly with vehicles. The information of the UUV energy source gained via analysis of the batteries, fuel cells, internal

combustion engines or other available energy sources is found in Jane's Underwater Technology Information. Important UUV power system performance metrics consist of energy and power, specific energy and power, usable state of charge, voltage response under load, calendar life and charge acceptance specifically, power and energy density and physical volume are critical to UUV system design. **Figure 3** [24] shows the specific power and energy properties of major UUV energy sources.

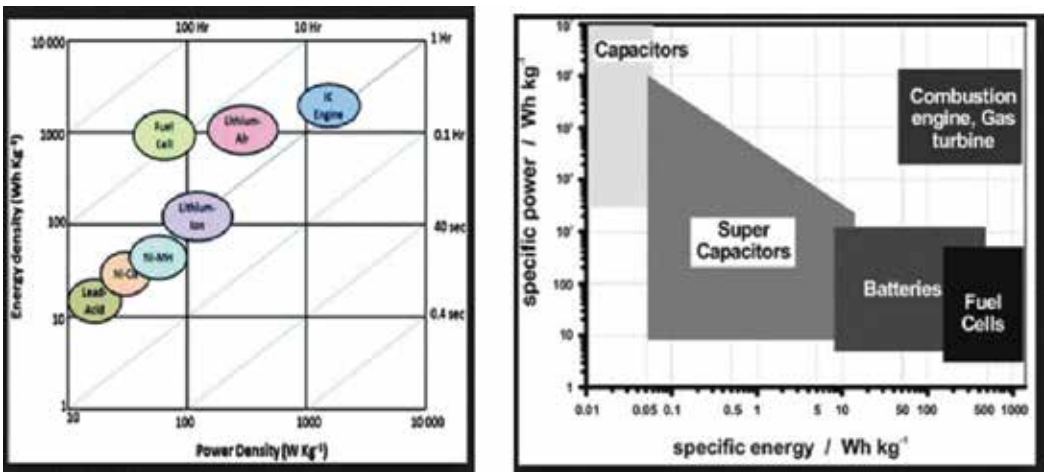

Figure 3. Energy source characteristics, Ragone Chart [24].

Based on current technology development of battery systems, high-performance battery is the most favorable choice for the autonomous vehicles based on performance, availability and cost-effectiveness. With battery applications, to facilitate the addition of battery packs to the vehicle, the hull shape should be redesigned to be longer or wider. Such hull reshaping reduces the overall vehicle drag coefficient and increases energy to UUV's propulsion power. As UUV energy systems are characterized by specific energy or power density per unit volume or weight, adding additional energy to the system increases the vehicle length [23]. When the battery packs are added, the midsection (D) must be longer (L) in order to house additional battery packs. This changes the aspect ratio, and increases the vehicle drag coefficient. Increased vehicle drag requires more propulsion power, which is a portion of added energy. The sensitivity to added battery packs is compensated for by changing the axial drag coefficients as and other conditions, including hotel loads, are unchanged.

Based on the Ragone Chart characteristics [23], the preferred long-term approach to using hydrogen is the fuel cell. Fuel cells use a process that is essentially the reverse of electrolysis to combine hydrogen and oxygen in the presence of a catalyst to generate electricity. Fuel cells are much more efficient than ICEs often topping 70% [24, 25]. The main problem with fuel cells is the cost, and the other primary issue with fuel cells is durability. Both of these renewable fuels have lower heating values (Btu/gallon) than their counterpart gasoline and diesel fuel, resulting in higher fuel consumption when measured on a volume basis. Diesel engine offer

http://dx.doi.org/10.5772/63795

better fuel savings over gasoline engines, battery and fuel cells on specific energy containment and gives good gas mileage on fuel consumption (gallon/mile) and load-specific fuel consumption (gallon per ton-moles), defending on the engines and operating conditions, diesel engine can provide up to 25% lower fuel consumption than gasoline engines.

Considering more than 50 days of field operation of MCM UUV and current technology development of battery systems, it could be a realistic combination for larger diameter long endurance MCM UUV system with diesel internal combustion engine (ICE) and effective battery systems. Internal combustion system gives relatively high specific power and is proven as a convenient technology, whereas battery systems give operational conveniences. We tried to integrate a small diesel engine connected to battery system, as well as to modify the hull of the UUV for a snorkeling operation [25]. This is for both recharging and the propulsion of the MCM UUV. This diesel battery hybrid power system is designed to be controlled by vehicle management computers and the main AI expert mission management system. In this power option, we consider appropriate snorkeling systems and structural accommodations.

2.9. CONOPS of hybrid mine countermeasure UUV

2.9.1. Prospective of concept of operations

The main concept of MCM operations using UUV systems is to reduce incoming threats for the naval fleet with the employment of a robust, highly autonomous vehicle unit which is capable of operation engagement and execution of neutralization procedures. Neutralization procedures include either moving the mine out of the original place, precise delivery of the charged device to a desired location or the acquirement of projectiles to blast previously localized, in volume, drift, floating and bottom mines in deep and shallow water zones [15, 16].

The main body of the new MCM UUV has fully trained AI expert systems with MCM data bases to implement mission movement, in addition to vehicle and contingency operational management. The MCM UUV system has expandable small UUV sensor/neutralizers with a formed charge, and it is able to acquire projectile reaching and explode designated mines. Before it begins actual disposal activities, the control module of UUV unit requests a confirmation of mine identification to the mother ship via acoustic and RF communication links [8].

In the envisioned concept of operations, a UUV unit uses its high capacity communication links to get prior mine target information from the MCM operation center at the mother ship which is located more than 50 miles standoff distance [6] at high sea as shown in **Figure 4**. The vehicle then initiates an adaptive engagement plan autonomously along its trajectory with the available information from the navigation sensors. While compensating for winds, waves and currents along the disposal range, it will try to navigate accurately to the designated mine target. All the way to the designated mine position, the launched disposal device maintains the targets in the field of the imaging sonar. After neutralizing the designated mine, the UUV unit performs a neutralization damage assessment, and reports that the mission has been accomplished [18].

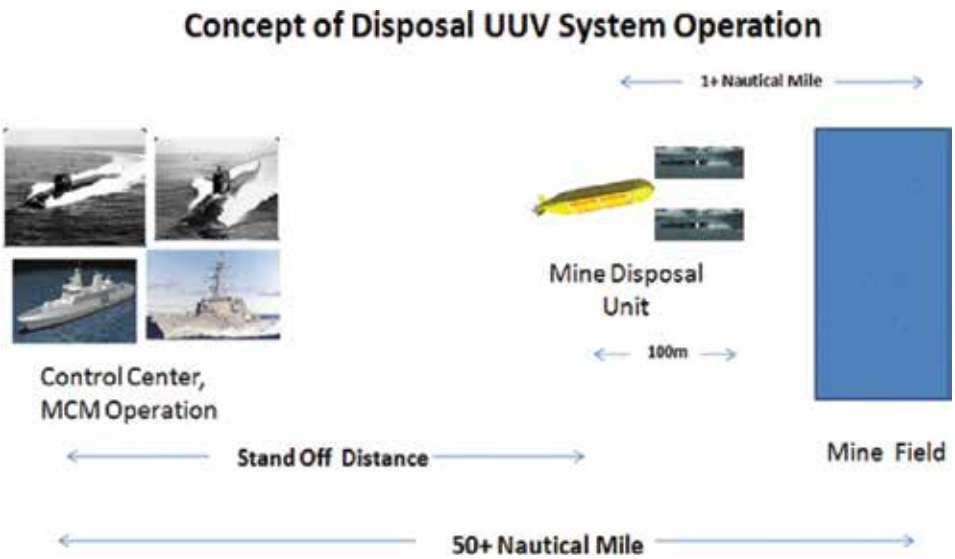

Figure 4. Concept of MCM UUV system operations.

3. System design of a large diameter MCM UUV unit

Current status of unmanned system technology and participation of unmanned vehicle fleets to naval operations can transform the concepts of future navy MCM tactics, weapons, and man machine interoperability in the field. In the near future, MCM vessels with C4I capability and MIW data base that act a main control center for a variety of unmanned vehicles in the enemy territory and doing a MCM operations without the presence of men in the mine field [9].

3.1. Large diameter UUV [16]

The conventional smaller diameter unmanned vehicle system has major operational difficulties in sensor system and vehicle endurance that give limited search, launch and recovery operations. If we can design larger unmanned vehicle, we will have more payload and energy storage for longer endurance. They can be a force multiplier for increasing the operational capability of submarines and surface ships [7].

The options for hull shape and various subsystem configuration of vehicle define the set of vehicle design options which are evaluated by the design requirements. Some important design options are the fineness ratio and block coefficient, which dictate the basic packaging spaces and sizing of all other vehicle subsystems [12].

3.2. Main control center configurations

The autonomy of the system and the spectrum of operations are fundamental characteristics on MCM operations. The main platform has mission management blocks that automatically

http://dx.doi.org/10.5772/63795

perform various MCM operational procedures such as contact of mines, obstacles from multiple sensor data sources and management of neutralization process, environmental data and bottom mapping [17]. For the mission accomplishment, organic MCM platforms, and operation with various sensors must undergo guidance of system management command, which is from rigorous analysis, experimentation, modeling and simulation on board [18]. The missions of MCM fleet operation is divided into five segments; launch, transit, execution of mission, return transit and recovery, each defined by key mission, and environmental parameters such as range, speed, ocean current and salinity and various MCM mission-related execution orders [12].

Advanced technologies applied for MCM main mission management system include situational reactive mission control suits, smart sensor system of systems, dynamic intelligent mine classification processors with MCM data bases. Vehicle management system controls precise intelligent undersea navigation, intelligent sensor systems and obstacle avoidance measures. Application of up to date AI technologies to the vehicle's functionality and mission effectiveness of MCM UUV system are implemented with expert system blocks, AI pattern classification and efficient power management systems in our works [12]. The MCM UUV unit provides autonomy of vehicle systems through incorporation with platform-independent autonomous controller that supports high degree of autonomy, highly precise low-power navigation and machine vision in support of automatic classification [26]. Mission management function block diagram of MCM UUV is given in **Figure 5**.

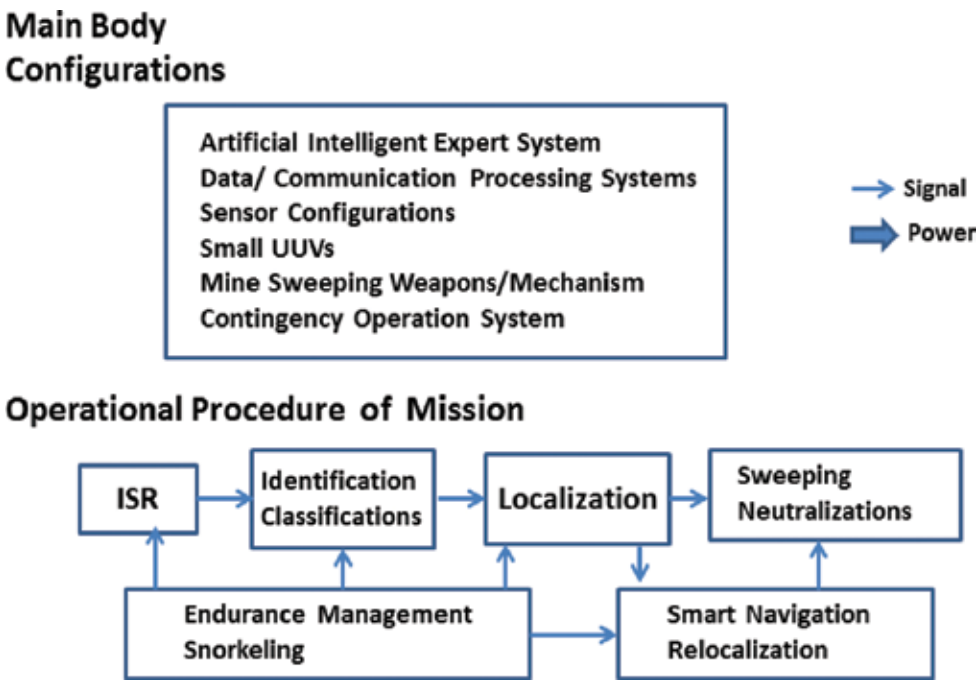

Figure 5. Function diagram of AI mission management system.

A capability of directing all aspects of the multifaceted MIW campaign plan is needed to bring the various MCM capabilities together, providing unity of effort in defeating the mine threat.

3.3. Neutralization weapon

There are several state-of-the-art weapon systems to dispose or detonate mines effectively, and economically such as the use of a laser gun, acquire gun and small charge delivery devices. Furthermore, the confidence for job completion requires the capability of accurate battle damage assessment (BDA). Underwater motion projectile is multipurpose in formed cavity water, due to its density, has a profound impact upon the terminal velocity of the implant at the target. A suitable weapon technology applied to MCM UUV is a lightweight composite 30 mm launcher that would implant a round filled with either high explosives (HE) for an explosive hard-kill or reactive material for a soft kill burn [3].

Similar technology was developed to counter roadside improvised explosive devices using 50 caliber weapons. A 30 mm implant would be usefully larger and could integrate a compliant fusing device, utilizing a detonator enables digital fusing, and affords either timed or controlled detonation, including detonation by an acoustically transmitted command. A 30 mm launcher provides sufficient terminal velocity to penetrate 5/10 inch cold rolled steel from a range of 30 feet [13, 26].

The currently achieved standoff range of 30 feet which the UUV should shot detonate the mine is not sufficient to ensure safety of MCM UUVs. Shooting from longer ranges requires significant basic research, and development, both in material strengths, and in achieving precise sonar fire-control accuracies before truly safe standoff ranges are achievable.

3.4. Energy and power managing section

Considering the operational combat field endurance limit of more than 50 days of MCM UUV and the current status of the battery systems technology, the combination of diesel internal combustion engine (ICE) and effective battery systems could become reality. The high specific power generation of the internal combustion system gives effective operation of the vehicle and can provide a stable recharge power source of the battery system. Integration of a small diesel engine connected to the battery systems, and modification of the UUV hull structure for the snorkeling operation could give better alternatives for both recharging and propulsion of the MCM UUV in the meantime [25].

A diesel submarine is a very good example of hybrid power supplying and sharing systems. The two or more sets of diesel engines in most diesel submarines can run propellers or can run generators that recharge a huge battery bank, or work in combination mode; one engine driving a propeller and others driving a generator. The submarines should run the diesel engines, they must surface or cruise just below the surface of water using snorkeling, and once the batteries are fully charged, the submarine can dive to underwater operations [8]. These diesel battery hybrid power systems are controlled by vehicle management computers and a main AI expert mission management system. Combined power generation, and the control system structure are given in **Figure 6**.

http://dx.doi.org/10.5772/63795

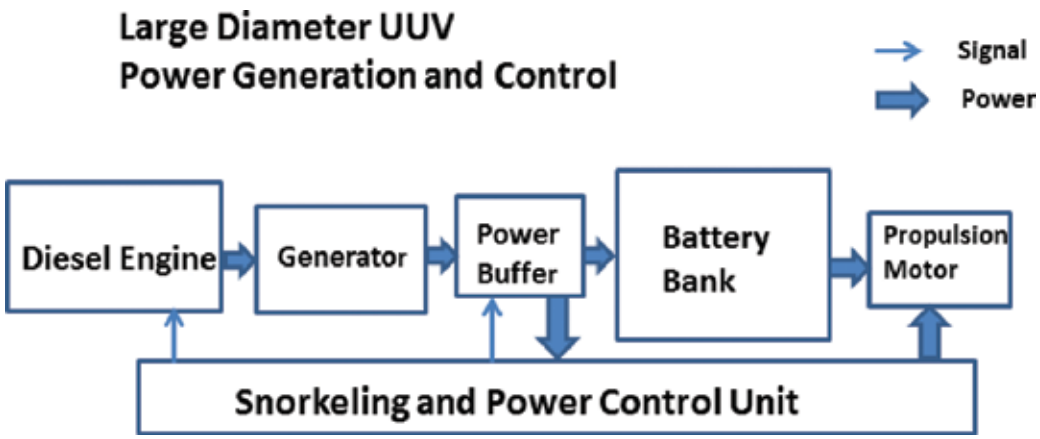

Figure 6. Power management system of MCM UUV.

4. System measure of effectiveness

4.1. System evaluation model

Recently, UUV systems have emerged as a viable technology for conducting underwater search and neutralization operations in support for the naval MCM missions. In the final phase of the system design process, either conceptual or actual, justification studies for the proposed design should be carried out with functional and cost-effectiveness evaluations. In this section, analytical frameworks for evaluating the proposed MCM disposal UUV unit are developed based on the part of current US naval underwater ship design procedure [27, 28].

The evaluation models provide means to relate the effectiveness matrices to the system-level performance parameters. These individual capabilities can be stated in terms of vehicle subcomponents, such as sensors, data storage, processing unit, communication systems, navigation instrumentations, and disposal payload items. The evaluation framework is based primarily on the approach that combines several well-known systems engineering practices and decision making methods in a framework suitable for naval ship design [29].

The general approach of measure of effectiveness (MOE) investigation is to make high-level model as generic as possible and to increase detail and resolution with each progression into the low-level models [27]. This is accomplished by developing separate model subcomponents and linking them together to form the overall system model.

4.2. System effectiveness model

For the entire MCM evaluation framework, the specific operational requirements can be defined as follows; the MCM operations with mine reconnaissance, classification, localization

and mine neutralization; the autonomous operations with minimal reliance on support platforms; safe recovery of the vehicle system unit. The effectiveness model has been established through considering the operational requirements for MCM autonomous vehicle systems and comparing those requirements to the existing MOE to determine where the changes are needed as in **Figure 7** [27].

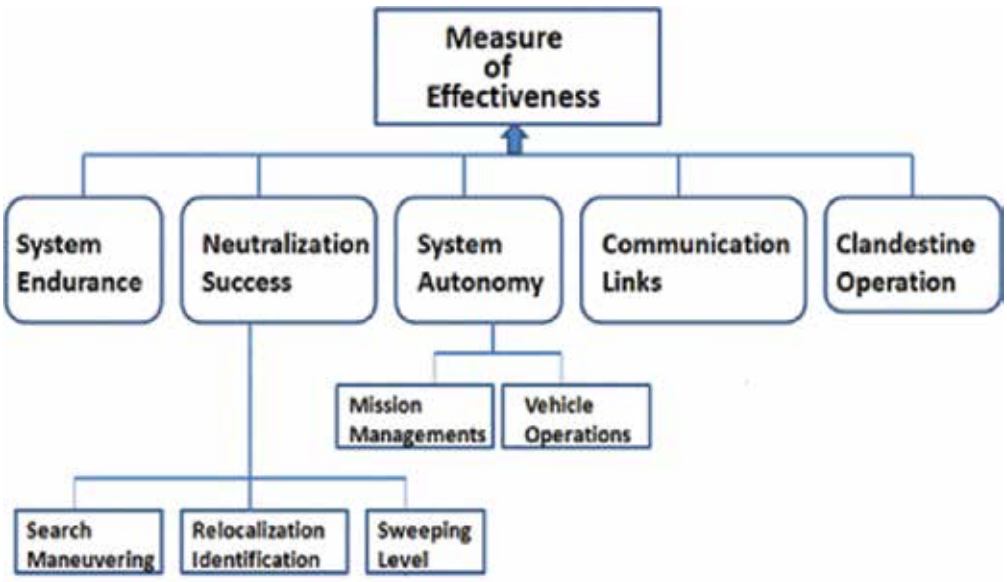

Figure 7. Structure of system MOE evaluations.

Thus, for the MCM UUV disposal system unit, the mission time, mission accomplishment, autonomy, communication and covertness form the highest level of the proposed MOE hierarchy [29]. As shown in **Figure 7**, the MOE evaluation for the proposed design has the following components: system endurance, neutralization success, system autonomy, communication links and clandestine operations.

The concepts for effective area coverage rates are better measured by time rate for mine search and actual neutralization activity, while operational time range is better for information, surveillance and reconnaissance (ISR) operations for long-term mine detection activities in wide areas. The effective area coverage rate can be defined as the ratio of the total search area to the total amount of time required to complete the MCM missions from launching to recovering of the UUV system. Duration of designed mission time is fundamentally based on UUV system hardware capability related to energy source, speed, operational load and hotel power consumptions [30].

Mine neutralization or sweeping success is the main object of MCM operations, and this MOE represents the estimated probability of search/classification of mines, as well as mission accomplishment for mine clearing. Mine reconnaissance and clearance are the two basic MCM

http://dx.doi.org/10.5772/63795

missions, and the major objectives of mine reconnaissance are accurate search, localization and containment of designated mine in the contacts. Search level refers to cumulative probability of mine detection and relocalization, classification and identification within specified MCM operational areas. For the mine hunting, and neutralization phase, the MOE will be scored from minesweeping levels and the search level, confirming relocalization accuracy. The measures of mine neutralization success are defined by performances of the individual disposal weapon system and by successful identification of mines, which is expressed by the probability measures based on the history of mission maneuvering trajectory, performances of identification sensor systems and conditions of complex underwater environments [28].

The autonomy measure represents mission management, and vehicle operations related to the independence of the system from human oversight for the mission tasks. The area of mission managements consists of execution/service commands, communication links among MCM operations and logistics support relating to launch and recovery of the small UUV unit. The mission management requirement is specified in terms of discrete host responsibility alternatives, such as performance of system platforms, remote command and control (C2) and integration of mission activity by subdivisions via operation executions [28].

Measure of dynamic vehicle operations is also based on the degree of intelligence of vehicle maneuvering, obstacle avoidances and optimal path planning. The degree of autonomy of vehicle operations is determined by the level of guidance/navigation/control (GNC) of vehicles and obstacle avoidance/optimal path planning required during the MCM mission operations. The nature of this kind of MOE characteristics is well defined in the department of defense(DoD) level of autonomy for autonomous vehicle criteria by the number, capability of processing unit and data base capacity for decision making within specific missions [29, 30].

5. Summary

In this study, we investigate the current MCM systems and evaluate the technologies to be improved for future mine neutralization operations. The configuration of hybrid MCM UUV systems has an effective future system design figure that relays a battery power system in conjunction with a diesel engine and an integrated AI expert applied autonomous system.

We try to make a larger and heavier UUV system with typical MCM missions and mission management algorithms with appropriate hardware configurations. Proposed larger displacement UUVs will be integrated into new platform designs in order for these systems to become viable organic assets. Realization of the full potential of the UUV as a truly autonomous undersea vehicle (AUV) in warfare with UUV system structure, functional specification of expert system controlled MCM UUV subsystem [30]. Hybrid power system is introduced and effectiveness discussions were presented and give the progressive transition guide line for a future larger displacement vehicle.

Author details

Kwang Sub Song*

Address all correspondence to: Kssong@ nps.edu

Oceanography Department, Naval Postgraduate School, Monterey, California, USA

References

[1] National Research Council. Oceanography and Mine Warfare, *Ocean Studies Board, National Academy Press, Washington, D.C.*, 2000.

[2] Hendrickson D, Carroll A, Wilcox M, and Douser L. Modular Remote Mine Reconnaissance System (MRMRS), *Applications of Technology to Demining, Part II Naval Mine Countermeasure, The Society for Counter Ordnance Technology*, July 2005.

[3] Office of the Assistant Secretary of the Navy. Unmanned vehicles (UV) in Mine Countermeasures, *Naval Research Advisory Committee Report*, Nov. 2000.

[4] Curtin BT, Crimmins MD, Curcio J, Benjamin M, and Rope C. Autonomous Underwater Vehicle: Trends and Transforms, *Marine Technology Society Journal*, 2005; 39(3): 65–75.

[5] Lorenson A, and Kraus D. 3D Sonar Image Formation and Shape Recognition Techniques, *Technical Report, Hochschule Bremen, University of Applied Sciences*, 2009.

[6] Nicholas CP. Buried Target Image Quality, Applications of Technology to Demining, Part II Naval Mine Countermeasure, *The Society for Counter Ordnance Technology*, July 2005, 203–207.

[7] Malerud S, Else F H, Geir E, and Karasten B. Assessing the Effectiveness of Maritime C2 Systems – Measures of Merit, *Norwegian Defence Research Establishment (FFI) Internal Report*, 2001.

[8] Levis HA. Measuring the Effectiveness of C4I Architectures, *C3 Architectures Laboratory C3I center Report, GMU/C31-186-P, George Mason University*, May 1997.

[9] NATO Report, Integration of Tools and Processes for Affordable Vehicles, Chap 5, Sea Vehicles, *NATO Report RTO-TR-AVT-093*, 2002.

[10] Wernli LR. Recent U.S. Navy Underwater Vehicle Projects, *Space and Naval Warfare Systems Center Report*, 2002.

[11] Nativi A. UUV Development Accelerates, *Aviation Week's Defense Technology International*, Sep. 2010.

http://dx.doi.org/10.5772/63795

[12] Committee for Mine Warfare Assessment National studies Board, National Research. Naval Mine Warfare: *Operational and Technical Challenges for Naval forces, Committee Report*, 2001.

[13] Pollitt W G. Mine Countermeasure Requirements to Support Future Operational Maneuver, *Johns Hopkins APL Technical Digest*, 2000; 21(2): 280–287.

[14] Evans B, Davies G, Myers V, Bellettini A, Pinto M, and Munk P. Implementation of Autonomous Mission Control for Mine Reconossaince AUVs, *NATO Report RTO-MP-AVT-146*, 2007.

[15] Brown C, and Clark P R. Using Novel Conceptual Design Utility to Evaluate a Long Range, Large Payload UUV, *OCEANS 2010 MTS/IEEE Seattle, Seattle, Washington*, Sep. 2010, 100513-016.

[16] Deitz D. Large UUV Technologies, *ONR Report Code* 32, Oct. 2010.

[17] Batlle J, Ridao P, Garcia R, Carreras M, Cufi X, El-Fakadi A, Ribas D, Nicosevici T, and Battlle E. URIS: Underwater Robotic Intelligent System, Technical Report, *Computer Vision and Robotic Group, University of Girona, Spain*, Fall 2005.

[18] Woodrow I, Purry C, Mawby A, and Goodwin J. Autonomous AUV Mission Planning and Replanning Toward True Autonomy, *System Engineering & Assesment LTD, Internet Report, Beckington Castle, United Kingdom*, 2010.

[19] Nehme CE, Stacey SD, Cumming ML, and Furusho CY. Generating Requirement for Futuristic Heterogeneous Unmanned Systems, In *Proceedings of HFES 2006, San Francisco, CA*, Oct. 2006.

[20] Weiss L. Unmanned Systems Common Control (USCC), *Georgia Tech Research Institute Report*, May 2010.

[21] Schuette L. Innovating for the Future, *Office of Naval Research S&T Presentation*, 10th Annual Science & Engineering Technology Conference/DoD Tech Exposition, April 21-23, 2009 Embassy Suites/Convention Center Charleston, SC.

[22] Bailey T, and Durrant-Whyte H. Simultaneous Localization and Mapping (SLAM), Part II, Tutorial, *IEEE Robotics and Automation Magazine*, Vol.13, Issue 3, Sep. 2006, 108–117.

[23] Hughes G. Thomas. The impact of power system type and vehicle size on range and payload for UUV'S. *Applied Research Laboratory Report, The Pennsylvania State University, State College, Pennsylvania*, 2000.

[24] Griffiths G. Energy and Power for AUVs: Batteries or Fuel Cell? *Southampton Oceanography Center Report*, 2004.

[25] Zimmerman S. Submarine Technology for the 21st Century. 2nd ed. Victoria: Trafford, 2000, 220p. ISBN:1-55212-330-8.

[26] Chu PC and Fan CW. Mine Impact Burial Model (IMPACT35) Verification and Improvement Using Sediment Bearing Factor Method. *IEEE Journal of Oceanic Engineering*, 2007; 32(1): 34–48.

[27] Bullock K.R. Theory of Effectiveness Measurement, *Doctoral Dissertation, Air Force Institute of Technology*, Sep. 2006.

[28] Osmundson S J, and Huynh VT. A Systems Engineering Methodology for Analyzing Systems of Systems, *Department Internal Report, Department of Information Science and Systems Engineering, NPS*, 2006.

[29] Green MJ. Establishing System Measures of Effectiveness, *Raytheon Naval & Marine Integrated Systems Report*, 2000.

[30] Song BW, Zhu QF, and Liu ZY. Research on Multi-objective Optimization Design of the UUV Shape Based on Numerical Based Simulation, *ICSI 2010, PartI LNCS* 6145, 2010, 628–635.

Edited by Andrzej Zak

Autonomous vehicles, despite their relatively short history, have already found practical application in many areas of human activity. Such vehicles are usually replacing people in performing tasks that require long operating time and are held in inaccessible or hazardous environments. Nevertheless, autonomous robotics is probably the area that is being developed the most because of the great demand for such devices in different areas of our lives. This book is a collection of experiences shared by scientists from different parts of the world doing researches and daily exploiting autonomous systems. Giving this book in the hands of the reader, we hope that it will be a treasure trove of knowledge and inspiration for further research in the field of autonomous vehicles.

ISBN 978-953-51-5789-2

Photo by Zapp2Photo / iStock

IntechOpen